Microwave-Assisted Synthesis of Phosphorus Based Flame Retardants

by

Robbie Mahaffey Humphries

A Thesis Submitted in Partial Fulfillment of the Requirements for the Degree of

Master of Science in Chemistry

Middle Tennessee State University

May 2021

Thesis Committee:

Dr. Dwight Patterson, Chair

Dr. Kevin Bicker

Dr. Greg Van Patten

Acknowledgments

I would like to thank Dr. Dwight Patterson for his endless patience and encouragement. His teachings were instrumental within the lab, classroom, workplace, and life in general. I truly believe he pushed me to be better in every aspect and I have cherished having him as my mentor.

I would also like to express my gratitude to Dr. Chusuei, Dr.Van Patten, and Dr. Bicker for their participation as my thesis committee. My gratitude also goes to Dr. Ooi, for allowing me to use the CEM microwave. Dr. Chong for always advising with analytical instruments and Mr. Weatherly for always taking care of the instrumentation and assisting with any issues. Dr. Patricia Patterson, thank you for teaching me how important it is to "make the doughnuts". My gratitude to the entire department and MTSU is endless.

As for my friends who have come and gone throughout the years, you are all an important part of my academic career. Learning and teaching one another during this journey, has been one of my greatest joys.

I would like to thank my husband, Christopher, who never lets me falter in any task, met me each day with love and understanding and who always kept me well fed. A special thanks to my father, Eddie Lee Mahaffey, who always supported me and encouraged me to keep learning. He never missed an opportunity to cheer me on as I know he always will. My entire family has provided me with the support that I needed as

I pushed through to finish this journey. I am grateful and incredibly blessed to have had you all in my life.

Abstract

Using microwave synthesis, chemists may decrease reaction times drastically to produce, in this case, three phosphorus-based flame retardant additives in under twenty minutes to an hour.[1] Traditionally, these three products typically take twenty-four to forty-eight hours with traditional reflux methods.[2] The popular and daily use of vehicles, computers, televisions and other household items that can easily become fire hazards, civilization requires the means of fire prevention for these synthetically composed polymer products. Materials must have the ability to resist flames and interrupt the combustion cycle of the flame. Due to environmental concerns, a non-halogenated and phosphorus-based compound is a solution that is already in use.[3] The phosphorus-based compounds are going to be synthesized into solid products to enhance thermal stability and to make handling easier. It is hypothesized that flame retardants are best in the solid phase, which allows for higher molecular weight. The synthesis process of 1,3,5-tris(diphenoxyphosphoryl)benzoate, 1,3,5-tris(phenoxyphosphoryl) dibenzoate, and 1,3,5-tris(phenoxyphosphoryl) tribenzyldicarboxylic acid were done via microwave synthesis in bulk.[2] Lastly, the final products were characterized using Fourier transform infrared spectroscopy (FTIR), differential scanning calorimetry (DSC), nuclear magnetic resonance (NMR), and thermogravimetric analysis (TGA) to determine each compounds capability as a high-quality flame retardant additive for polymer compounds.

Table of Contents

LIST OF TABLES

LIST OF FIGURES

Chapter I

Introduction

Synthetic polymers are a major part of most of our daily lives. Cell phones, vehicles, household items and appliances are all items that contain synthetic polymers. Polymers can be synthesized to have various properties and physical performance depending on the choice of monomers. Additives can enhance the performance of these polymers. A flame retardant (FR) additive functions by interrupting the combustion cycle and causing the polymer to char.[4] The ability of the flame retardant to cause charring to occur is a highly desirable property. Synthetic materials often utilize FR compounds as they are readily available to be used as an additive compound or applied as a coating.[2,4] As fire prevention has been prioritized in recent years, various additives have been synthesized with cost, performance, and commercial utilization all in consideration. However, fire safety is not considered a recent scientific discovery as it is thought that FR additives were used by Greek historian Herodotus due to his observation of flame resistance by the use of alum and later again when Romans used Bromine to protect their siege towers.[2,5,6] Chemists have optimized the abilities of flame retardants throughout the years and they are now a large part of synthetically designed polymer compounds. The increased usage of FRs has led to environmental and health concerns. This chapter will discuss the various types of FR's used as well as the mechanisms associated with each reaction. Additionally, the different methods of testing FR's and the rising health and environmental concerns of FR's will also be examined. To conclude Chapter 1, the

purpose of this study will be briefly discussed. Furthermore, the analytical techniques that are used to characterize the products are also discussed.

A. Origin of Microwave-Assisted Synthesis

It all began in 1946, a self-taught engineer by the name of Percy Spencer, was working with a chocolate bar in his pocket. Percy worked for Ratheon on a radar project when he noticed that the chocolate bar in his pocket had melted.[7] Once he made this discovery, he observed what would happen to popcorn and then continued to observe what would happen to an egg. By 1947, Percy had patented and built the first microwave appliance, which was called Radarange microwave oven.[8] This microwave was not like one would imagine, as it stood almost six feet tall and weighed approximately seven hundred and fifty pounds. It wasn't too much longer that microwaves became an affordable household item owned by many.[9]

In the 1980's, microwaves found their way into laboratories. Since then, manufacturers have found more innovative ways to improve this technology so that it is smaller, safer, and easier to use.

B. Microwave-Assisted Heating vs Traditional Heating

Microwave-assisted synthesis allows the heating of a solution to be direct and volumetric. This method of heating differs from the traditional hotplate because microwave energy heats matter with dielectric heating.[10,11] The Figure 1 is an example of

the oscillating electromagnetic radiation that is composed of an electric field and

magnetic field.
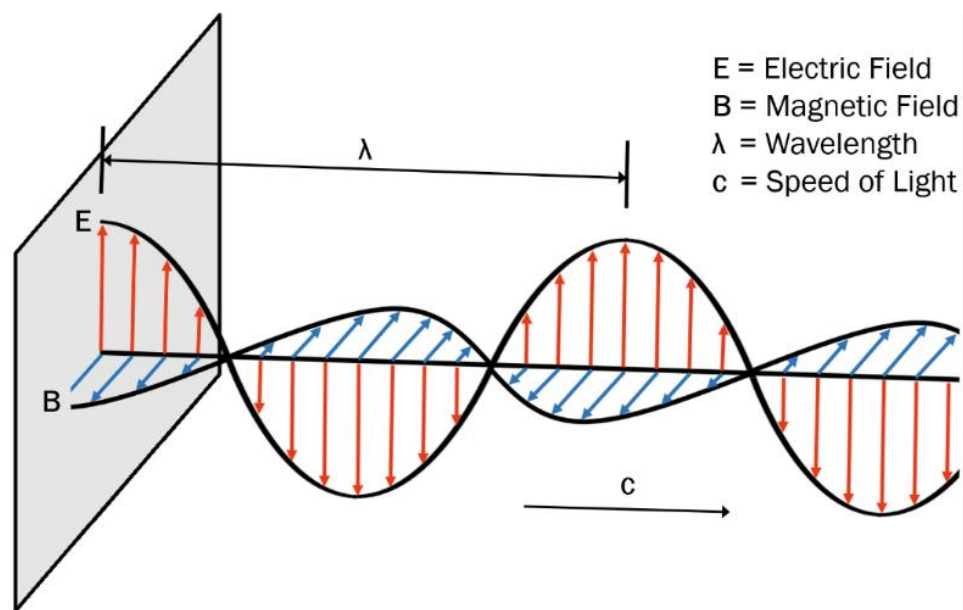
Figure 1: Oscillating electromagnetic radiation. Image from
https://cem.com/de/microwave-heating-mechanism-and-theory.

The electric field is responsible for dielectric heating.[8] The final conversion of

electromagnetic energy turns into kinetic energy. This occurs as electromagnetic

radiation causes the stimulation of dipolar molecules to oscillate.[9] Dielectric heating

relies heavily on a solvent to absorb and convert microwave energy for a more even

distribution of energy and faster reaction time.[13,14]

C. Benefits of Microwave-Assisted Synthesis

Microwave-assisted synthesis has been proven beneficial in the laboratory to many different fields and industries. It can be found in a lab making peptides, organic compounds, or polymer compounds. It has been used in the biological labs, the food industry, and more. Microwave-assisted synthesis offers a shorter reaction time, a controlled environment and multiple heating methods, higher yield, ability for bulk syntheses, and safer than traditional heating methods.[1,7, 14]

D. Fire Statistics of 2019

In 2019, local fire departments had responded to 1,291,500 fires, resulting in 3,700 civilian fire fatalities and 16,600 civilian fire injuries. Home fires make up seventy-five percent of the deaths and seventy-three percent of the injuries.[15] The devastation caused $14.8 billion in property damage. The National Fire Protection Agency (NFPA) studies and reports the statistics each year. The concerns of manufacturers as well as others have led to strict material regulations, educational improvements as well as motivation for optimized properties of materials that are deemed fire safe.[15]

E. Polymer Combustion Cycle

Polymers are often highly combustible due to their structure. With a specific amount of heat, which is dependent on the specific polymer, they pyrolyze producing combustible gases.[4,16] Under ambient conditions, the gases then mix with the oxygen in the air and become ignitable. Ignition is possible by an external source such as a flame or a spark as well as impulsively. An ignition that impulsively ignites is possible due to a

temperature being reached, which then reaches the activation energy fueling the combustion cycle.[4,16] Once ignited, the released heat furthers the decomposition process, which then has the possibility of a generating a self-sustaining combustion cycle.[16]

F. Types of Flame Retardants

The FR's mechanism interrupts the combustion cycle.[6] This interruption may occur physically or chemically.[2,4,16] Examples of physical interruption would include dilution of combustible gases by the production of inert gases, as well as decreasing the temperature due to the production of decomposition products.[2] Chemical interruption occurs when the FR reacts in the gas or condensed phase of the combustion cycle. The condensed phase occurs after the production of char.[2,16]

There are four categories of flame retardants that will be discussed, and each has its own general mechanism of interrupting the combustion cycle. Each of the four categories has a mechanism in a different phase of the combustion cycle that will interrupt according to its specific mode of action. Halogenated based FRs are used to help prevent or hold back fumes. Silicon slows down the decomposition by slowing the release of the gases that fuel the combustion cycle.[17] The nitrogen based stops the decomposition process and prevents flammable gases from being released. Lastly, the phosphorus based FRs stimulate charring and also prevent flammable gases from being released.[17]

i.   Halogenated Based Flame Retardants

Halogenated based flame retardants are often used due to their availability, cost, and broad knowledge of use in industry.[16] During thermal decomposition, halogenated FRs

release hydrogen halides, which can then react in the gas phase of the combustion process. The ability of scission to occur between the halogen and the carbon that the halogen is attached is important for the FR to interrupt the right phase of the combustion cycle. Halogenated FRs react in the gas phase of the decomposition process by radical mechanisms.[2,4,16] Figure 2 below is an example of the radical mechanism in a polymer with a flame retardant vs a polymer without the flame retardant. Note that the O_2 feeds the flame in the reaction without the FR, but the polymer containing the FR reacts as a radical reaction to interrupt the combustion cycle.
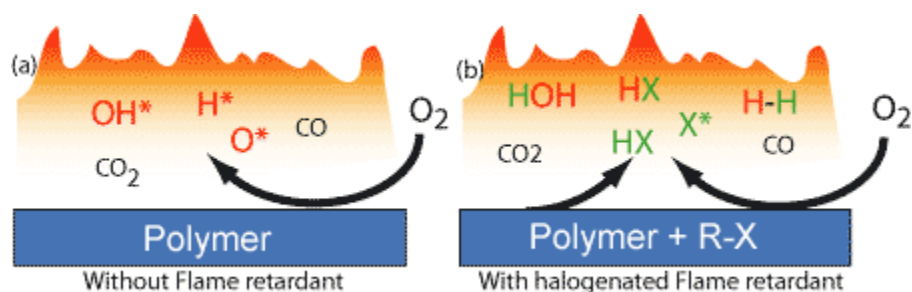
Figure 2: Mechanism of Halogenated FR. Image from https://polymer-additives.specialchem.com/selection-guide/flame-retardants-for-fire-proof-plastics/flame-retardants-mechanism-of-action-and-chemistries.

Fluorine is an exception as it is not an efficient radical acceptor due to the strong bond that it forms with carbon. This strong bond prevents interruption during the gas phase. In the opposite respect, iodine has such a weak bond to carbon that it is released before pyrolysis even occurs.[19]

Of all halogens, bromine is often considered the most effective and most frequently preferred. Aliphatic compounds containing bromine are better suited for polymers with lower decomposition temperatures because they are easier to breakdown, although bromine may also be bound aromatically.[19]

ii.   Silicon- Containing Flame Retardants

Until recently, silicon based FRs were considered some of the best co-additives. Current research indicates that silicon could also serve as a stand-alone additive. Silicones have diverse applications and can be found in cosmetic, electrical, and aerospace industries as well as several others. When pure, silicones burn slowly during the combustion cycle without the production of toxic smoke, dripping, and only small amounts of carbon monoxide gas.[16]

The mechanism occurs in the condensed phase and produces a char type residue. Therefore, once the polymer is exposed to heat, it will decompose and leave a residue that is composed of inorganic silica. The silica residue that has built up then behaves as a barrier preventing the combustion cycle from continuing.[16] Figure 3 examines the mechanism of a silicon-based FR additive that is used in textiles.
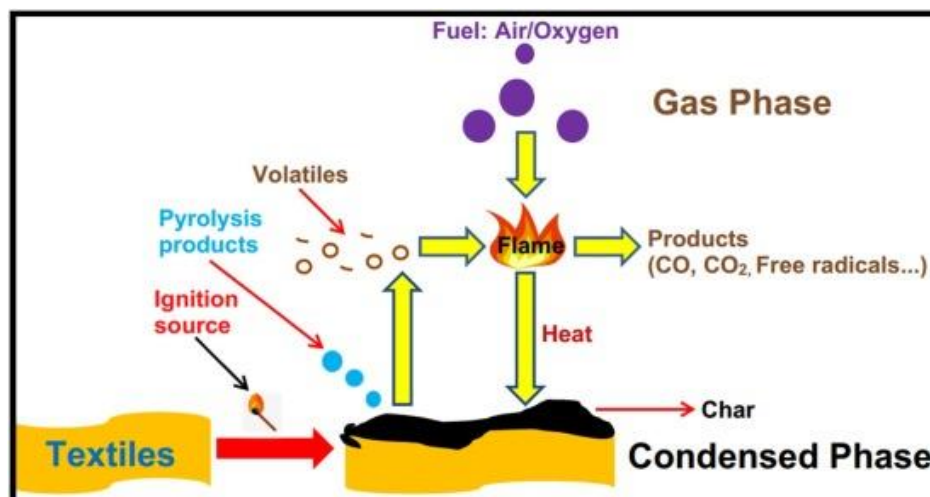
Figure 3: Mechanism of silicon-containing FR. Image from
https://www.sciencedirect.com/science/article/abs/pii/S0014305720316256.

iii.   Nitrogen Based Flame Retardants

The most commonly used nitrogen-based FR is melamine, which mechanistically

takes place in the condensing phase of the polymer combustion cycle just as phosphorus-

based FRs do. Melamine, which is a crystalline solid FR, also has a commonly used

derivative, melamine phosphate. Once thermal degradation takes place, melamine

phosphate releases melamine and phosphoric acid. [2,21] The release of phosphoric acid

causes the FR to function similarly to the phosphorus-based FR. A side effect of this

reaction is that the melamine degrades a resin of interest until it eventually releases

ammonia making it a less desired option.[2,21]

iv.   Phosphorus-Based Flame Retardants

Phosphorus-based FRs are sought after due to their low toxicity levels during production as well as during and after degradation.[3,22] Due to an extensive variety of both inorganic and organic compounds, it is important to understand that the phosphorus-based FR may be used as either an additive or a coating.[3] Due to the variance, the phosphorus- based FRs can mechanistically interrupt the gas phase or the condensed phase; therefore, it has the ability to act as a radical and also react to form a char.[2] Figure 4 is an example of the mechanism reacting in the gas phase as well as the condensed.
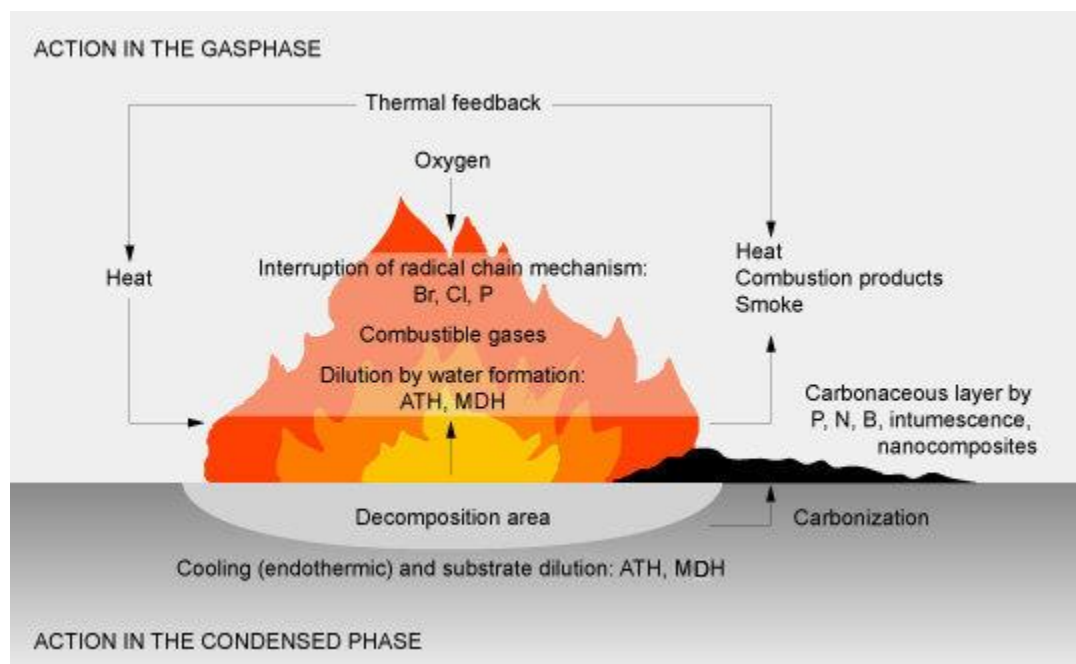
Figure 4: Mechanism of phosphorus-based flame retardants. ATH represents alumina trihydrate and MDH represents magnesium hydroxide. Image from https://www.flameretardants-online.com/flame-retardants/mode-of-action.

In the condensed phase mechanism, it appears that a phosphorus FR forms phosphoric acid and after decomposition leaves pyrophosphate and water. The gas phase mechanism reacts much like the halogen FRs, as a radical, but after degradation produces phosphine. Phosphine is highly toxic.[2,4] Fortunately, the phosphorus-based FR that causes the production of phosphine has not been used as much as halogenated FRs. The condensed mechanism is more desired due to the charring. This is because the charring is known to be a safer product of decomposition.[2]

G. Environmental Concerns

The absence of broad-based recycling has become a concern for the environment as well as its inhabitants. Recent studies have shown that some FRs do not decompose quickly over time.[4,24] Studies that began thirty years ago, in a third-world country, have concentrated on proving that dumping halogenated FRs in an electronic landfill is going to lead to large concentrations of harmful pollutants that do not decay quickly. The electronic landfills containing these materials, as well as other harmful elements, have accumulated over the years and will continue to increase as manufacturing and the use of polymers containing FRs also grows.[4,24] It has become society's responsibility to begin looking into healthier and more environmentally friendly flame retardants.[11,24]

H. Health Concerns

Health-related studies of human and animal species will continue to develop as the use of items containing flame retardants grows endlessly. Evidence of potential adverse health effects from the composition of FR's are now associated with the strength of

immune system, neurological function, reproductive issues, endocrine/thyroid disruption, fetal development, childhood development, and cancer. Studies have shown that children often have higher concentrations of FR within their body in comparison to adults because of developmental vulnerabilities in relation to hygiene and physical height.[25,26]

I. Recent Studies of Flame Retardant Studies Utilizing Microwave-Assisted Synthesis Techniques

Recent microwave -assisted syntheses have eliminated the need of an added catalyst and formed a new type of FR, that is both phosphorus and nitrogen containing (DOPO) and reacts in the condensed phase. [27,28] The DOPO flame retardant is being studied for polyester and polyurethane materials and forms an intumescent char in response the combustion cycle. [27,28] Studies have shown that they are more environmentally friendly and have not shown any adverse health effects at this time. [27,28]

There are a plethora of sources and articles discussing the benefits of synthesizing flame retardants using microwave-assisted synthesis. Microwave-assisted techniques have also been used to identify organophosphate flame retardants that are present in water sources.[25] The study explained that the microwave was coupled with GC-MS, electron impact (EI), and chemical ionization (CI) for sample analysis. [29]

J. Purpose of this Study

The overall goal of this research is to shorten the reaction time of three potential FR additives from 24-48hrs to only a few hours or less. The reaction times for the three condensation reactions were drastically reduced using microwave-assisted synthesis

instead of the conventional method. These three molecules were synthesized for potential evaluation as high molecular weight, phosphorus-based FR additives for use in engineering resins. The idea of a high molecular weight FR compound is that as the molecular weight increases, the compound is expected to be a solid and easier to handle versus the liquid phosphate FR compounds.[2]

K. Synthesis

The three compounds synthesized in this study, were successfully established using a previous thesis project. For the prior project, the compounds were constructed and based off other oligomeric phosphates found in literature and patents.[2] The three synthesized products are not currently used in industry and were chosen as alternative flame retardants. Each reaction contains trimesic acid (1,3,5 benzenetricarboxylic acid) introducing several carboxylic acids that react with either diphenyl chlorophosphate (DPCP) or phenyldichlorophosphate (PDCP). Since this is a condensation reaction, the mechanism results in the loss of HCl(g). The loss of HCl(g) occurs as the nucleophilic agent (DPCP or PDCP) contains chlorines that will react with the electrophilic hydrogen of the carboxylic acid group (provided by trimesic acid).[2] This reaction then results in the preparation of each phosphate compound. The three synthesized compounds are as listed: 1,3,5-tris(diphenoxyphosphoryl)benzoate (1,3,5-DPP), 1,3,5-tris(phenoxyphosphoryl)dibenzoate (1,3,5-PPDB), and 1,3,5-tris(phenoxyphosphoryl) tribenzyldicarboxylic acid (1,3,5-PPTBDA). Figure 5 depicts the CEM (Discovery) microwave set-up used in the following reactions. The acronym for CEM represents

the founders of the company as one was a chemist (C), another was an electrical

engineer (E), and the last was a mechanical engineer (M).[8]

.

Figure 5: CEM microwave used for syntheses.

The CEM used in the experiment was run as an open vessel reaction, allowing for a

water-cooling system and a caustic scrubber. The lowest molecular weight product

synthesized is shown in Figure 6. This figure denotes the phenyl functional group as Ph.

Figure 7 is the most relaxed state of the molecular 3-D model representing 1,3,5-DPP.

Figure 8 and Figure 9 represent the molecular structure and a most relaxed state of the 3-

D model for 1,3,5-PPDB. Figure 10 and Figure 11 represent the 1,3,5-PPTBDA

compound. Ph denotes a phenyl group for these structures as well. Each structure is an

increase of molecular weight.
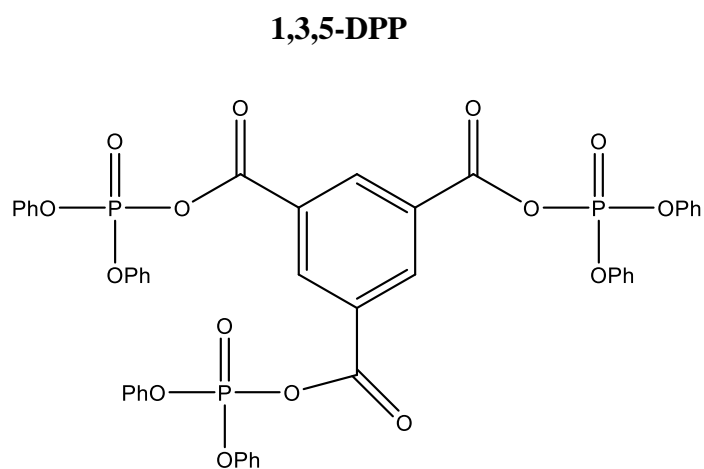
1,3,5-DPP

Chemical Formula: $C_{45}H_{33}O_{15}P_3$

Molecular Weight: 906.67g/mol

Figure 6: The molecular structure of 1,3,5-DPP.
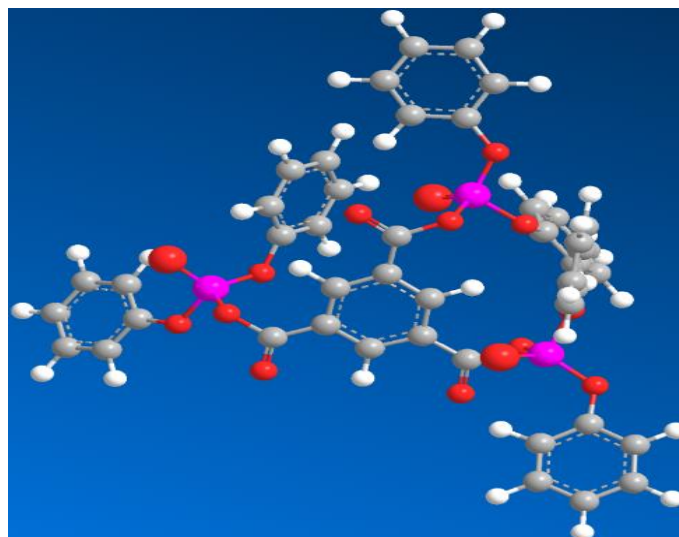
Figure 7: 3-D molecular structure of 1,3,5-DPP in the most relaxed state.

1,3,5-PPDB
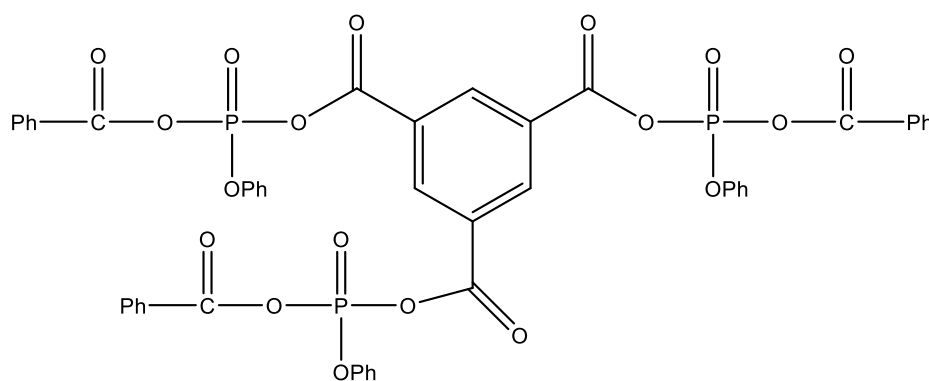
Chemical Formula: $C_{48}H_{33}O_{18}P_3$

Molecular Weight: 990.70g/mol

Figure 8: Molecular structure of 1,3,5-PPDB.
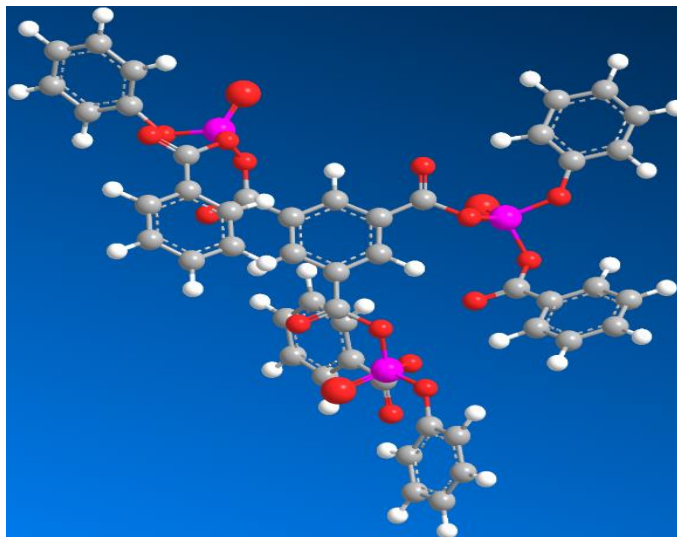
Figure 9: A 3-D molecular structure of 1,3,5-PPDB in the most relaxed state.
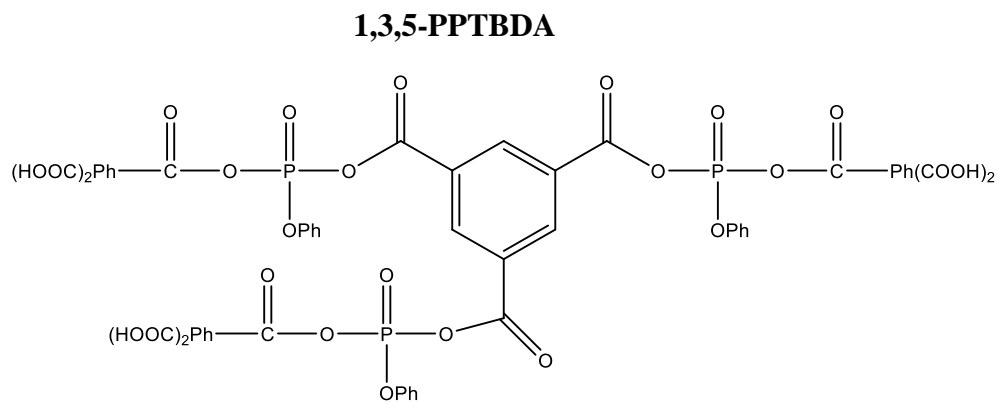
1,3,5-PPTBDA

Chemical Formula: $C_{54}H_{39}O_{30}P_3$

Molecular Weight: 1260.80g/mol

Figure 10: Molecular structure of 1,3,5-PPTBDA.
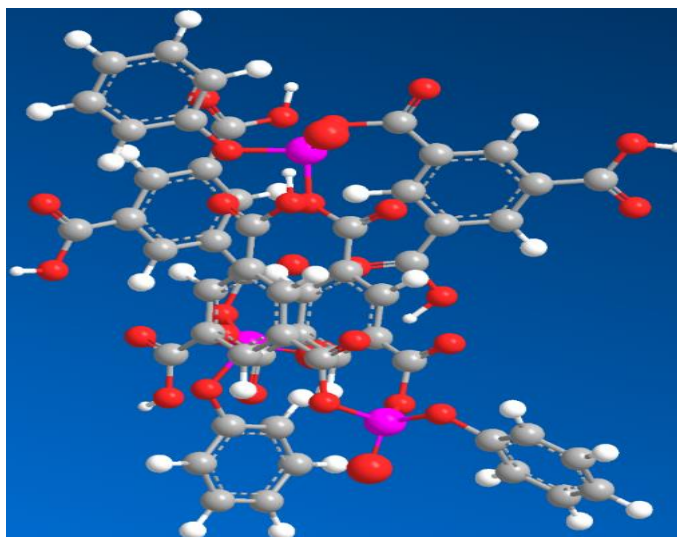
Figure 11: A 3-D molecular structure of 1,3,5-PPTBDA in the most relaxed state.

L. Analytical Techniques Used to Evaluate the Flame Retardants Synthesized

i.   Fourier-Transform Infrared Spectroscopy (FTIR)

IR spectroscopy is an analytical method that aids in identifying the functional groups

present in a sample using infrared radiation. FTIR identified the functional groups present

in each synthesized product to detect whether the reaction had partially reacted or fully

reacted. This method of analysis does not require a large amount of sample and is useful

for quick analysis. IR is a useful technique for identifying unknowns, oxidation,

decomposition, and contamination by observing and characterizing the absorption

bands.[26,27] It is a valuable technique for clear observation of changes during a synthesis or

purification process and is often used in industry for quality control. Samples may be

analyzed in the form of a solid, liquid, or gas. Functional groups have a unique absorption

band at certain frequencies and IR works by sending energy through the sample and the functional group will absorb the energy passing through. Once the functional groups have absorbed the energy, the spectrum is produced where the frequencies are characterized in relation to the absorption.[27] IR instruments have an array of accessories and libraries that aid in analyzing and characterizing a sample. In this study, the attenuated total reflection (ATR) accessory will be used. ATR is fast and reliable method of analysis that uses internally reflected IR beam to generate an evanescent wave. The sample is placed on a crystal surface for measurement. The crystal essentially creates the pathway between the sample and the infrared beam that the detector records as an interferogram signal. The interferogram signal then produces the IR spectra used for analysis.[28]

ii.   Thermogravimetric Analysis (TGA)

TGA is a thermal technique that heats a sample under a vacuum or controlled atmospheric conditions and measures the change in mass as the sample is heated. This can be a simple ramp heat or an isothermally run sample where heat is applied as a function of time. A TGA can heat a sample from room temperature up to 1000°C and does not require a large amount of sample (1-150mg). It is used to observe the thermal degradation of a given sample and is a good technique to use before analyzing a sample by Differential Scanning Calorimeter.[29] For this project, comparisons of the TGA profiles onset degradation temperatures and the percentage of material left after the degradation gave insight on the synthesized additives degradation steps without its addition to a polymer resin.

iii.   Differential Scanning Calorimetry (DSC)

DSC analysis measures the heat gain or heat loss by the sample containing pan in comparison to an empty reference pan. DSC is a thermal analysis technique that measures changes in physical properties such as the melting point (T_m), glass transition temperature (T_g), degradation decomposition temperature (T_D), and crystallization temperatures (T_c).[26] This project used the standard heat/cool/heat method to identify thermal events such as the T_m and T_g.

iv.   Nuclear Magnetic Resonance (NMR) Spectroscopy

NMR spectroscopy is an analytical technique for determining a molecular structure and the content and purity of a sample. When nuclei of atoms in the sample are placed within a magnetic field and then irradiated with a specific radio frequency; signals are then produced. These signals yield a spectrum that is then analyzed. [30]

Chapter II

Experimental

The original experimental design was designed in a low, medium, high format regarding time, temperature, and power. Time, temperature, and power were varied according to Table 1. This table was modified throughout the process as well as whether the reaction should be open vessel or closed. This study will only include the reactions that were open vessel.

Table 1: The original experimental design.

Proposed Experimental Design			
	Time (min)	Temperature(°C)	Power (W)
Low	10	150	100
Medium	15	150	100
High	20	150	100
Low	10	160	100
Medium	15	160	100
High	20	160	100
Low	10	170	100
Medium	15	170	100
High	20	170	100

i. Materials

The trimesic acid (TMA), magnesium chloride($MgCl_2$) , diphenyl chlorophosphate (DPCP), and dimethyl sulfoxide (DMSO) were purchased from Sigma Aldrich. The phenyl dichlorophosphate (PDCP) was purchased from Alfa Aesar.

ii. Synthesis of 1,3,5-tris(diphenoxyphosphoryl) benzoate (1,3,5-DPP)

Trimesic acid (TMA) and diphenylchlorophosphate (DPCP) were reacted with magnesium chloride (MgCl$_2$) acting as a Lewis acid catalyst. The reaction can be found below in Scheme 1.
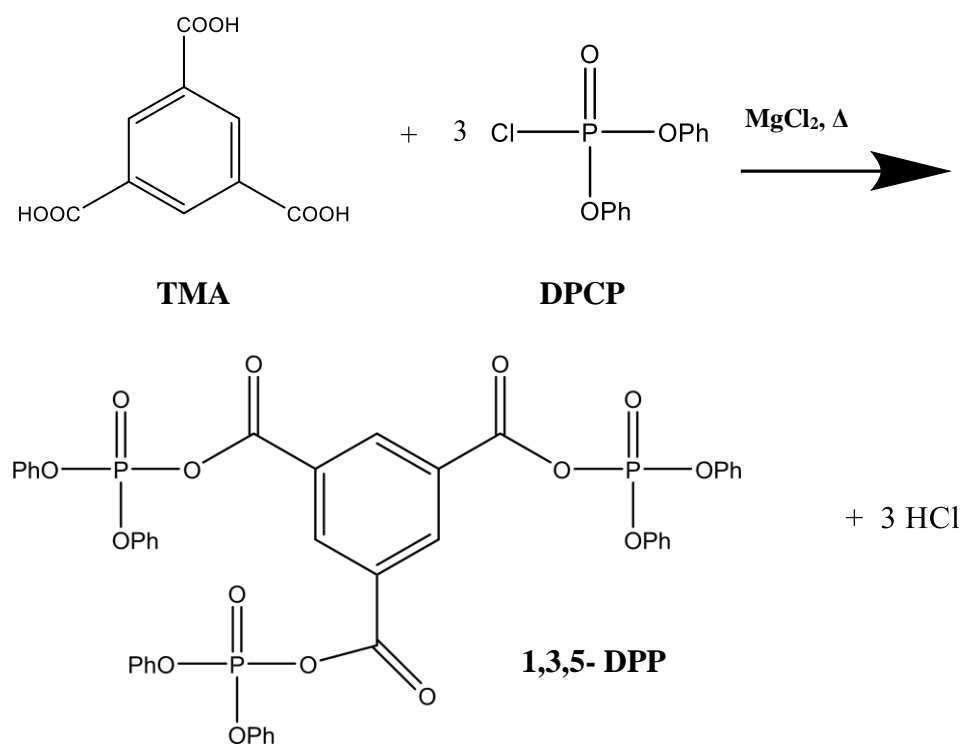
Scheme 1: The synthesis of 1,3,5-tris(diphenoxyphosphoryl) benzoate (1,3,5-DPP).

The reaction apparatus uses a 50 mL round bottom flask with a long neck. The round bottom flask was connected to a reflux condenser so that an inert atmosphere of Nitrogen

gas was used as a continuous purge. Note that nitrogen or argon could be used to purge the system. The condenser was water cooled. The byproduct of the reaction is HCl(g) and therefore a caustic scrubber, sodium bicarbonate ($NaCO_{3)}$, was added to trap and neutralize the HCl (g). The scrubber is connected to the condenser outlet.

A magnetic stir bar was placed in the round bottom flask. Trimesic acid was weighed out as a 1.00 g (0.00476 mol) sample as well as 0.10 g of $MgCl_2$ catalyst. Both were added to the flask. Lastly, 3.11mL (0.0143 mol) of DPCP was added to the round bottom flask. The reaction flask was connected to the apparatus and placed within the CEM microwave. The reaction was then purged with N_2 (g) for approximately 30-45 minutes.

The beginning of this experiment found that recording the temperatures throughout the synthesis manually would be important for later observations. This was due to variation in microwave performance. Multiple users may introduce inconsistencies.

Power, temperature, time, and pressure were entered into the instrument using the standard heating method of the CEM. Table 2 represents the settings used in the synthesis of 1,3,5-DPP.

Table 2: CEM microwave settings used for the synthesis of 1,3,5-DPP.

Sample I.D.	Time (min)	Power (W)	Temperature (°C)	Pressure Open Vessel
EM100419B	2	50	150	Atmospheric
EM031019A	2	100	150	Atmospheric
EM091319A	6	50	130	Atmospheric
EM092119	10	50	130	Atmospheric
EM031719B	10	100	150	Atmospheric
EM100419	15	50	130	Atmospheric

Once the reaction was completed, the apparatus was left to continue purging and cooled to room temperature. Purification began after the microwave-assisted synthesis. Once the reaction was cooled, DMSO was added to the flask. Once the product was in solution, the sample was then reprecipitated by adding the DMSO solution (approximately 40-50 mL) to a 1:1 MeOH: DI solution (approximately 500-600 mL). The solution was then refrigerated for 24-48 hrs minimum.

The precipitate was then washed in a 1:1 Methanol: DI solution and centrifuged for thirty minutes at 4000 rpm. Each product was washed with the Methanol: DI solution three times. After the wash, the product was dried at 50°C in a vacuum oven until dry.

iii. Synthesis of 1,3,5-tris(phenoxyphosphoryl) dibenzoate (1,3,5-PPDB)

Trimesic acid (TMA) and phenyldichlorophosphate (PDCP) are reacted in the first step. The second heating step occurs after the addition of benzoic acid. Magnesium

Chloride serves as an added catalyst in the first step. The reaction can be found below in Scheme 2.

COOH

HOOC   COOH

+   3   Cl—P—OPh

MgCl₂, Δ

3 HCl +

TMA   **PDCP**

PhO—P—O   O—P—OPh

Cl   Cl

PhO—P—O

Cl

+   3   Ph—C—OH

Benzoic Acid

Phosphate Intermediate

Δ

Ph—C—O—P—O   O—P—O—C—Ph

OPh   OPh

Ph—C—O—P—O

OPh

+ 3 HCl
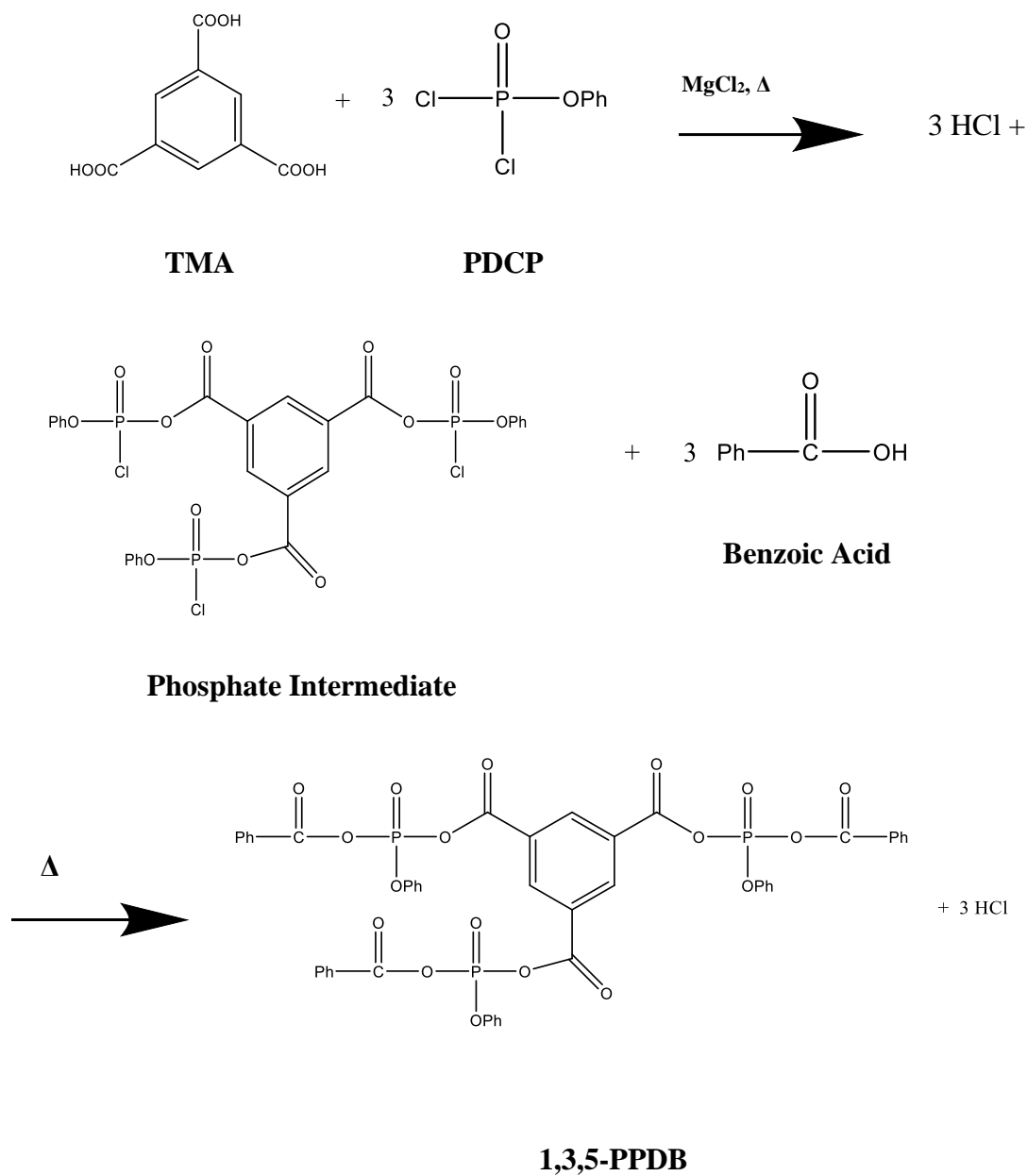
1,3,5-PPDB

Scheme 2: Synthesis of 1,3,5-tris (diphenoxyphosphoryl) benzoate (1,3,5-PPDB)

Trimesic acid was weighed out as a 1.00 g (0.00475 mol) sample as well as 0.10 g of MgCl$_2$ catalyst. Both were added to the flask. Lastly, 2.13 mL (0.0143 mol) of PDCP was added to the round bottom flask. The reaction flask was connected to the condenser apparatus and placed within the CEM microwave. The reaction was purged with N$_2$ (g) for approximately 30-45 minutes. Setting up the experiment with similar methods did not always yield the same results. For this reason, the time and temperature were noted and later graphed. Table 3 represents the conditions used for the microwave-assisted heating.

Table 3: CEM microwave settings used for the synthesis of 1,3,5-PPDB.

Microwave 1 of 2				
Sample I.D.	Time (min)	Temperature (°C)	Power (W)	Pressure Open Vessel
EM020720	6	130	50	Atmospheric
EM022320	8	130	50	Atmospheric
EM030120	10	130	50	Atmospheric
EM030620	12	130	50	Atmospheric
EM081720	15	130	50	Atmospheric
EM082720	15	130	50	Atmospheric
EM082820	15	130	50	Atmospheric
EM111320	20	130	75	Atmospheric
EM081716	30	160	150	Atmospheric
EM080516	60	160	300	Atmospheric
EM080316	80	160	220	Atmospheric

After the first microwave, the samples were cooled to room temperature and

approximately 1.77 g (0.0145mol) of benzoic acid was added to the reaction flask. This

step took place in the hood attached to a condenser, scrubber, and inert atmosphere. To

prevent uncontrollable reactions with the addition of the benzoic acid, the reaction

product from the first step and the benzoic acid mixture was heated in an oil bath for

about an hour or until it reaches 110°C. The benzoic acid was thoroughly mixed into the

solution, in order to prevent an exothermic reaction that occurs with undissolved benzoic

acid during the second microwave step.

The round bottom flask was placed back into the CEM and purged 30-45 minutes.

Table 4: CEM microwave settings used for the synthesis of 1,3,5-PPDB.

Microwave 2 of 2				
Sample I.D.	**Time (min)**	**Temperature (°C)**	**Power (W)**	**Pressure Open Vessel**
EM030620	5	130	50	Atmospheric
EM081720	5	130	50	Atmospheric
EM082820	6	130	50	Atmospheric
EM082720	7	130	50	Atmospheric
EM111320	7	130	50	Atmospheric

Purification began after the second microwave step. The samples were cooled and

DMSO was added. The samples were soluble in approximately 35-40 mL of DMSO and

reprecipitated in a 500-600 mL solution of (1:1) Methanol:DI. The samples were

precipitated and then refrigerated for 24-48 hrs. The products were then centrifuged at

4000 rpm for 30 minutes and washed three additional times before the drying step. The samples were dried in a vacuum oven at 50°C.

iv. Synthesis of 1,3,5-tris(phenoxyphosphoryl) tribenzyldicarboxylic acid (1,3,5-PPTBDA)

Trimesic acid (TMA) and phenyldichlorophosphate (PDCP) are reacted in the first step. The second heating step occurs after the second addition of trimesic acid. Magnesium Chloride serves as an added catalyst in the first step. The full reaction can be found below in Scheme 3.

Scheme 3: Synthesis of 1,3,5-tris (phenoxyphosphoryl) tribenzyldicarboxylic acid (1,3,5-PPTBDA)

Trimesic acid was weighed out as a 1.00 g (0.00475 mol) sample as well as 0.10 g of

$MgCl_2$ catalyst. Both were added to the flask. Lastly, 2.13 mL (0.0143 mol) of PDCP was

added to the round bottom flask. The flask was then purged with Nitrogen gas. The

reaction flask was connected to the condenser apparatus and placed within the CEM

microwave. The reaction was then purged with N_2 (g) for approximately 30-45 minutes.

Setting up the experiment did not always yield the same results. For this reason, the time

and temperature were noted and later graphed.

Table 5: CEM microwave settings used for the synthesis of 1,3,5-PPTBDA.

Microwave 1 of 2				
Sample I.D.	**Time (min)**	**Temperature (°C)**	**Power (W)**	**Pressure Open Vessel**
EM081620	2	130	50	Atmospheric
EM080920	10	130	50	Atmospheric
EM092520	15	130	50	Atmospheric
EM092520B	15	130	50	Atmospheric
EM100120	20	130	50	Atmospheric
EM100820	20	130	75	Atmospheric
EM101020	25	130	75	Atmospheric

After the first microwave, the samples were cooled to room temperature and

approximately 3.00 g (0.0143mol) of trimesic acid was added to the reaction flask.

Before proceeding to the microwave, this step took place in the hood attached to a

condenser, scrubber, and inert atmosphere. The mixture was heated in an oil bath for

about an hour and until it reaches 110°C. Trimesic acid was thoroughly dissolved into the

mixture before being placed in the CEM for the second microwave step. Table 6

represents the CEM microwave settings.

Table 6: CEM microwave settings used for the synthesis of 1,3,5-PPTBDA.

Microwave 2 of 2				
Sample I.D.	Time (min)	Temperature (°C)	Power (W)	Pressure Open Vessel
EM092520B	5	130	50	Atmospheric
EM103120	5	115	75	Atmospheric
EM100820	10	130	50	Atmospheric
EM110520	10	115	90	Atmospheric
EM092620	15	130	50	Atmospheric
EM110820	15	115	100	Atmospheric
EM101020	20	130	50	Atmospheric
EM111220	20	115	90	Atmospheric

The round bottom flask was placed back into the CEM and purged 30-45 minutes. After the second microwave, the samples were cooled and DMSO was added. The sample was then purified. The samples were soluble in approximately 35-40 mL of DMSO and reprecipitated in a 500-600 mL solution of DI water. The samples were added to the DI water and refrigerated for 24-48 hrs. The products were then centrifuged at 4000 rpm for 30 minutes and washed three additional times with DI water before the drying step. The samples were dried in a vacuum oven at 50°C.

B. Percent Yield of Samples Discussed

Table 7 is a summary of the percent yields for samples of interest before and after purification.

Table 7: Percent Yield			
Sample I.D.	**Molecule**	**Crude Yield %**	**Purified Product Yield %**
EM100419	1,3,5-DPP	94.8	2.9
EM081720	1,3,5-PPDB	91.4	22.4
EM082820	1,3,5-PPDB	89.7	19.2
EM092520B	1,3,5-PPTBDA	95.7	38.4
EM103120	1,3,5-PPTBDA	94.3	51.1
EM110520	1,3,5-PPTBDA	94.0	44.0
EM110820	1,3,5-PPTBDA	91.9	4.9
EM111220	1,3,5-PPTBDA	90.3	13.1

C. FTIR Spectroscopy

Samples were analyzed using the iS50 ATR accessory of a Thermo Scientific IR spectrometer. Each sample was scanned 64 times.

D. NMR Spectroscopy

JOEL ECA 500MHz was the spectrometer used for NMR sample analysis. Samples were dissolved in DMSO-d. Proton, carbon-13, and phosphorus-31 spectroscopy was performed if samples were soluble in DMSO-d. The ^{13}C samples were scanned 16,384 times, the ^{1}H samples were scanned 32 times and the ^{31}P samples was scanned 2,048 times. TMS served as the reference chemical shift agent for the proton and carbon NMR. Phosphoric acid served as a reference chemical shift agent for the phosphorus NMR spectroscopy.

E. TGA

A TA Instruments Q500 was the instrument used for sample analysis. Samples weighing approximately 8-20 mg were placed into an alumina sample pan and heated at 10°C/minute to a maximum temperature of 1000°C. During the TGA, the sample was purged with Nitrogen gas.

F. DSC

The instrument used for DSC analysis was the TA instruments Q2000 with a Refrigerated Cooling System 90 cooling accessory from TA. The amount of sample used was approximately 3 mg and the samples were crimped inside a hermetically sealed

aluminum pans. Using a standard heat/cool/heat method, the samples were first cooled to -50.0°C for an equilibrium temperature and then heated at a rate of 10°C/minute to a maximum temperature of 250°C. The maximum temperature for some samples were as low as 80°C. The samples were purged using nitrogen gas.

Chapter III

Results and Discussion

A. Possible Discrepancies in Synthesis

Discrepancies were learned throughout the synthesis process showing how easily a microwave-assisted synthesis can have varying results based off small changes that often occurs with different users. For example, the PSI of the cooling air is set for the microwave to be between 25-30PSI, but if another user changes this setting it can cause a deviation in heating. Another important factor is the height and placement of the round bottom flask. Being consistent and using the microwaves base that holds the flask or vial centered in the microwave cavity is key. While the microwave will work, there appears to be inconsistent heating. The microwave heating method is often changed by different users. It is essential to understand the mode the microwave is in. Some modes on the microwave have a ramp time, others do not. Some modes offer high-speed stirring while others do not.

B. Temperature vs Time

The settings that were selected for the microwave synthesis did not often reflect the actual results. The results for 1,3,5-DPP are limited as this data was collected toward the end of the synthesis trials. The graphs represent the time and temperature of the actual runs as it was discovered the software was not able to print or save each run for record.

Figure 12 below is the recorded temperature and time during the reaction with data being noted every thirty seconds. The CEM microwave has a timer that counts down and therefore the beginning of the synthesis begins on the left side of the graph and ends at the maximum temperature on the right side of the graph. Figure 13 represents the time and temperature manually recorded every thirty seconds during the first microwave step of the synthesis for 1,3,5-PPDB.
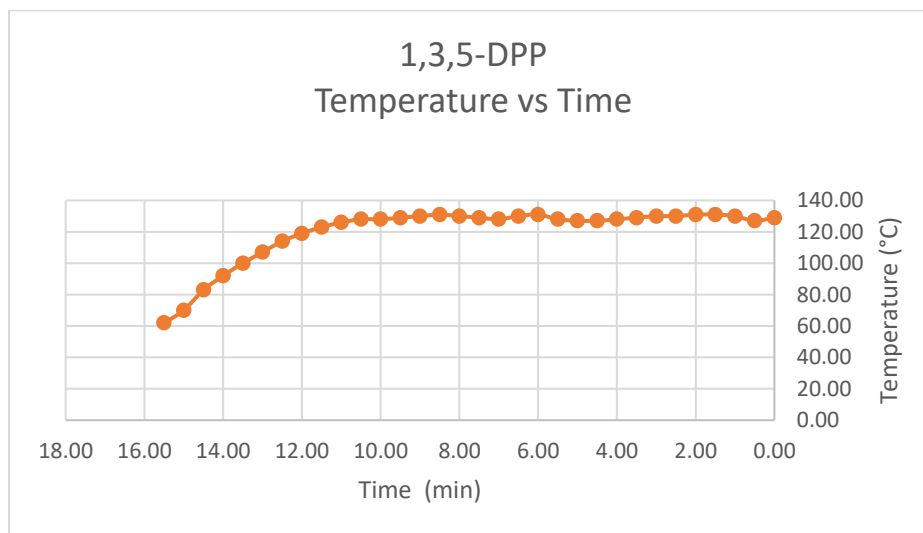
Figure 12: Temperature vs Time Profile for 1,3,5-DPP.
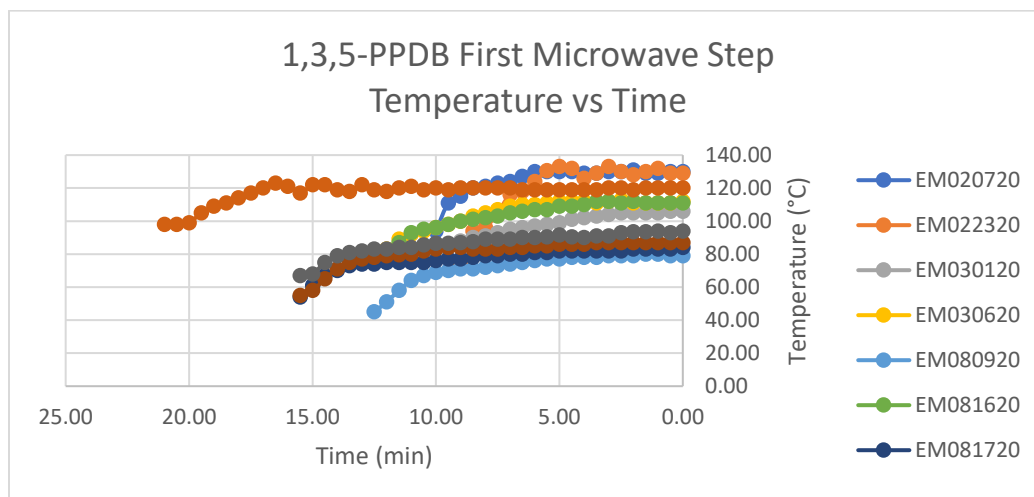
Figure 13: Microwave 1 Temperature vs Time Profile for 1,3,5-PPDB.

Figure 14 represents the second heating and should be noted that samples EM030620 and EM082720 charred during the second microwave step and had to be stopped sooner than intended. These samples will not be discussed as they are unknown chemically once the charing has taken place. The original experimental design changed due to the sensitivity of the reaction after the addition of benzoic acid.
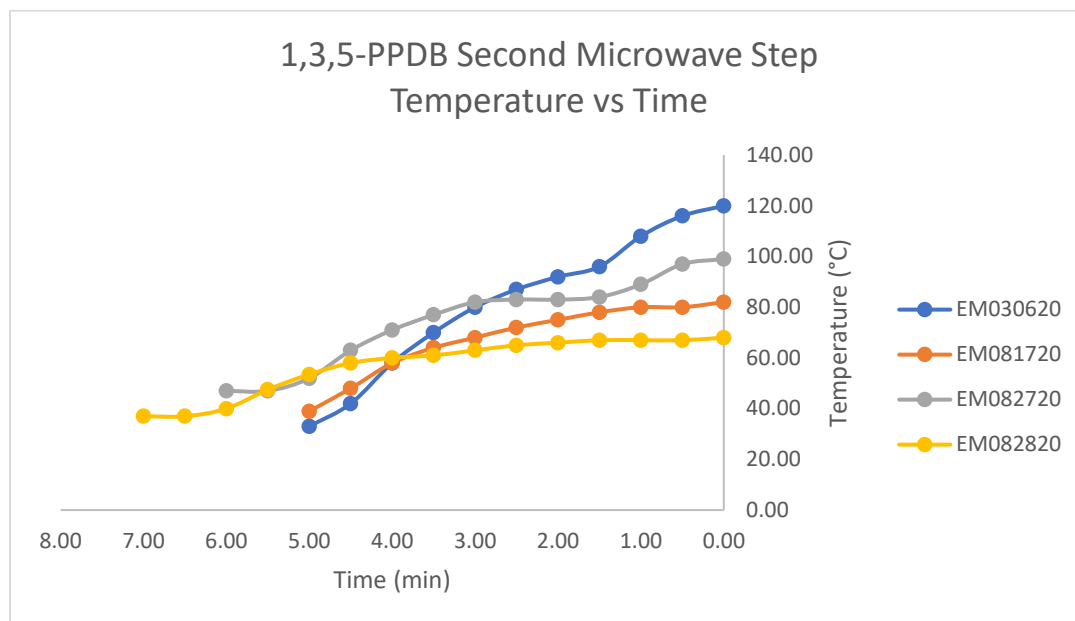
Figure 14: Microwave 2 Temperature vs Time Profile for 1,3,5-PPDB.

Figure 15 is the temperature vs time for the first microwave-assisted step for 1,3,5-PPTBDA. The first part of the synthesis was identical to the synthesis of 1,3,5-PPDB, therefore; more data had been previously established on what reaction times did not yield a completed reaction. Figure 15 is a plotted graph where the data was manually recorded every thirty seconds.
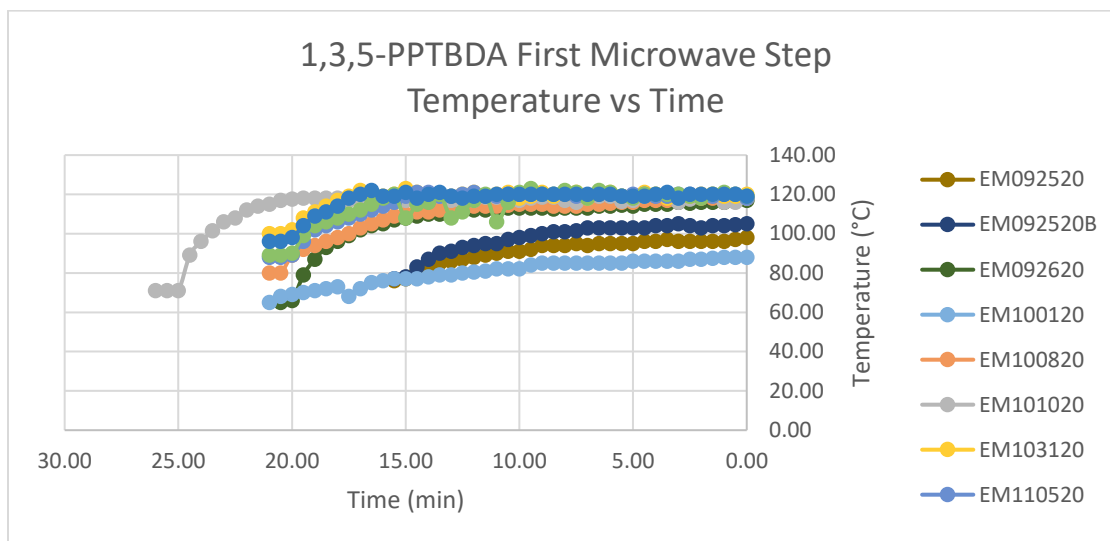
Figure 15: Microwave 1 Temperature vs Time Profile for 1,3,5-PPTBDA.

Figure 16 is an overview of the samples synthesized in the second microwave assisted

heating. Note that fewer samples charred with the 1,3,5-PPTBDA synthesis and therefore

yielded more samples for analysis
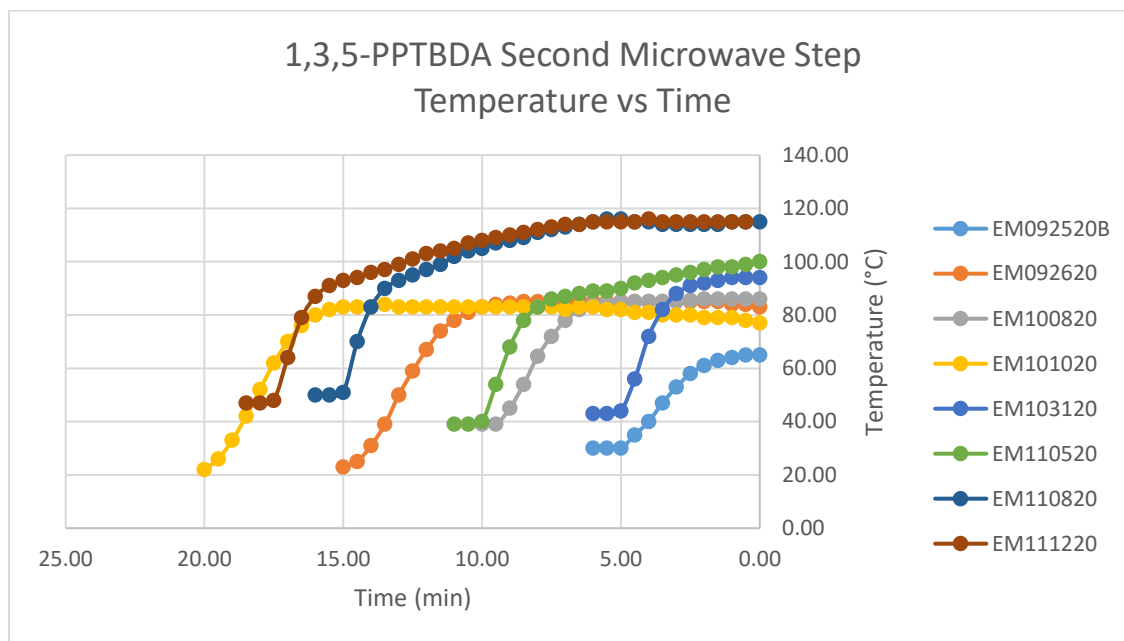
Figure 16: Microwave 2 Temperature vs Time Profile for 1,3,5-PPTBDA

C. FTIR

Each synthesized spectra was ATR and baseline corrected using the software algorithm in the Omnic software package before comparison. The synthesized products were compared to the starting materials and model compounds used for sample analysis. Figure 17 is a stacked plot of the starting materials used for all three products. Table 8 identifies the functional groups used for analysis in relation to the starting materials.

Table 8: FTIR spectroscopy of starting materials combined between each reaction.

FTIR Spectroscopy of Starting Materials				
	Carbonyl C=O(cm^{-1})	Aromatic C=C(cm^{-1})	P=O(cm^{-1})	Ester C-O(cm^{-1})
TMA	1696	1608,1454	-	-
DPCP	-	1588, 1488	1302	-
PDCP	-	1600,1587	1303	-
Benzoic Acid	1682	1600, 1583	-	-
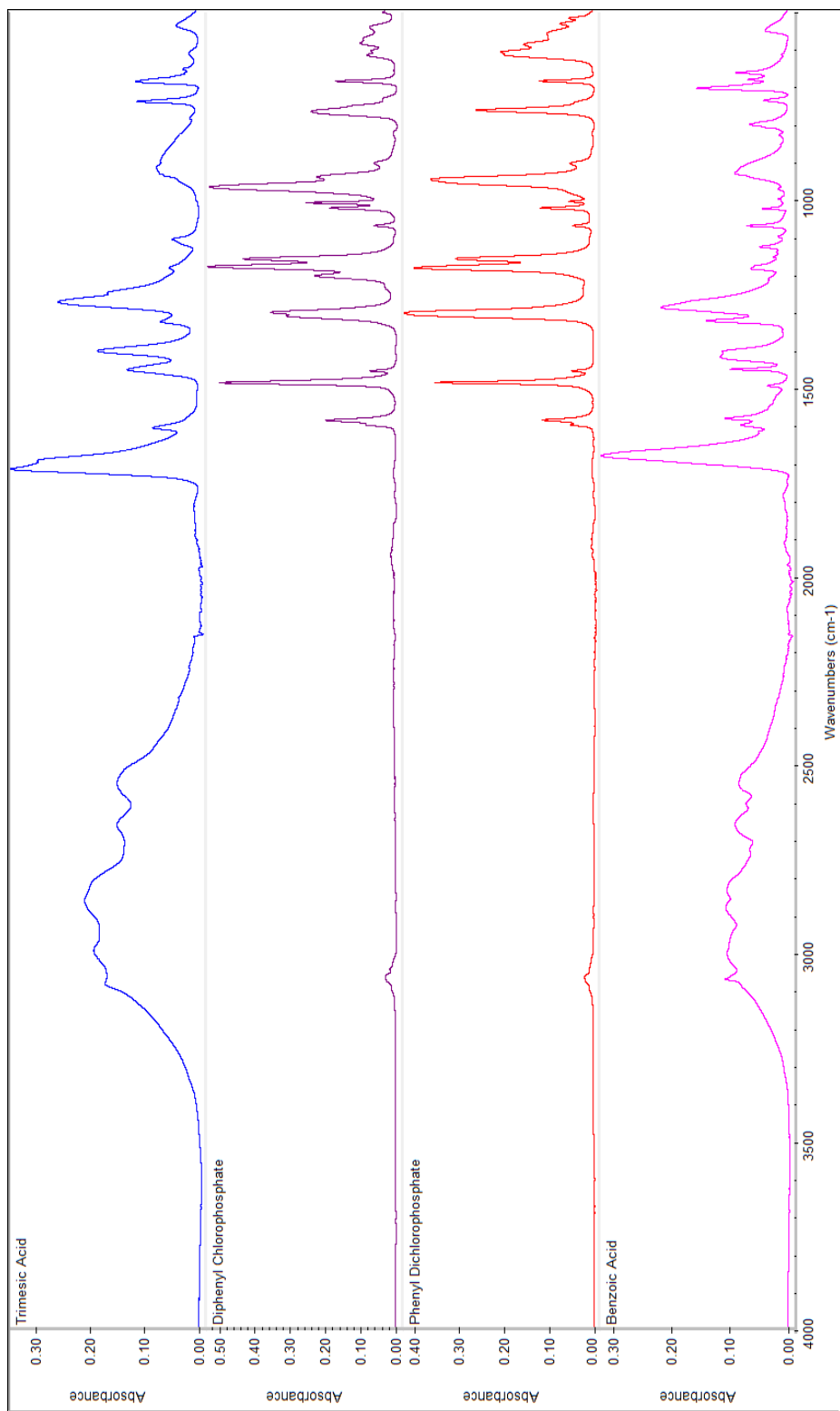
Figure 17: FTIR stacked spectroscopy of trimesic acid, diphenyl chlorophosphite, phenyl dichlorophosphate, and benzoic acid.

Figures 18 and 19 are the model compounds stacked plots for reference. Table 9

(below) notes the observed functional groups of the model compounds for this study. The

model compounds were for identifying possible by-products as well as for comparing the

possible substitution associated with the final products.

Table 9: FTIR spectroscopy of model compounds.

FTIR Spectroscopy of Model Compounds				
	Carbonyl C=O(cm^{-1})	Aromatic C=C(cm^{-1})	P=O(cm^{-1})	Ester C-O(cm^{-1})
1,3,5-benzenetricarbonyl Trichloride	1753	1594, 1433	-	-
Diethyl 1,3,5-benzenetricarboxylate	1739, 1683	1609, 1465	-	1281, 1166
Triethyl 1,3,5-benzenetricarboxylate	1719	1604, 1471	-	1238, 1023
Phenol	-	1595, 1532, 1499	-	-
Diphenyl Phosphate	-	1586, 1485	1269, 1182	-
Triphenyl Phosphate	-	1587, 1483	1293, 1174	-
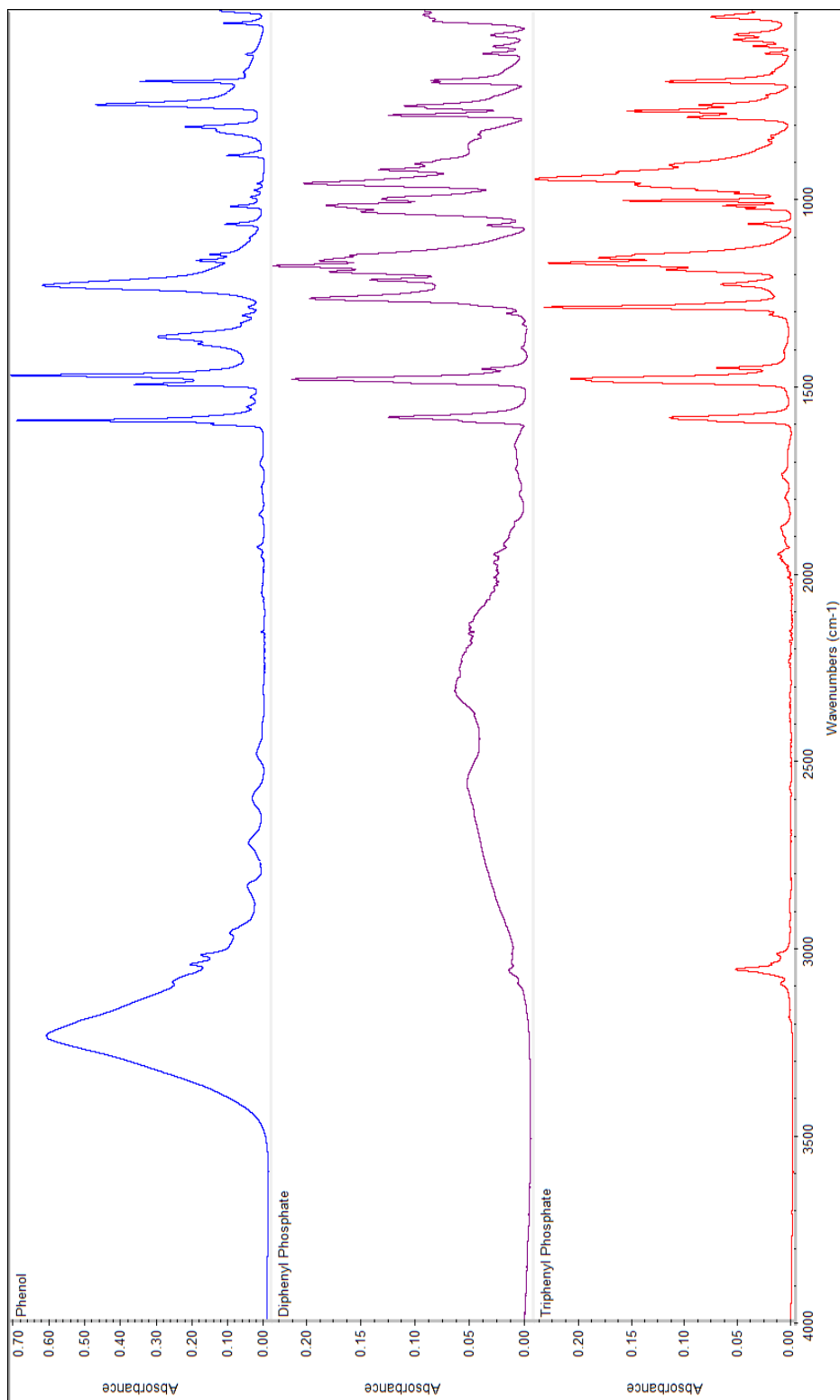
Figure 18: FTIR stacked spectroscopy of model compounds phenol, diphenyl phosphate, and triphenyl phosphate.
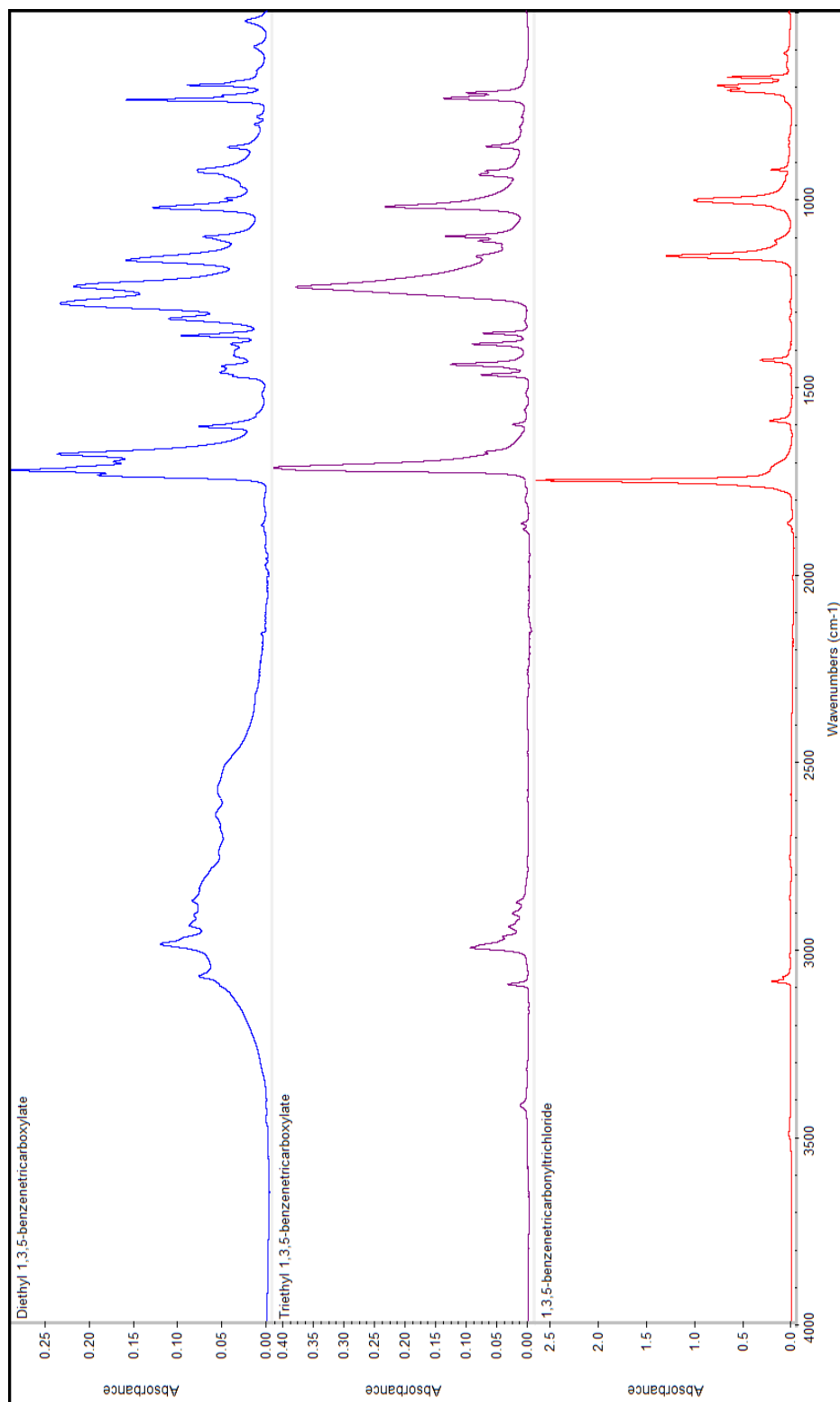
Figure 19: FTIR stacked spectroscopy of model compounds.

Figure 21-Figure 24 all examine sample EM100419 (1,3,5-DPP). The overlays have been adjusted to view the 1850-1550 cm^{-1}, 1550-1100 cm^{-1}, and 800-600 cm^{-1} range more closely. Figure 20 is an example of how samples were chosen after the first microwave-assisted heating. EM100419 was the sample chosen to represent 1,3,5-DPP in this study and the other two samples are examples of incomplete reactions of 1,3,5-DPP. This reasoning was based on the presence of multiple carbonyl absorption bands that can be seen zoomed in on Figure 22. The 1,3,5-DPP should only have one carbonyl peak. The other indicator on whether the reaction had reached completion was the absence of the hydrogen bonding stretch from the carboxylic acid functionality, which was provided by trimesic acid. The broad and strong peak from trimesic acid would stretch from approximately 3100-2100cm^{-1}.[31]

The unwashed sample of EM100419 and the washed final product of EM100419 have different carbonyl regions. The unwashed sample had one carbonyl at 1682 cm^{-1}, while the MeOH: DI washed sample had two peaks at 1738 cm^{-1} and 1657 cm^{-1}. Figure 23 showed that EM100419 contained an aromatic and phosphate region. Figure 22 also had an aromatic region around 1590cm^{-1}. The phosphate band (P=O) is broad and strong for sample EM100419. Figure 24 shows that EM100419 shares similarities to diphenyl phosphate and triphenyl phosphate around 800-740cm^{-1}. Values listed were combined for comparison in Table 10.

Based off the model compounds, the washed sample of EM100419 was a mixture of multiple products. EM100419 shared common peaks with the diphenyl and triphenyl

phosphate model compounds and the P=O band was broad with this sample, indicating

different phosphorus based species.

Table 10: FTIR spectroscopy of 1,3,5-DPP.

FTIR Spectroscopy of 1,3,5-DPP and 1,3,5-PPDB Samples				
Sample Name	Carbonyl C=O (cm^{-1})	Aromatic C=O (cm^{-1})	P=O (cm^{-1})	Ester C-O(cm^{-1})
EM100419 Unclean	1758	1590,1489	1302, 1188	1013
EM100419 Clean	1745, 1696	1590, 1487	1296, 1187	1010
EM031719	1738,1725	1594, 1488	1221, 1189	970
EM031619	1764	1590, 1489	1270, 1185	975
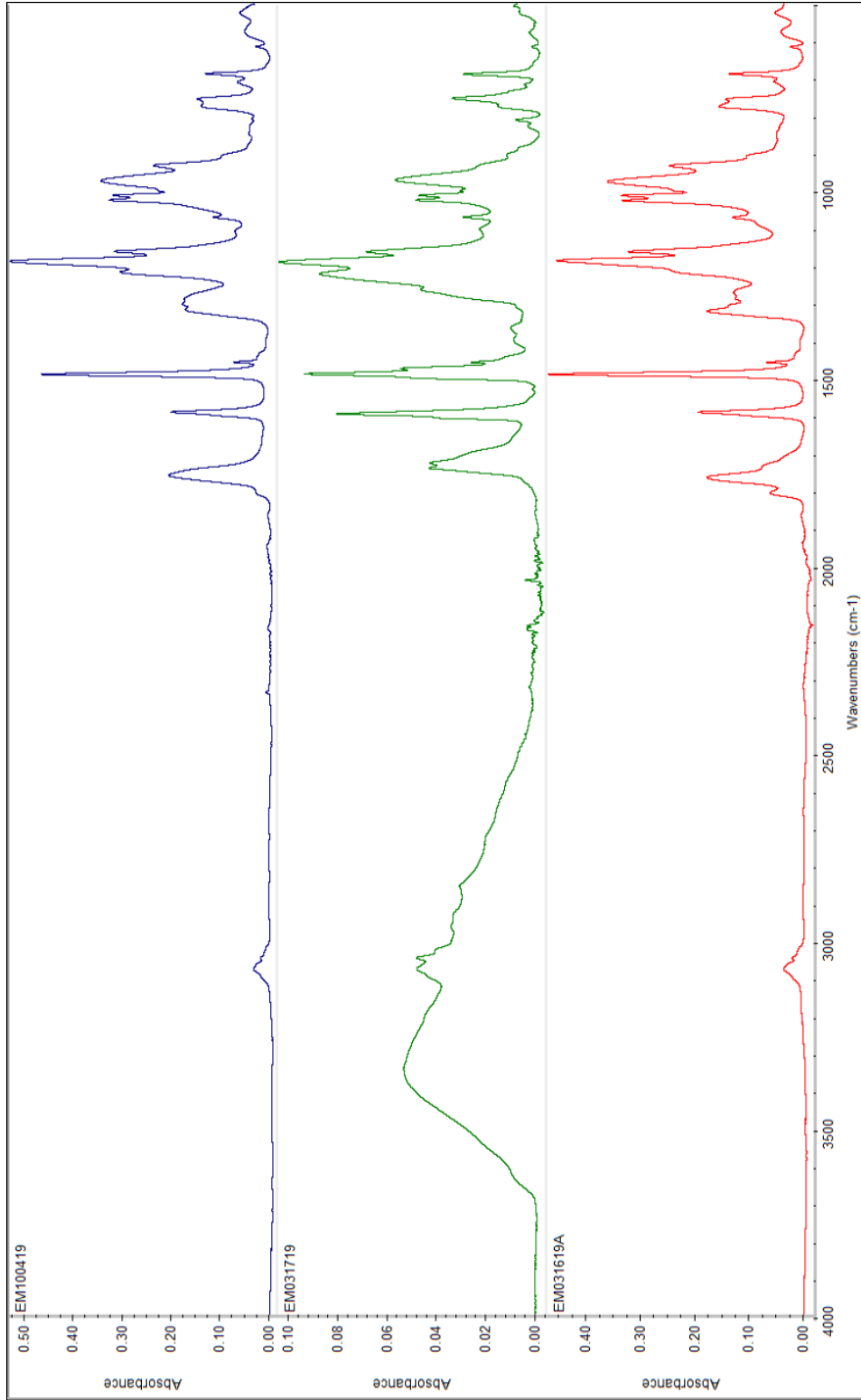
Figure 20: FTIR stacked spectroscopy of EM100419 with samples that did not completely react.

49
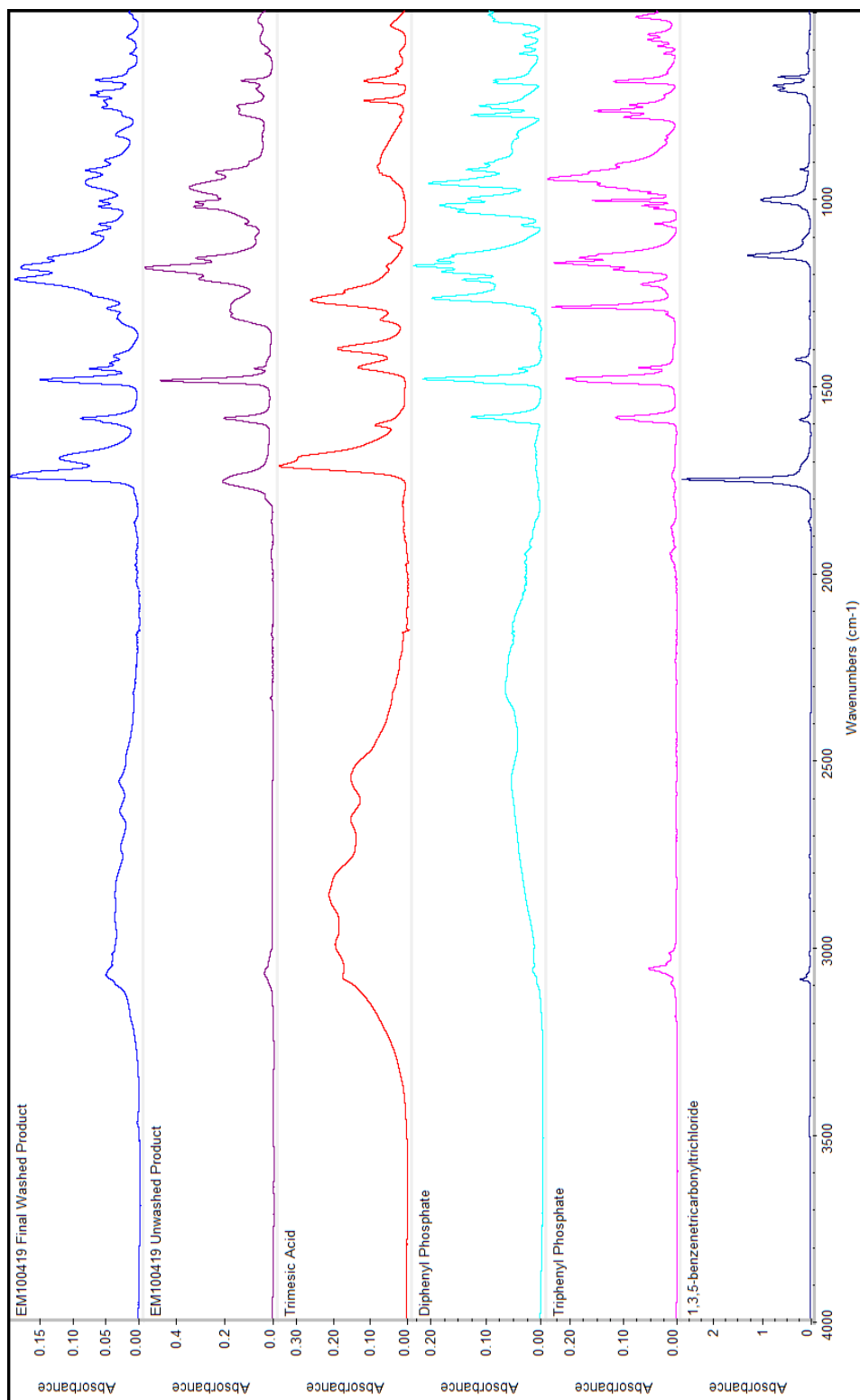
Figure 21: FTIR stacked spectroscopy of Sample EM100419 in reference to model compounds and trimesic acid.
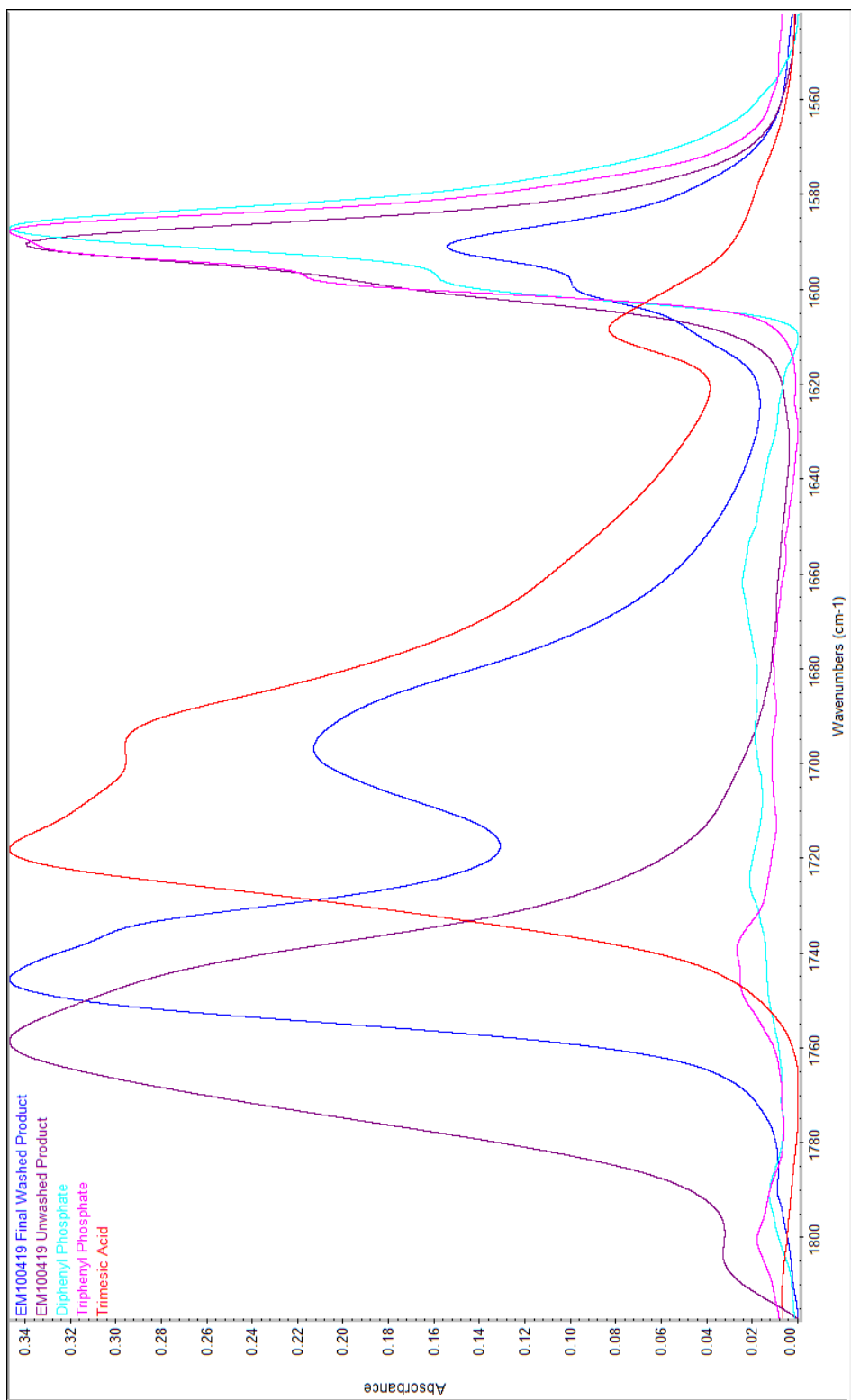
Figure 22: FTIR overlay of spectroscopy between 1850 and 1550 cm^{-1} of sample EM100419, model compounds, and trimesic acid.
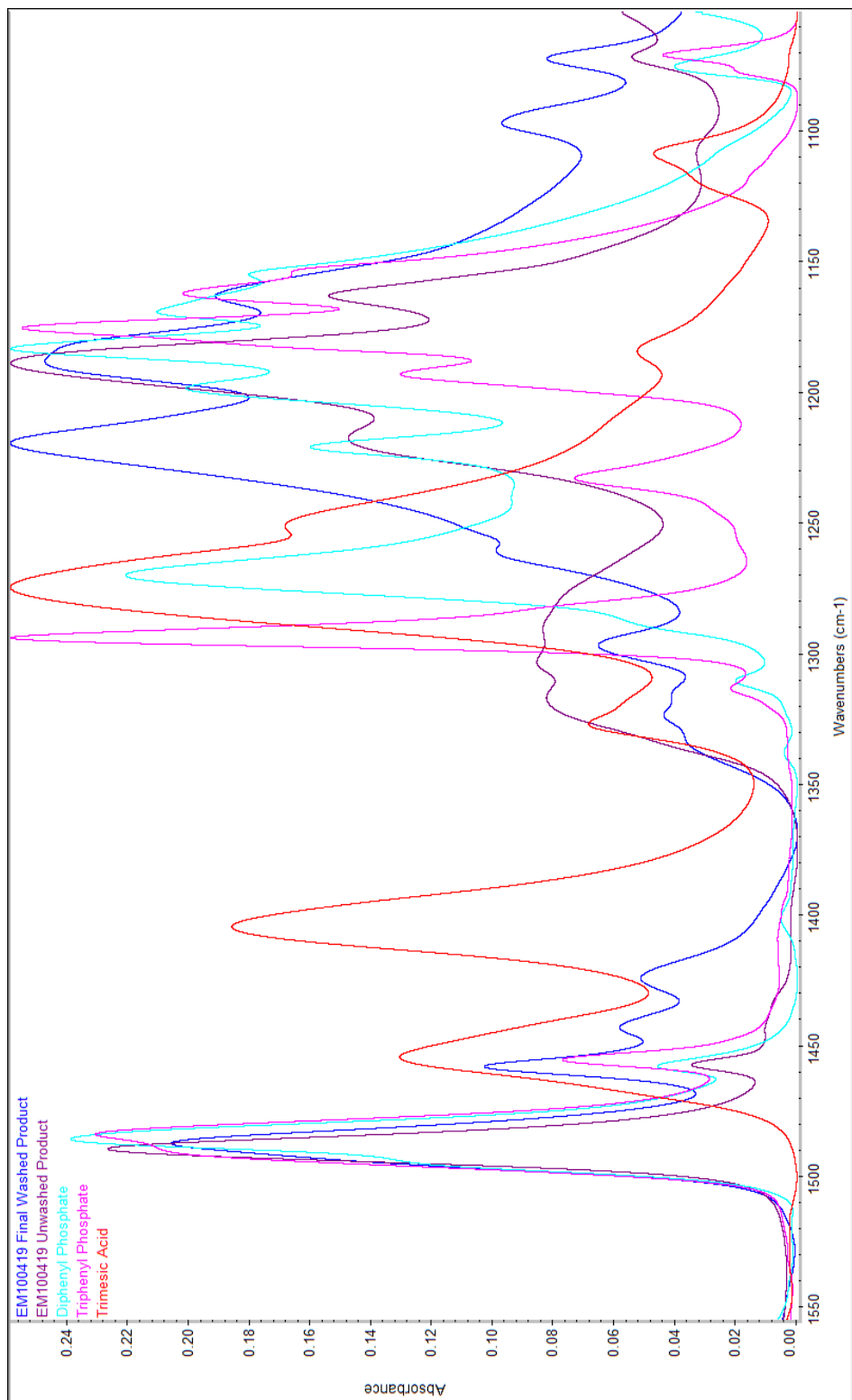
Figure 23: FTIR overlay spectroscopy between 1550 and 1100cm^{-1} of sample EM100419 ,trimesic acid and model compounds.
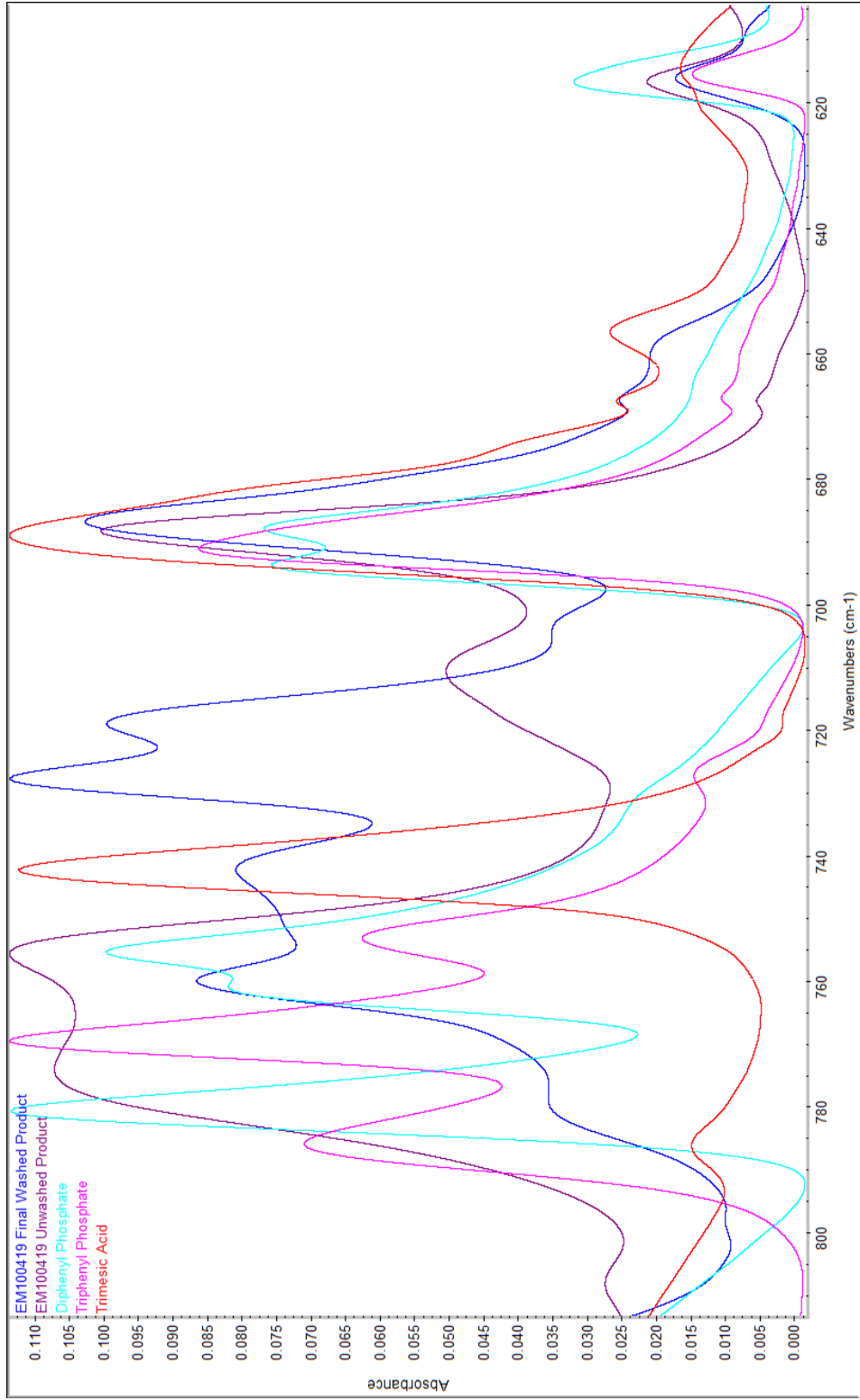
Figure 24: FTIR overlay of spectroscopy between 800-600cm^{-1} of sample EM100419, trimesic acid and model compounds.

Table 11: FTIR spectroscopy of 1,3,5-PPDB.

FTIR Spectroscopy of 1,3,5-PPDB Sample				
Sample Name	Carbonyl C=O (cm^{-1})	Aromatic C=O (cm^{-1})	P=O (cm^{-1})	Ester C-O(cm^{-1})
EM082820 Vial 2	1738, 1657	1597, 1486	1263, 1193	1102, 1000
TMA	1696	1608,1454	-	-
Benzoic Acid	1682	1600, 1583	-	-
Diethyl 1,3,5-benzenetricarboxylate	1739, 1683	1609, 1465	-	1281, 1166
Triethyl 1,3,5-benzenetricarboxylate	1719	1604, 1471	-	1238, 1023

Figure 25 is a stacked plot of EM082820, trimesic acid, benzoic acid, diethyl 1,3,5-benzenetricarboxylate, and triethyl 1,3,5-benzenetricarboxylate. The overlays for Figures 26-28 have been adjusted to view the 1850-1550 cm^{-1}, 1550-1100 cm^{-1}, and 800-600 cm^{-1} regions more closely. In Figure 26, sample EM082820 had two carbonyl peaks at 1738 cm^{-1} and 1657 cm^{-1}, which were similar to the carbonyl peaks of diethyl 1,3,5-tricarboxylate at 1739 cm^{-1} and 1683 cm^{-1}. The hydrogen bonding of the carboxylic acid provided by trimesic acid appears to be absent between 3100-2100cm^{-1}.[33] Figure 27 is a zoomed in region between 800-600 cm^{-1} for comparison. The phosphate band can be seen in Figure 28 stretching between 1190-1263 cm^{-1} EM082820 appears to have reacted completely regarding functional groups present vs what would be seen if trimesic acid were still present.

54
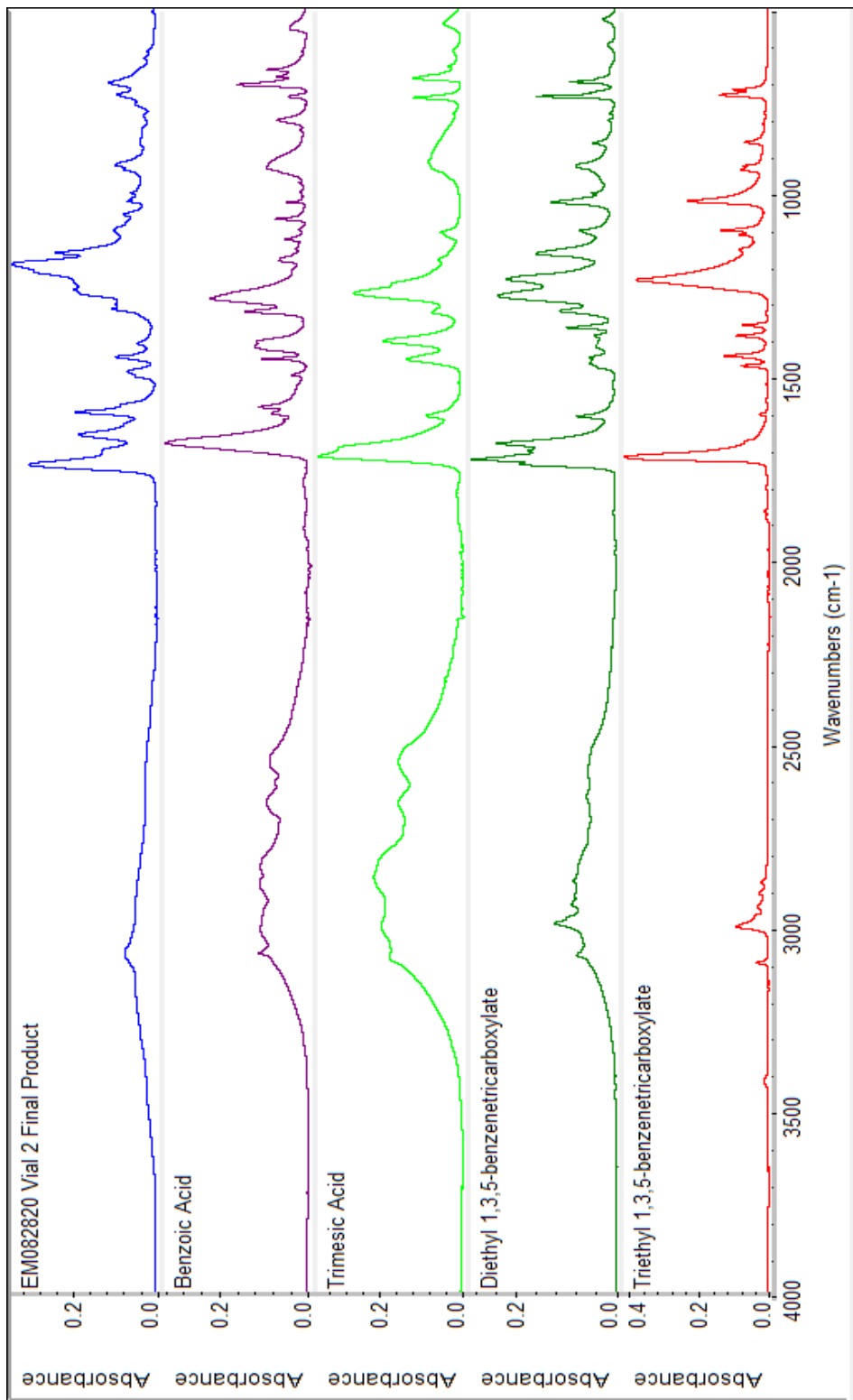
Figure 25: FTIR stacked spectroscopy of sample EM082820 Vial 2, starting materials, and model compounds.
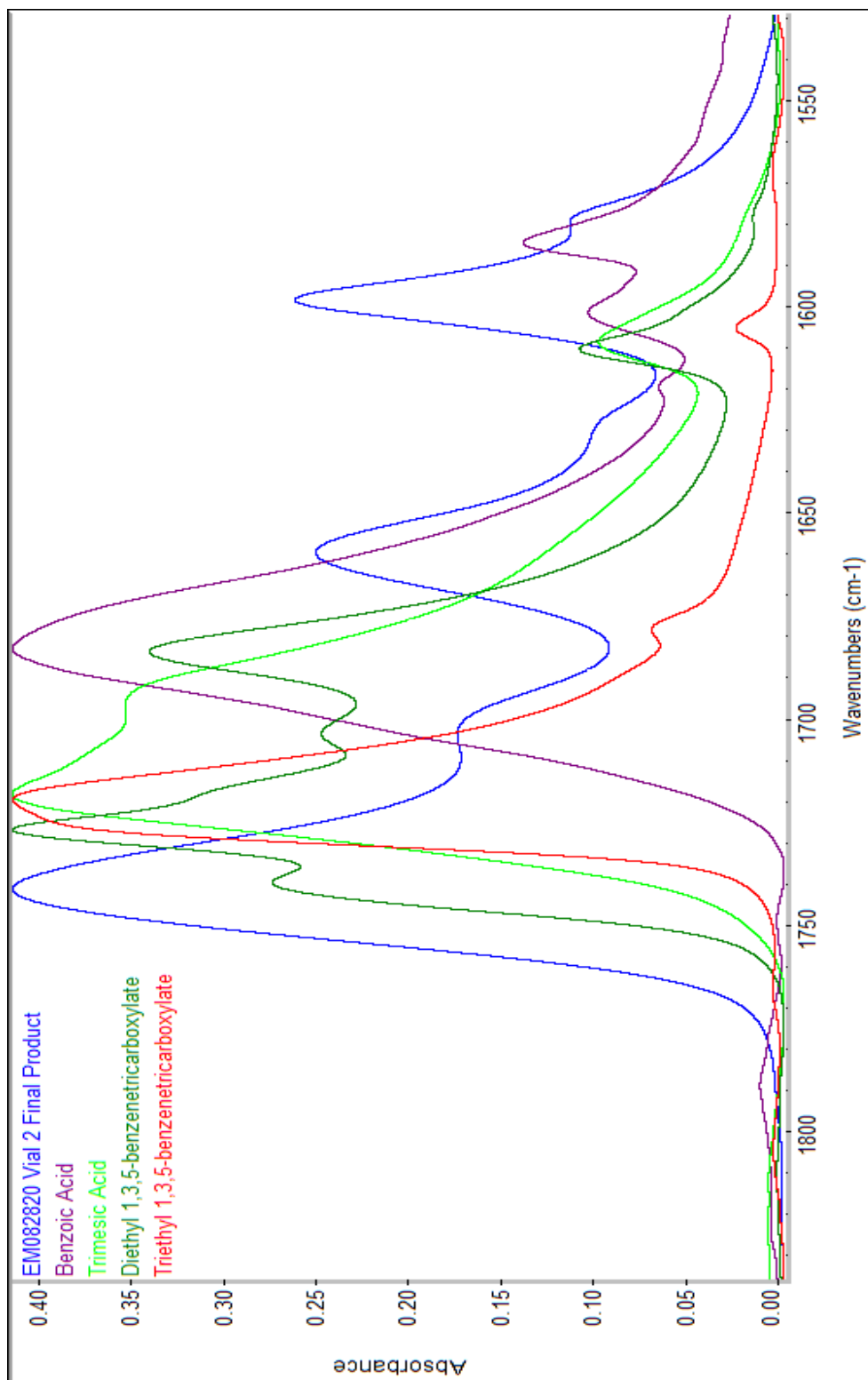
Figure 26: FTIR overlay plot between 1850-1550 cm^{-1} spectroscopy of sample EM082820 Vial 2, starting materials, and model compounds.
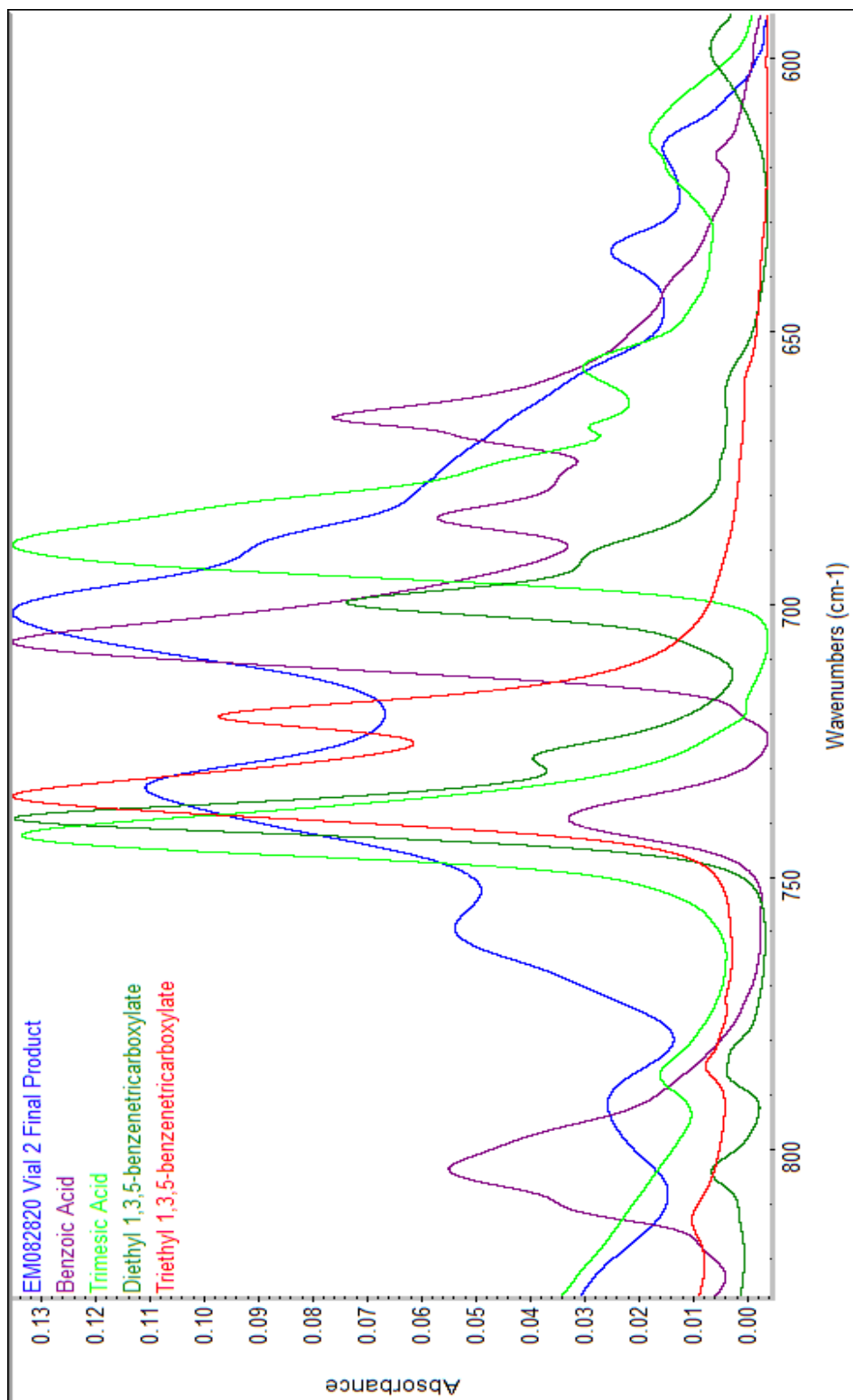
Figure 27: FTIR overlay plot between 850-600 cm^{-1} spectroscopy of sample EM082820 Vial 2, starting materials, and model compounds.
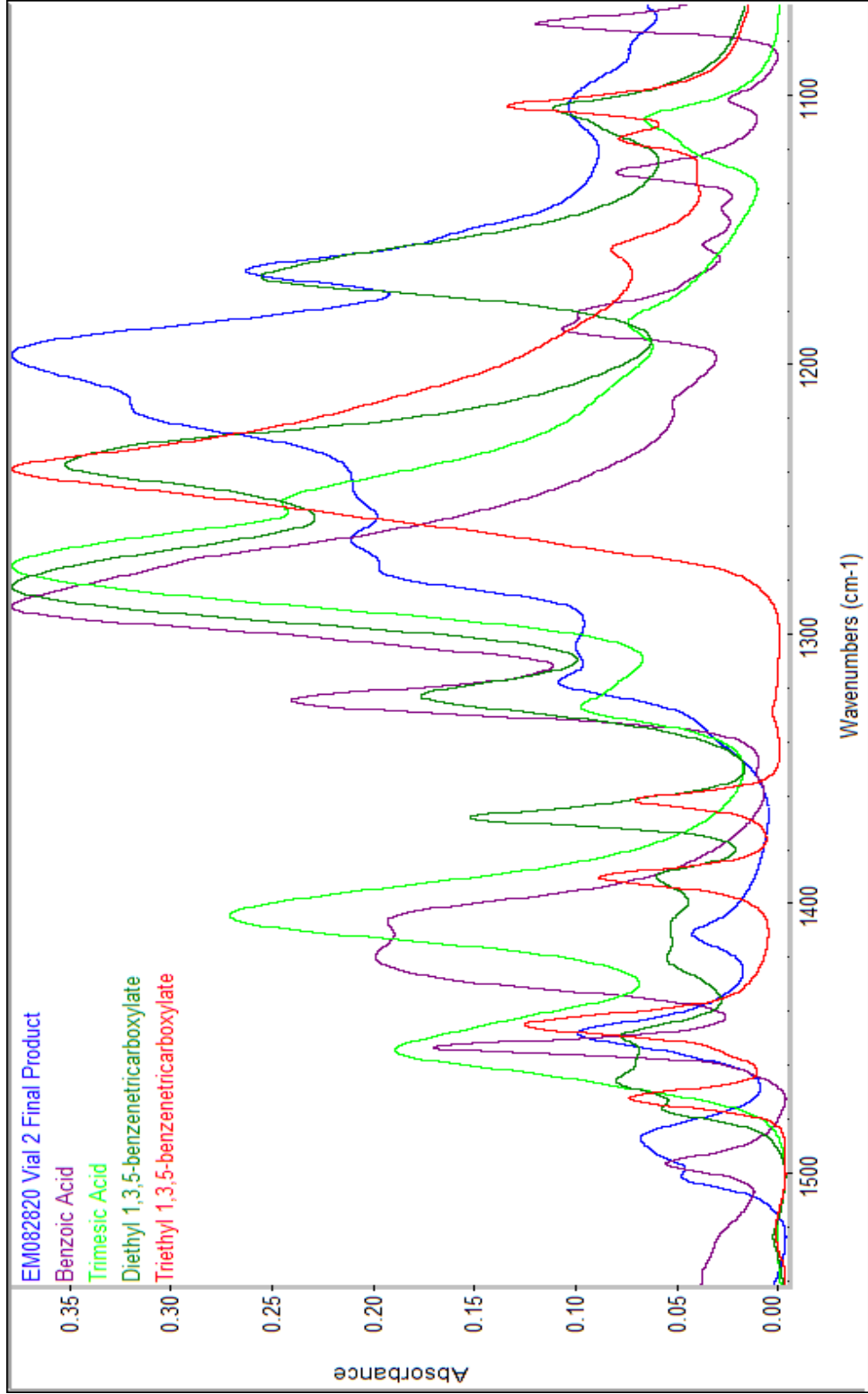
Figure 28: FTIR overlay plot between 1550-1100 cm^{-1} spectroscopy of sample EM082820 Vial 2, starting materials, and model compounds.

Figures 29-36 are soluble and insoluble products from the synthesis of 1,3,5-PPTBDA. The samples Vial 1 (Table 10) represent the samples soluble in DMSO and the Vial 2 samples (Table 11) represents the samples insoluble in DMSO that were seperated before the purification step due to slight difference in appearances. The soluble samples and insoluble samples were analyzed and compared seperately. Figure 29-32 are soluble samples and Figure 33-36 are the insoluble samples.

Figure 29 is a stacked plot of multiple samples of 1,3,5-PPTBDA and trimesic acid. Between $3400cm^{-1}$ and $2100cm^{-1}$, the presence of hydrogen bonding from the carboxylic acid hydroxyl group that is provided by trimesic acid was observed and was a good indicator since the final product was expected to have carboxylic acid ends. At $3500cm^{-1}$, a band appears in samples EM092520B and EM103120 indicating that non-hydrogen bonding was present from the presence of free hydroxyl groups.[31] Figure 30 is the carbonyl region where EM111220 appears to have a broad multipeak stretch that indicated that there were more types of esters present in this sample. The other samples in Figure 30 appear to have similar profiles. Figure 31 is the phosphate region between $1200-1160cm^{-1}$.[31] Sample EM111220 has a broad phosphate region in comparison to the other samples. Each sample has a phosphate band, but sample EM111220 is an outlier, which was also observed in Figure 32.

The analysis of these samples were observed to have similarities to the trimesic acid. Of course, these samples were capped with carboxylic acid groups and therefore it was

expected to observe these resemblances. The P=O bands appeared less broad with some

of these samples as well. Peak values may be observed in Table 11.

Table 12: FTIR Spectroscopy of 1,3,5-PPTBDA soluble samples.

FTIR Spectroscopy of 1,3,5-PPTBDA Soluble Samples				
Sample Name	Carbonyl C=O (cm^{-1})	Aromatic C=O (cm^{-1})	P=O (cm^{-1})	Ester C-O(cm^{-1})
EM110520 Vial 1	1715	1607, 1453	1272, 1184	1107
EM103120 Vial 1	1724, 1693	1610, 1452	1277, 1208	1109
EM111220 Vial 1	1731, 1702, 1666	1599, 1486	1216, 1163	1104
EM092520B Vial 1	1700	1608, 1453	1276, 1183	1108
TMA	1696	1608,1454	-	-
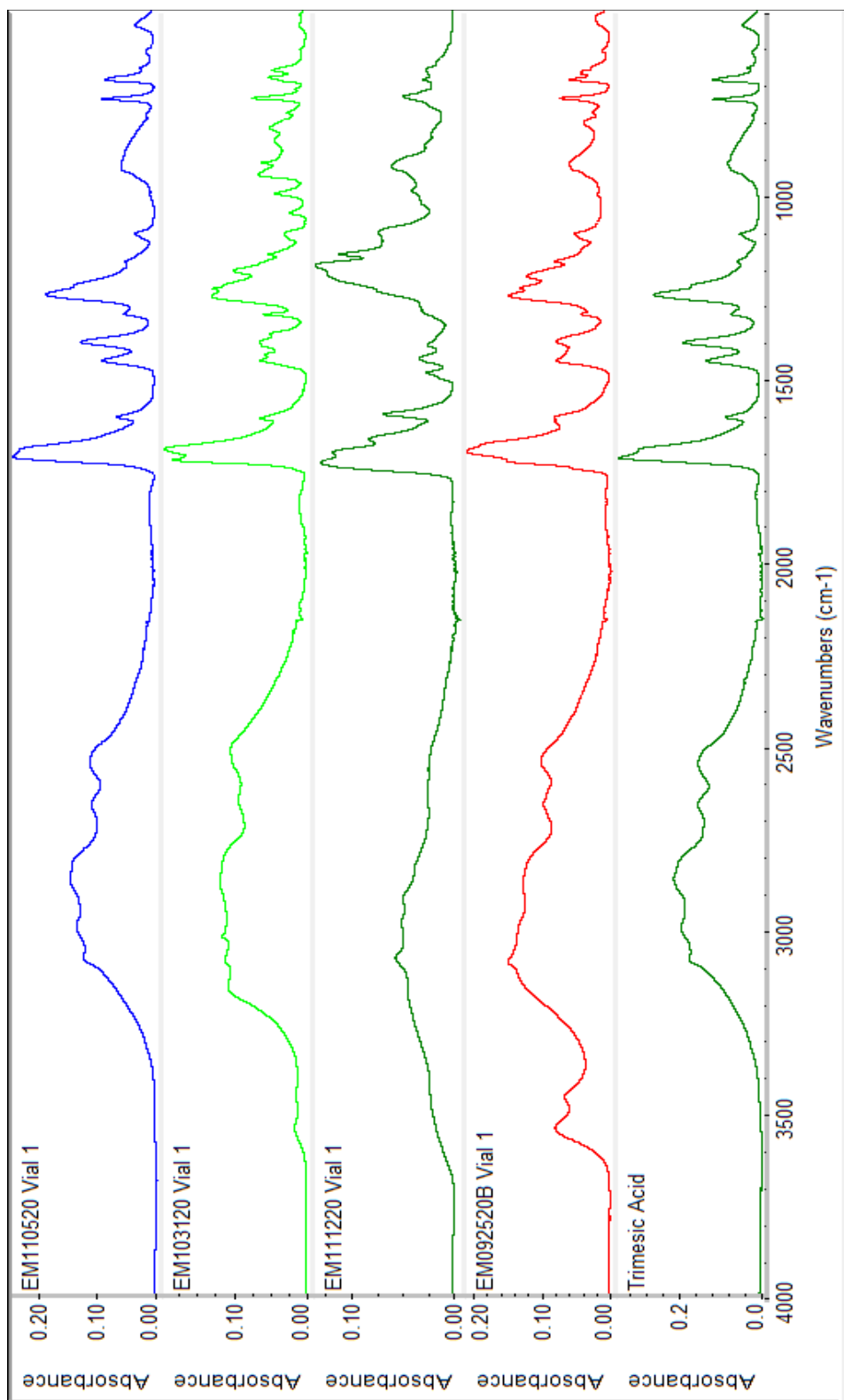
Figure 29: FTIR stacked spectroscopy of soluble samples of 1,3,5-PPTBDA and trimesic acid.

60
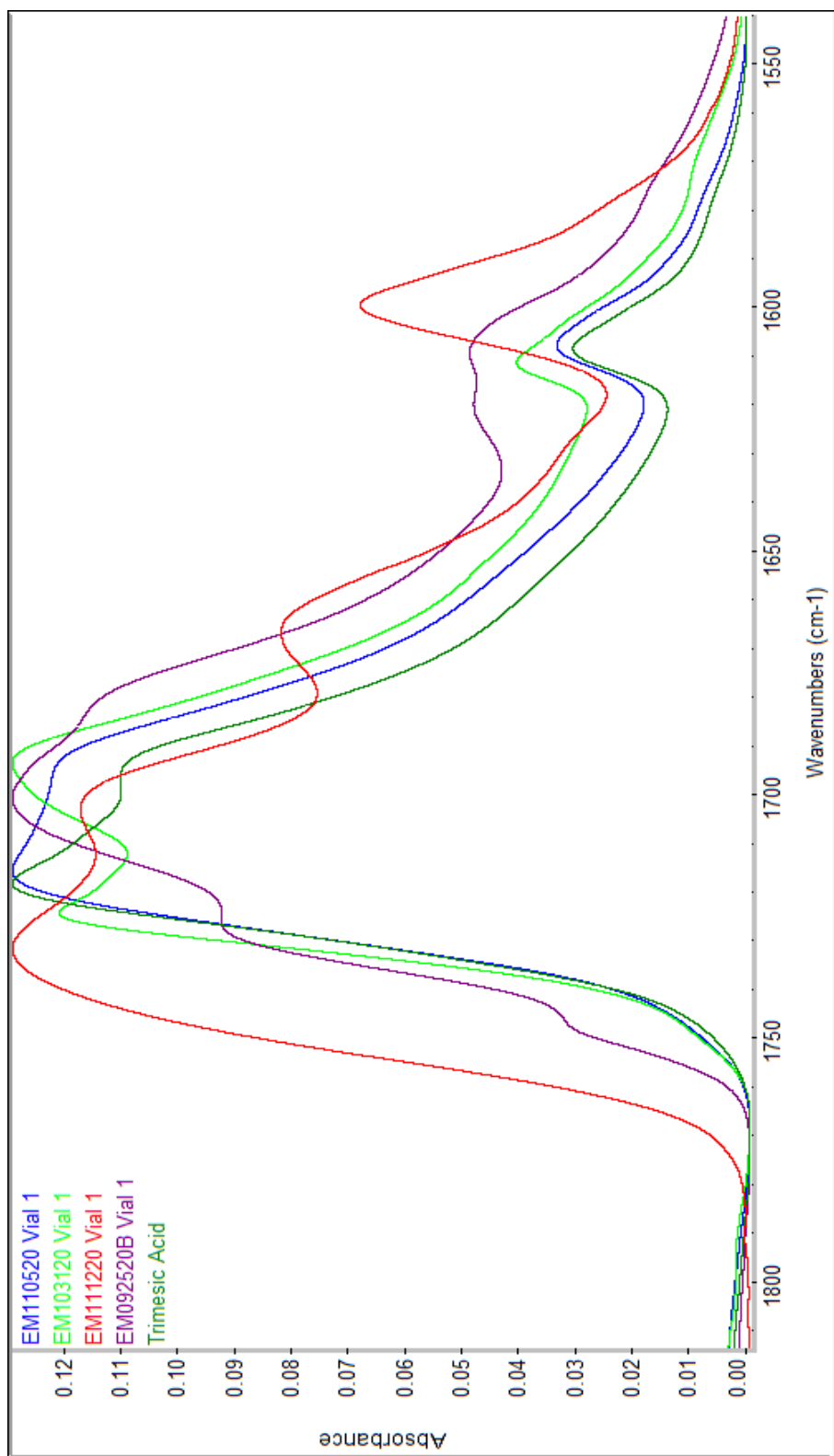
Figure 30: FTIR overlay between 1800 and 1550cm^{-1} spectroscopy of soluble samples of 1,3,5-PPTBDA and trimesic acid.
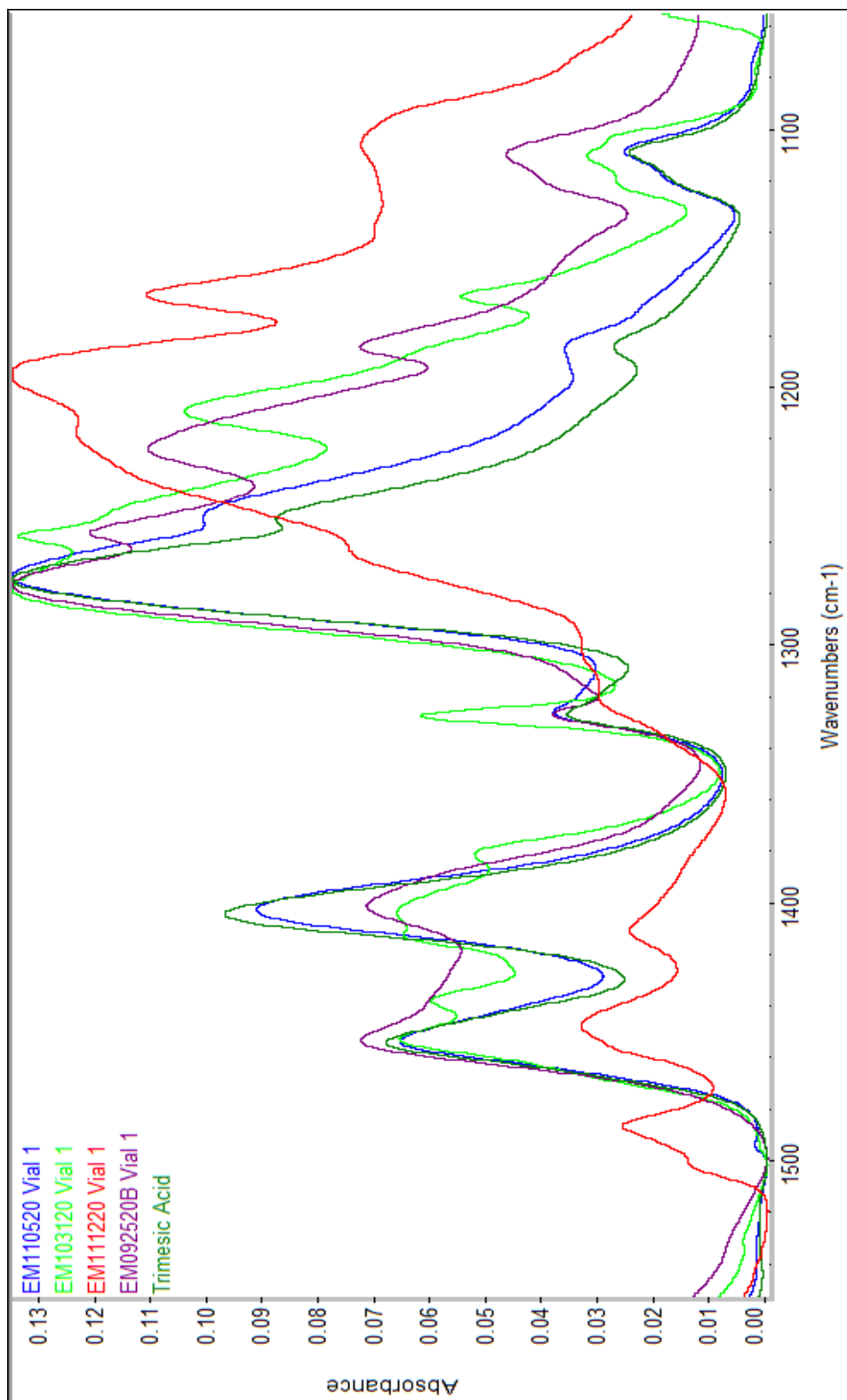
Figure 31: FTIR overlay of spectroscopy between 1550 and 1100cm^{-1} of soluble samples of 1,3,5-PPTBDA and trimesic acid.
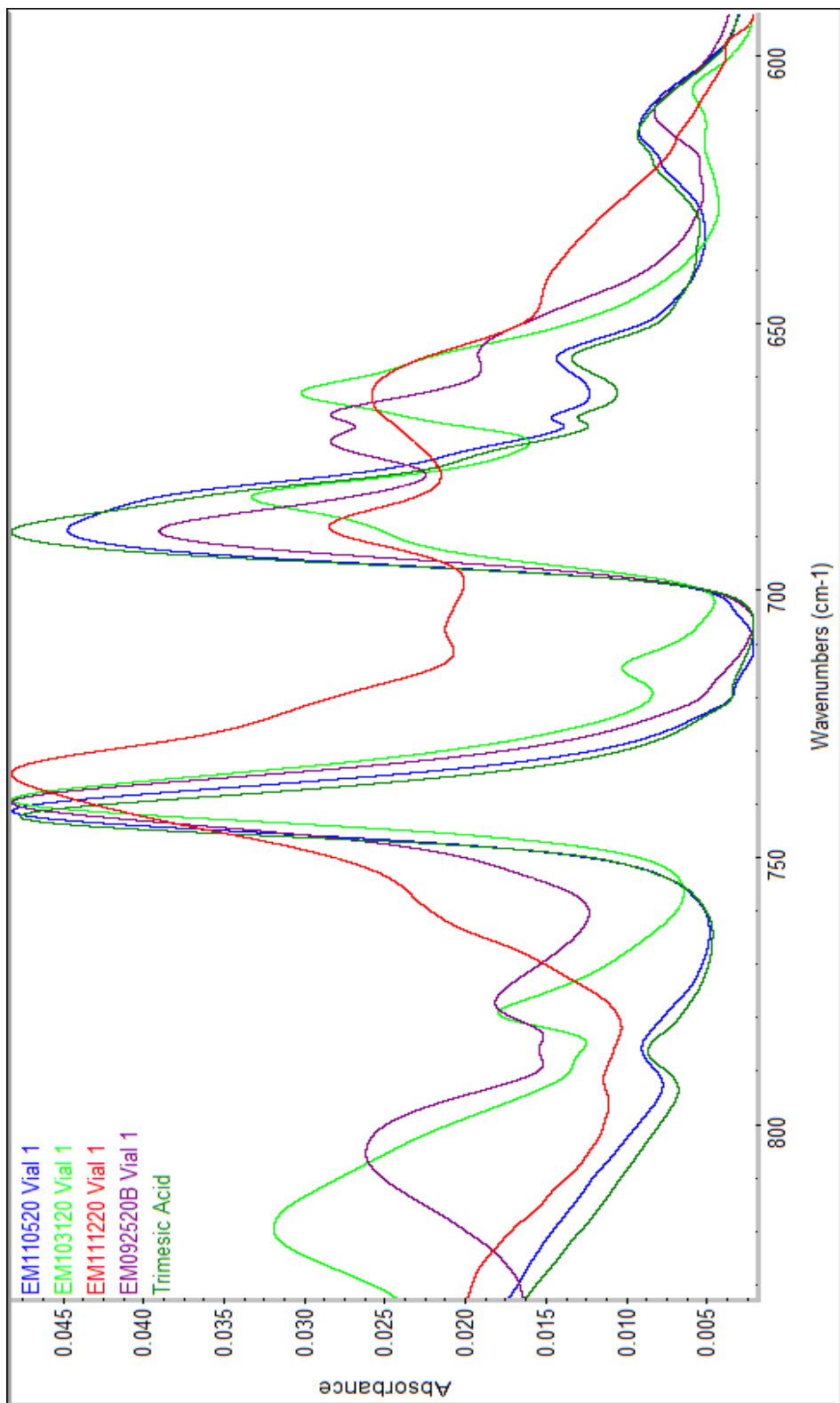
Figure 32: FTIR overlay of spectroscopy between 850 and 600cm^{-1} of soluble samples of 1,3,5-PPTBDA and trimesic acid.

The insoluble 1,3,5-PPTBDA samples in Figure 33 showed that the broad absorption functionality from the hydrogen-bonding from the carboxylic acid were present in the insoluble samples as well. Sample EM103120 had a broad band at 3500 cm^{-1} indicating non hydrogen bonding from free hydroxyl groups. Figure 34 is the carbonyl region where the samples all share a similar carbonyl peak around 1720 cm^{-1} and samples EM103120 and EM092520B both have peaks at 1693cm^{-1}. Trimesic acid has a carbonyl at 1696 cm^{-1} indicating a strong similarity to EM103120 and EM092520B.

Figure 35 is the phosphate region and part of the aromatic region. Each sample appeared to have a phosphate band and aromatic indicators. Sample EM111220 indicated broad peaks and appeared to be an outlier from the other insoluble samples in Figure 36 between 800-600 cm^{-1}.

Table 13: FTIR Spectroscopy of 1,3,5-PPTBDA insoluble samples.

FTIR Spectroscopy of 1,3,5-PPTBDA Insoluble Samples				
Sample Name	**Carbonyl C=O (cm^{-1})**	**Aromatic C=O (cm^{-1})**	**P=O (cm^{-1})**	**Ester C-O(cm^{-1})**
EM110520 Vial 2	1718	1608, 1454	1273, 1236	1096
EM103120 Vial 2	1725, 1693	1611, 1436	1256, 1207	1101
EM111220 Vial 2	1733	1601, 1448	1236, 1165	1097
EM092520B Vial	1717, 1693	1608, 1453	1273, 1249	1106
TMA	1696	1608,1454	-	-
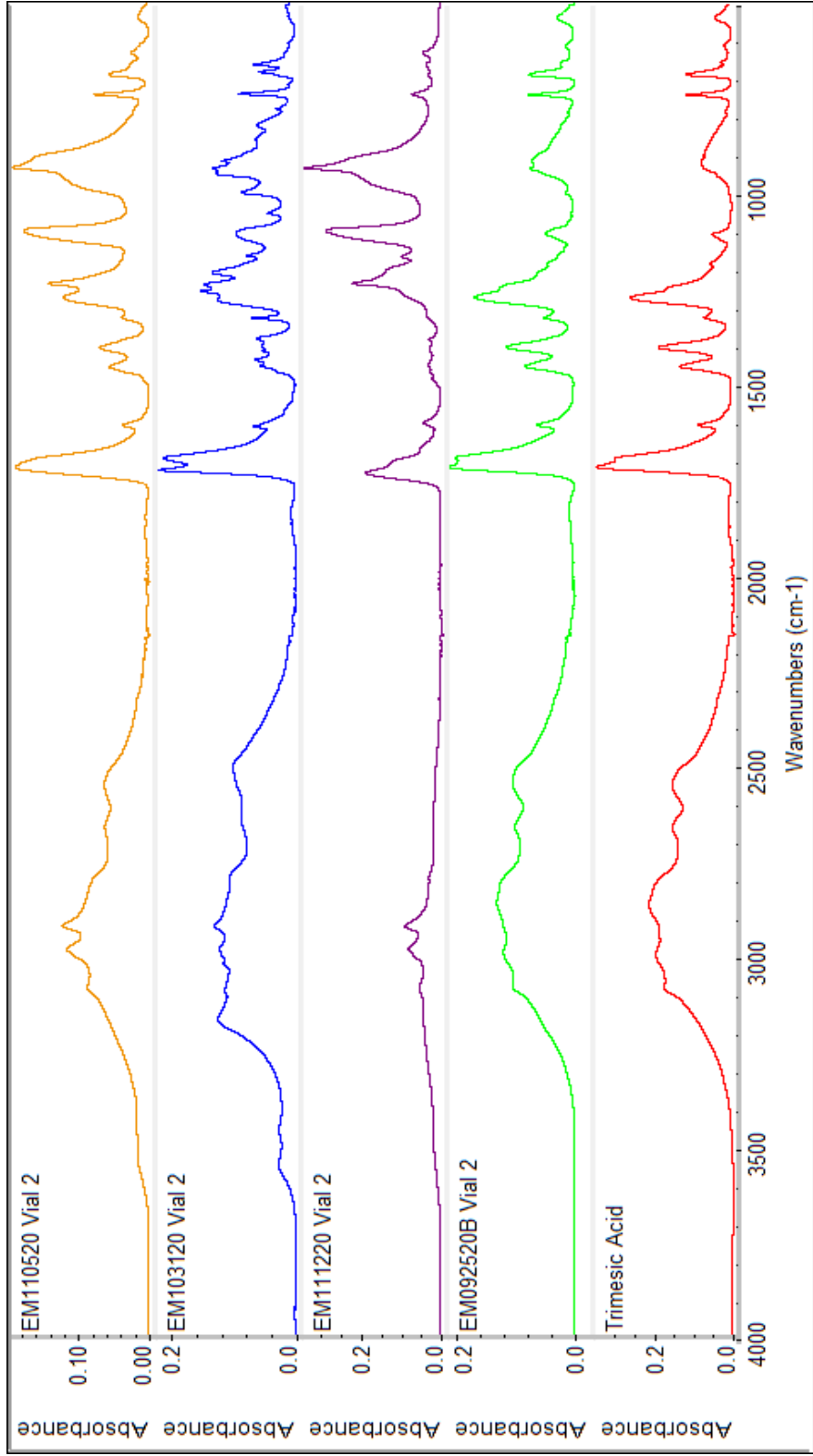
Figure 33: FTIR stacked spectroscopy of insoluble samples of 1,3,5-PPTBDA and trimesic acid.
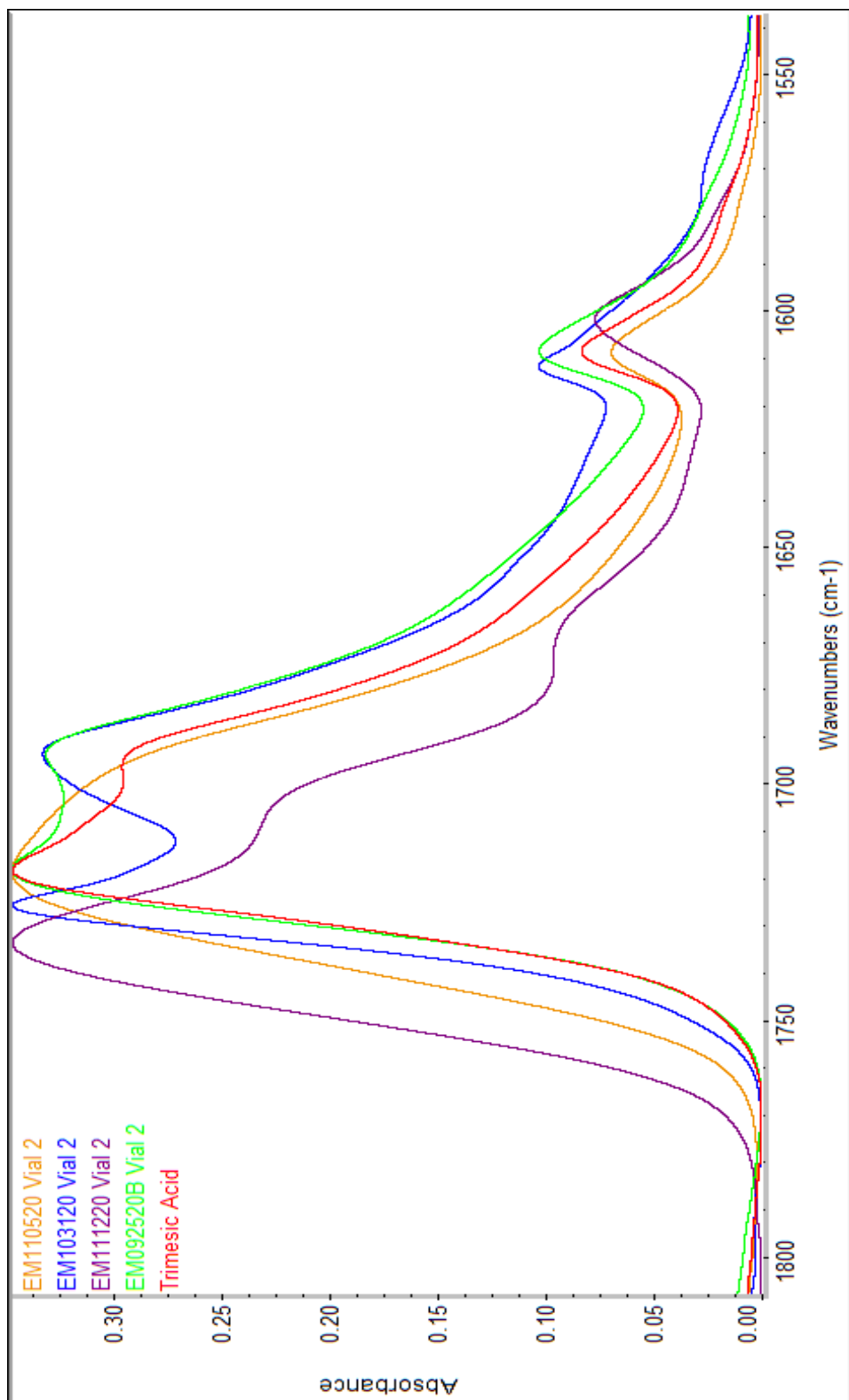
Figure 34: FTIR overlay of spectroscopy between 1800-1550cm^{-1} of insoluble samples of 1,3,5-PPTBDA and trimesic acid.
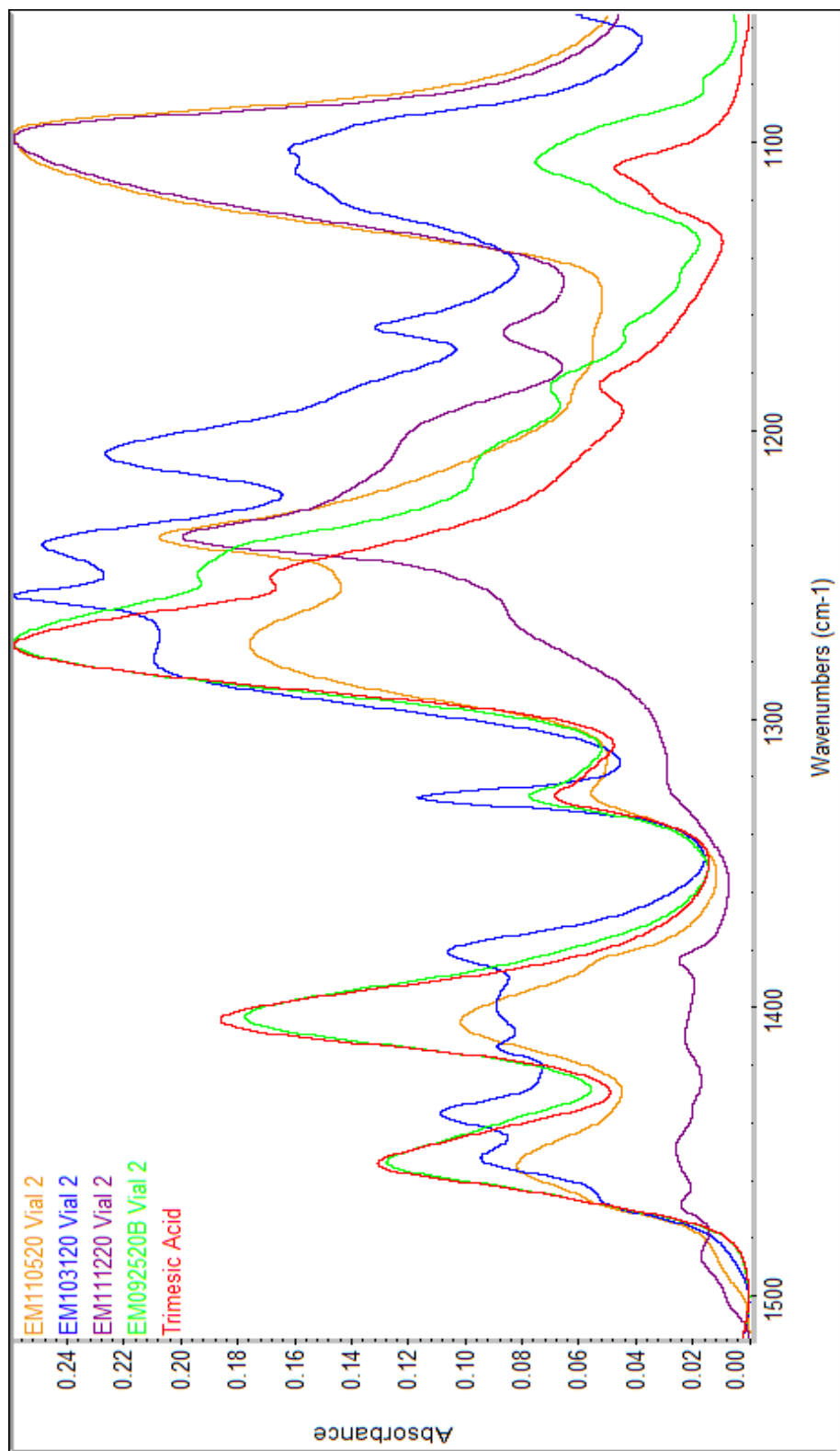
Figure 35: FTIR overlay of spectroscopy between 1500-1100cm^{-1} of insoluble samples of 1,3,5-PPTBDA and trimesic acid.
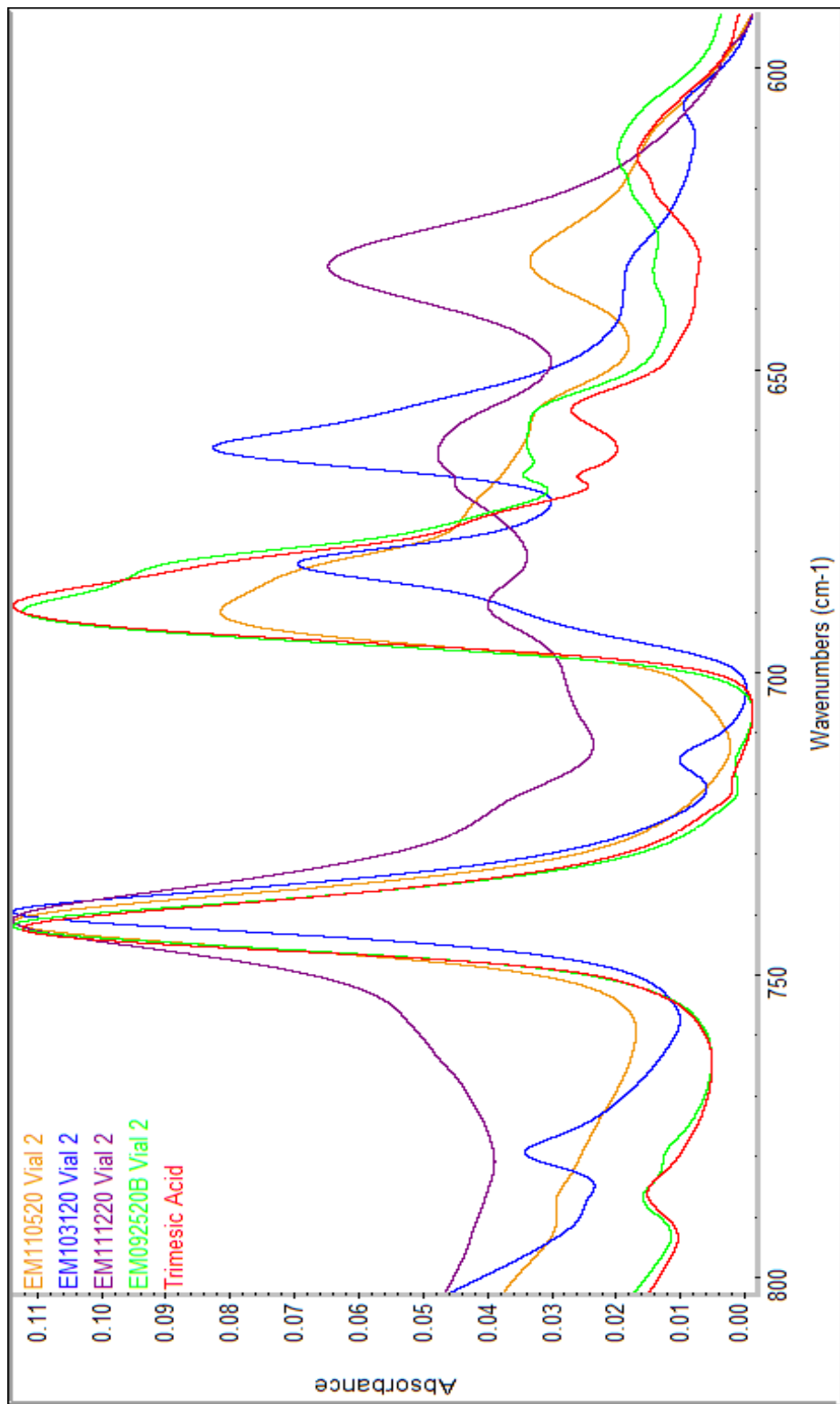
Figure 36: FTIR overlay of spectroscopy between 800-600⁻¹ of insoluble samples of 1,3,5-PPTBDA and trimesic acid.

D. TGA

TGA analysis observes the degradation of the FR additives. The samples displayed some variation between onset temperatures, loss in mass, and stability plateaus. This does not indicate whether the additive will perform well within a polymer system, but it does show which samples have common profiles and behavior in thermal analysis.

Some of the samples had a broad degradation while others were narrow with less thermal stability. TGA must be done before DSC to prevent samples degradation in a DSC analysis, the onset and loss in mass are noted as a preventative measure for the DSC. Samples with low temperature degradation are unable to be heated at higher temperatures in the DSC.

Figure 37 displays the weight loss versus temperature for sample EM100419, which is 1,3,5-DPP. EM100419 had a high temperature onset of degradation with 8% mass remaining at 600°C. Table 14 below summarizes the data from the thermogram in Figure 37. The derivative weight confirms the broad degradation temperature range.

70

Table 14: TGA analysis of 1,3,5-DPP.

Degradation of 1,3,5-DPP	EM100419
Stability Plateau (°C)	RT-200
Onset of Degradation	242
Weight Percent at A50°C (%)	100
Weight Percent at 80°C (%)	99
Weight Percent at 100°C (%)	99
Weight Percent at 150°C (%)	99
Weight Percent at 200°C (%)	96
Weight Percent at 250°C (%)	86
Weight Percent at 300°C (%)	59
Weight Percent at 350°C (%)	23
Weight Percent at 400°C (%)	15
Weight Percent at 600°C (%)	8
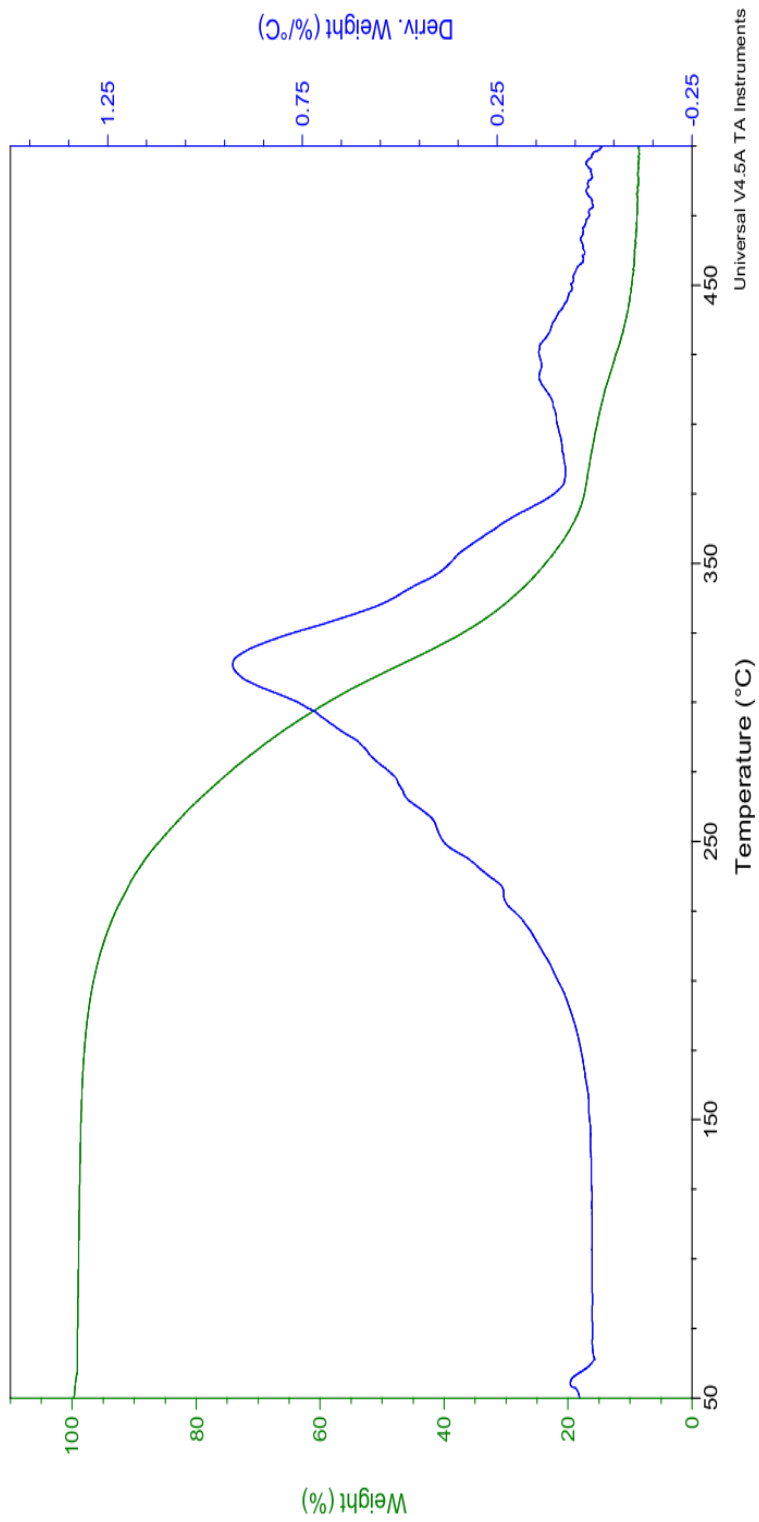
Figure 37: EM100419 TGA and derivative.

The TGA thermogram for the three different 1,3,5-PPDB samples are shown in Figure 38 and Figure 39. Figure 38 shows the weight loss vs temperature. Figure 39 is the weight loss derivative vs temperature. Both figures confirm a low temperature onset of degradation for samples EM111320 and EM081720. According to Figure 39, sample EM081720 had four different degradative steps and sample EM111320 had five degradative steps. Sample EM082820 had the highest onset of degradation temperature with 28% of the sample remaining at 600°C. The high mass percent remaining may indicate crosslinking in sample EM082820. Table 15 summarizes the data gathered from the thermograms.

Table 15 summarizes the weight loss profile for 1,3,5-PPDB samples.

Table 15: TGA analysis profile of 1,3,5-PPDB samples.

Degradation of 1,3,5-PPDB	EM081720 Vial 1	EM111320 Vial 1	EM082820 Vial 2
Stability Plateau (°C)	RT-75	RT-45	RT-125
1st Onset of Degradation	96	55	188
2nd Onset of Degradation	285	108	-
3rd Onset of Degradation	-	216	-
4th Onset of Degradation	-	279	-
Weight Percent at 50°C (%)	100	97	100
Weight Percent at 80°C (%)	97	90	100
Weight Percent at 100°C (%)	91	76	99
Weight Percent at 150°C (%)	54	31	96
Weight Percent at 200°C (%)	45	23	92
Weight Percent at 250°C (%)	44	21	83
Weight Percent at 300°C (%)	30	16	71
Weight Percent at 350°C (%)	5	12	56
Weight Percent at 400°C (%)	5	12	45
Weight Percent at 600°C (%)	3	9	28
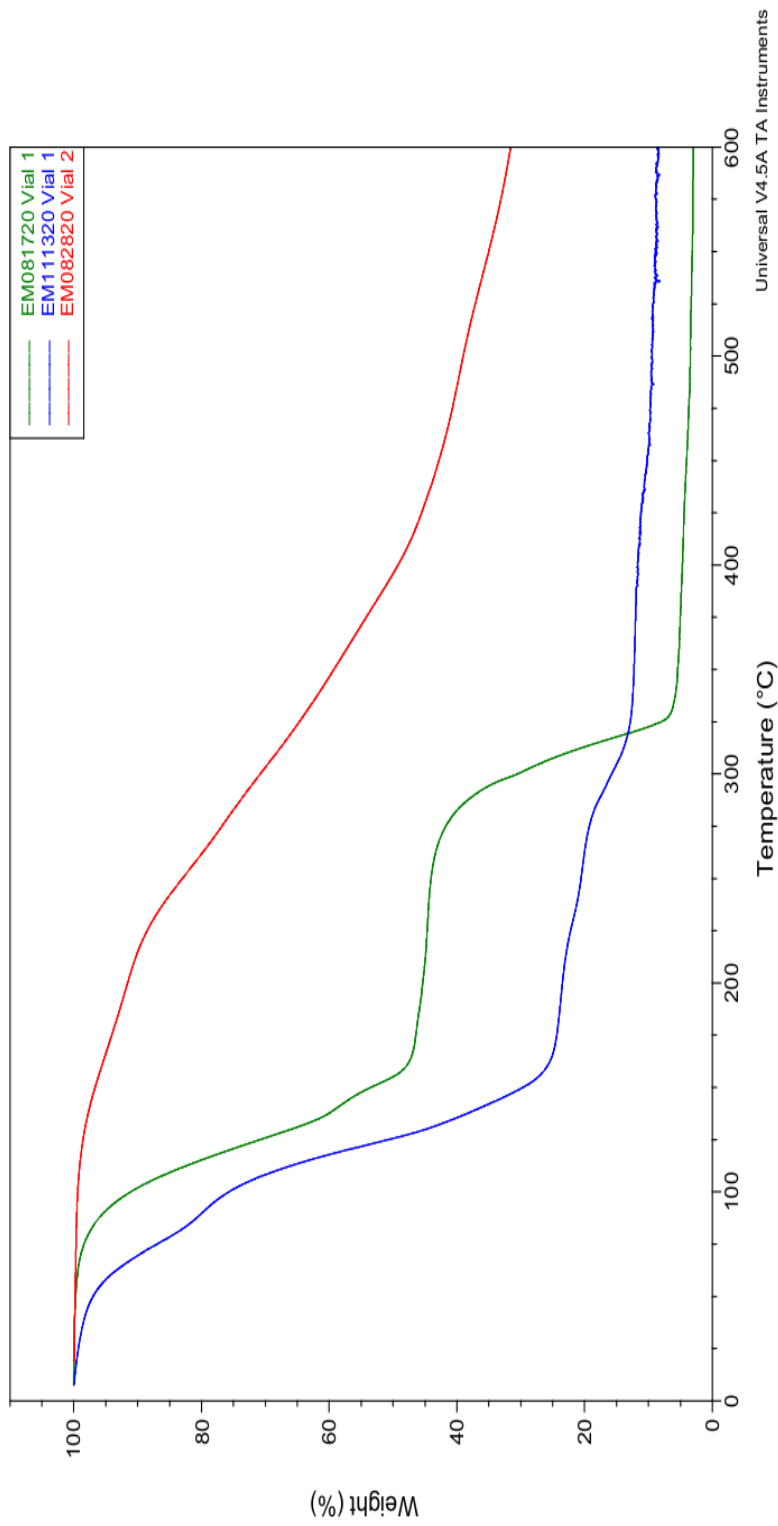
Figure 38: TGA overlay of 1,3,5-PPDB Products.
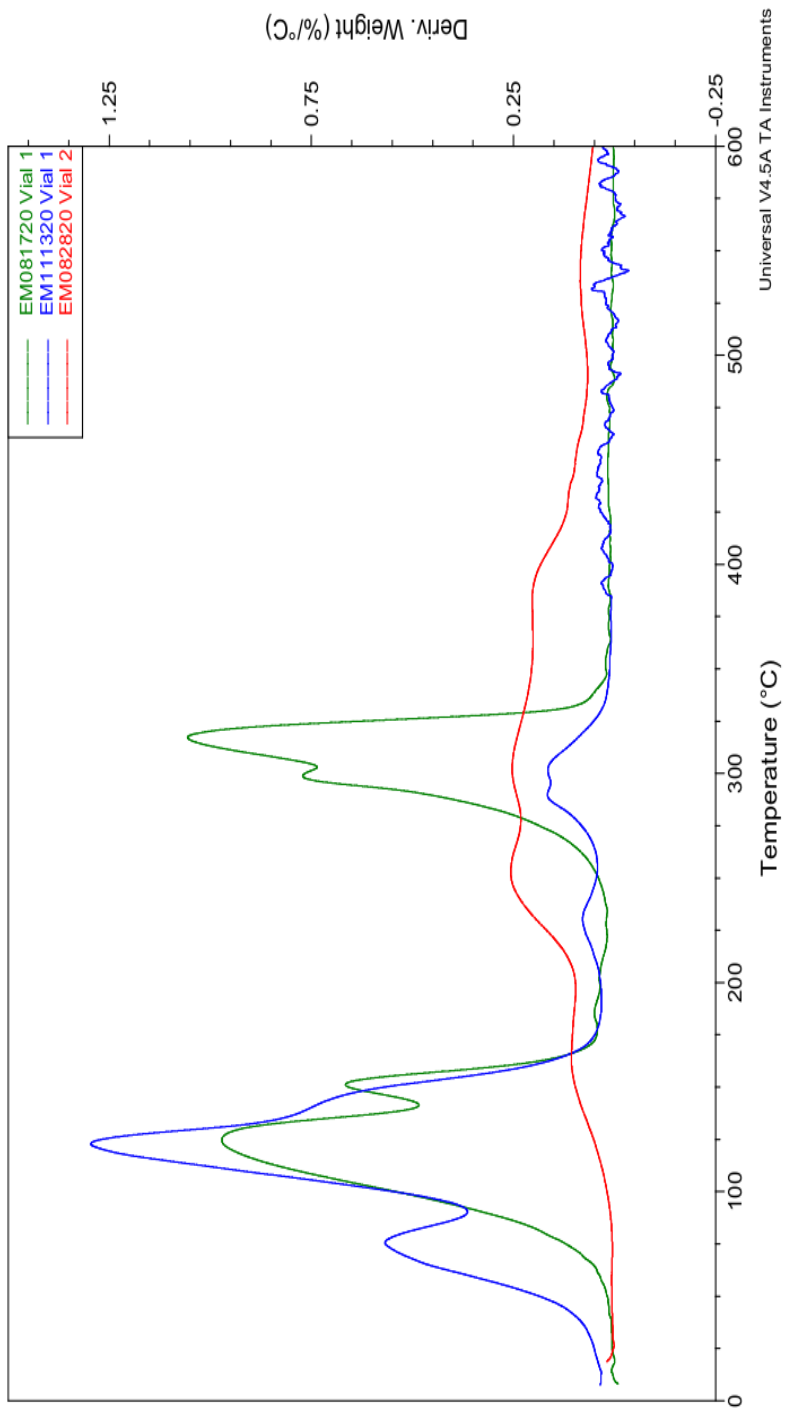
Figure 39: 1,3,5-PPDB Derivative Weight.

The soluble 1,3,5-PPTBDA products overlay in Figure 40 indicated that the samples all had similar profiles. The samples in Figure 40 all likely have low molecular weight species volatizing at lower temperatures. The samples had lower onset of degradation temperatures and at 600°C, each sample had under 10% mass remaining. Table 16 is a summary of the data gathered from the thermograms.

Table 16: TGA analysis profile of 1,3,5-PPTBDA soluble products.

Degradation of 1,3,5-PPTBDA	EM092520B Vial 1	EM092620 Vial 1	EM101020 Vial 1	EM110520 Vial 1	EM103120 Vial 1
Stability Plateau (°C)	RT-65	RT-100	RT-100	RT-100	RT-100
1st Onset of Degradation	72	137	135	135	140
2nd Onset of Degradation	130	313	313	310	317
3rd Onset of Degradation	311	427	420	420	418
4th Onset of Degradation	439	-	-	-	-
Weight Percent at 50°C (%)	100	100	100	100	100
Weight Percent at 80°C (%)	97	100	100	100	99
Weight Percent at 100°C (%)	97	100	100	100	99
Weight Percent at 150°C (%)	92	93	92	96	94
Weight Percent at 200°C (%)	90	84	80	92	84
Weight Percent at 250°C (%)	89	83	79	91	84
Weight Percent at 300°C (%)	82	77	72	83	78
Weight Percent at 350°C (%)	23	36	26	42	35
Weight Percent at 400°C (%)	7	10	7	12	14
Weight Percent at 600°C (%)	3	4	3	4	9
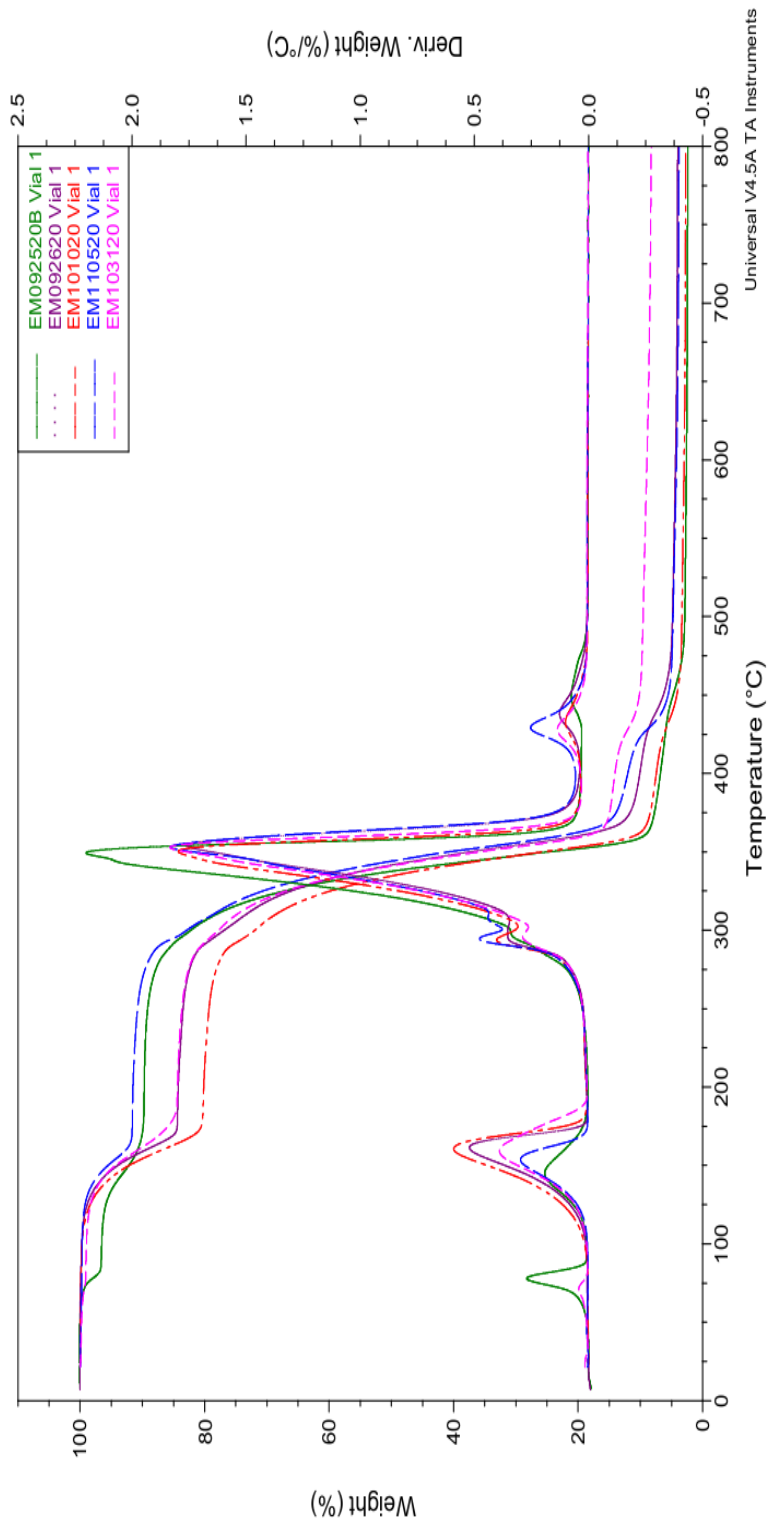
Figure 40: 1,3,5-PPTBDA Soluble Products TGA and weight derivative overlay.

Soluble sample outliers are pictured in Figure 41. Sample EM110520 Vial 1 was compared to samples EM110820 and EM111220. The two soluble outliers had comparable onset of degradation temperatures, but had almost 40% mass remaining at 600°C. Table 17 summarizes the data gathered from the thermograms.

Table 17: TGA 1,3,5- PPTBDA sample outliers profile compared to sample EM110520 Vial 1.

Degradation of 1,3,5-PPTBDA	EM110820 Vial 1	EM111220 Vial 1	EM110520 Vial 1
Stability Plataeu (°C)	RT-50	RT-50	RT-100
1st Onset of Degradation	122	97	135
2nd Onset of Degredation	285	262	310
3rd Onset of Degredation	448	450	420
Weight Percent at 50°C (%)	99	99	100
Weight Percent at 80°C (%)	98	98	100
Weight Percent at 100°C (%)	97	97	100
Weight Percent at 150°C (%)	93	91	96
Weight Percent at 200°C (%)	91	89	92
Weight Percent at 250°C (%)	88	86	91
Weight Percent at 300°C (%)	83	75	83
Weight Percent at 350°C (%)	71	63	42
Weight Percent at 400°C (%)	64	60	12
Weight Percent at 600°C (%)	39	37	4
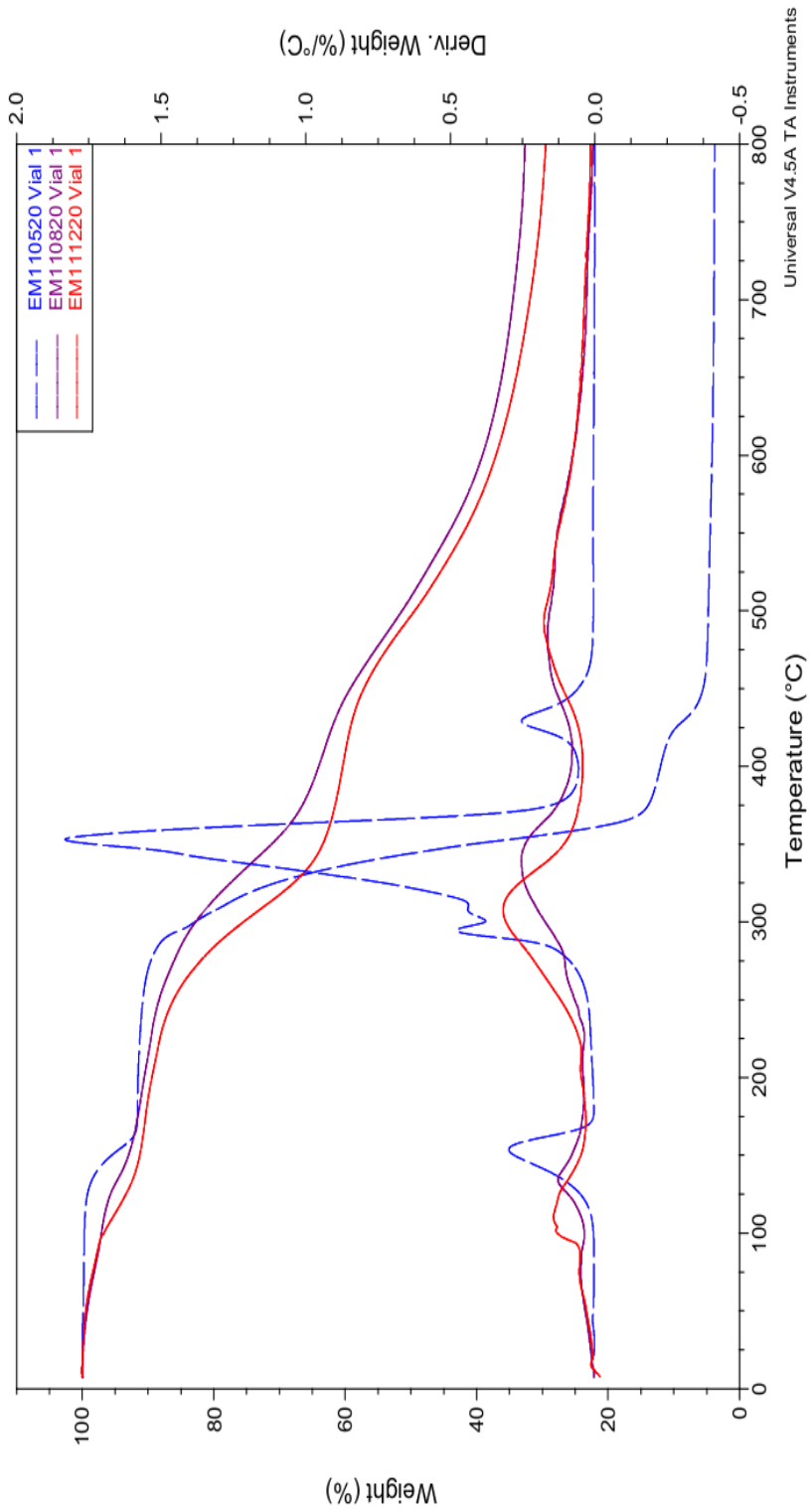
Figure 41: 1,3,5-PPTBDA soluble product outliers compared to EM110520.

Insoluble samples EM110820 and EM111220 were washed as separate products due to slight differences in color and appearance. After the wash, the samples were evaluated separately. Figure 42 examines how these products from the same reaction flask compare to one another. Table 18 is a summary of the data from the thermograms. The insoluble samples had similar degradative profiles in comparison to one another with onset of degradation temperatures around 60°C and 17-24% mass remaining at 600°C. The low temperature onset of degradation indicated that the samples have have low molecular weight species volatizing.

Table 18: TGA 1,3,5-PPTBDA Insoluble Sample Profile.

Degradation of 1,3,5-PPTBDA	EM110820 Vial 2	EM110820 Vial 3	EM110820 Vial 4	EM111220 Vial 2	EM111220 Vial 3
Stability Plateau (°C)	RT-40	RT-40	RT-40	RT-40	RT-40
1st Onset of Degradation	68	60	60	57	55
2nd Onset of Degradation	126	128	125	120	107
3rd Onset of Degradation	272	274	266	258	271
4th Onset of Degradation	437	459	454	448	439
Weight Percent at 50°C (%)	99	98	98	98	97
Weight Percent at 80°C (%)	95	93	91	89	84
Weight Percent at 100°C (%)	91	89	86	85	78
Weight Percent at 150°C (%)	65	69	66	60	61
Weight Percent at 200°C (%)	51	56	54	49	57
Weight Percent at 250°C (%)	48	53	51	47	55
Weight Percent at 300°C (%)	41	48	46	38	44
Weight Percent at 350°C (%)	32	41	41	32	32
Weight Percent at 400°C (%)	30	39	39	30	31
Weight Percent at 600°C (%)	17	24	23	19	23
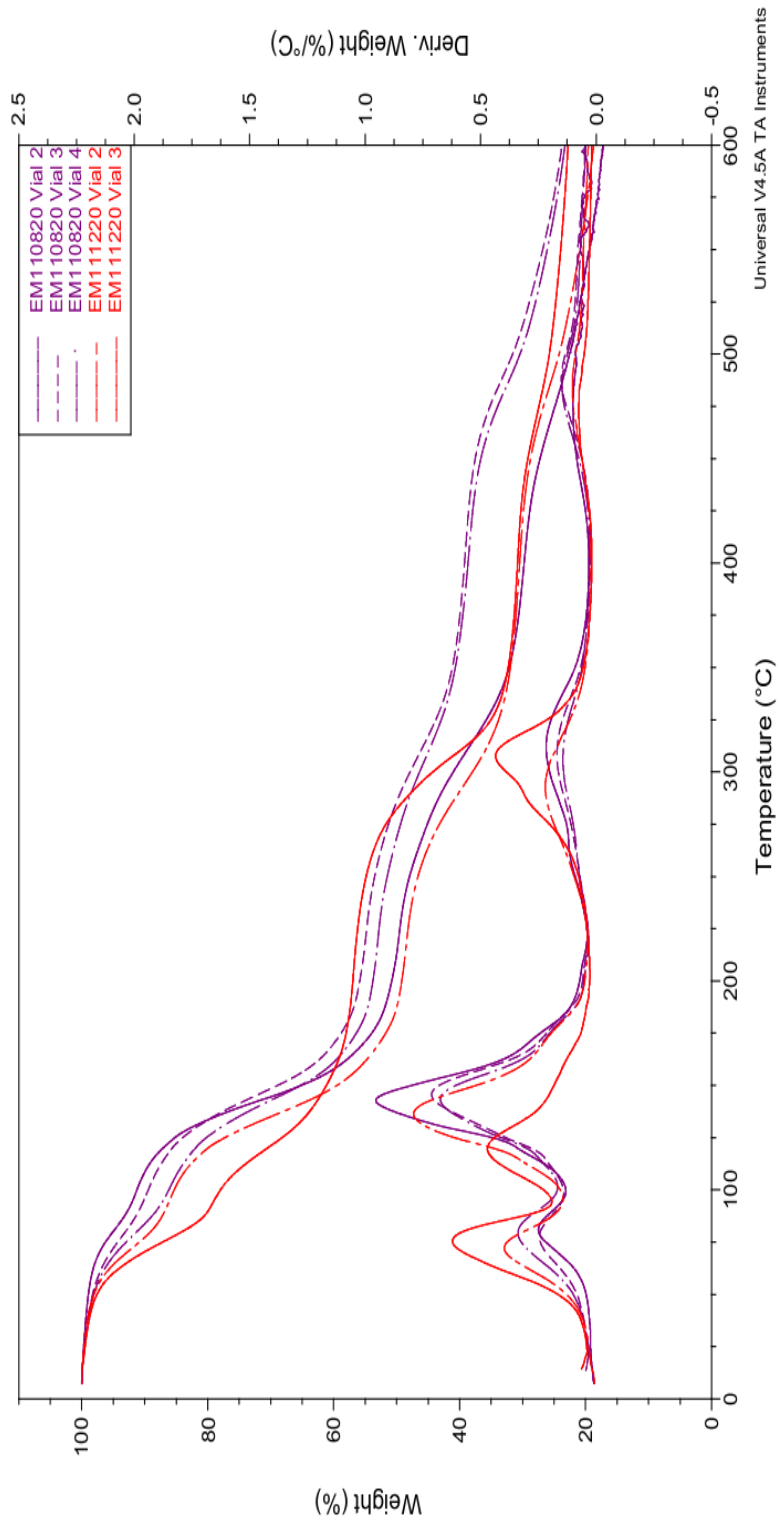
Figure 42: 1,3,5-PPTBDA insoluble products separated before purification.

Insoluble product outliers were compared to EM110820 Vial 4 in Figure 43. Table 19

summarizes data from the thermograms. The onset of degradation temperature was not as

low as the samples from Figure 42, but the mass remaining at 600°C was between 0-10%.

Table 19: TGA Insoluble Product Outliers of 1,3,5-PPTBDA.

Degradation of 1,3,5-PPTBDA	EM092520B Vial 2	EM103120 Vial 2	EM110520 Vial 2	EM110820 Vial 4
Stability Plateau (°C)	RT-90	RT-50	RT-80	RT-40
1st Onset of Degradation	107	129	94	60
2nd Onset of Degradation	311	301	157	125
3rd Onset of Degradation	412	-	279	266
4th Onset of Degradation	-	-	406	454
Weight Percent at 50°C (%)	100	100	100	98
Weight Percent at 80°C (%)	100	96	98	91
Weight Percent at 100°C (%)	99	95	86	86
Weight Percent at 150°C (%)	94	84	69	65
Weight Percent at 200°C (%)	94	79	55	54
Weight Percent at 250°C (%)	93	77	51	52
Weight Percent at 300°C (%)	85	66	32	46
Weight Percent at 350°C (%)	26	1>	10	41
Weight Percent at 400°C (%)	5	0	9	39
Weight Percent at 600°C (%)	0	0	5	23
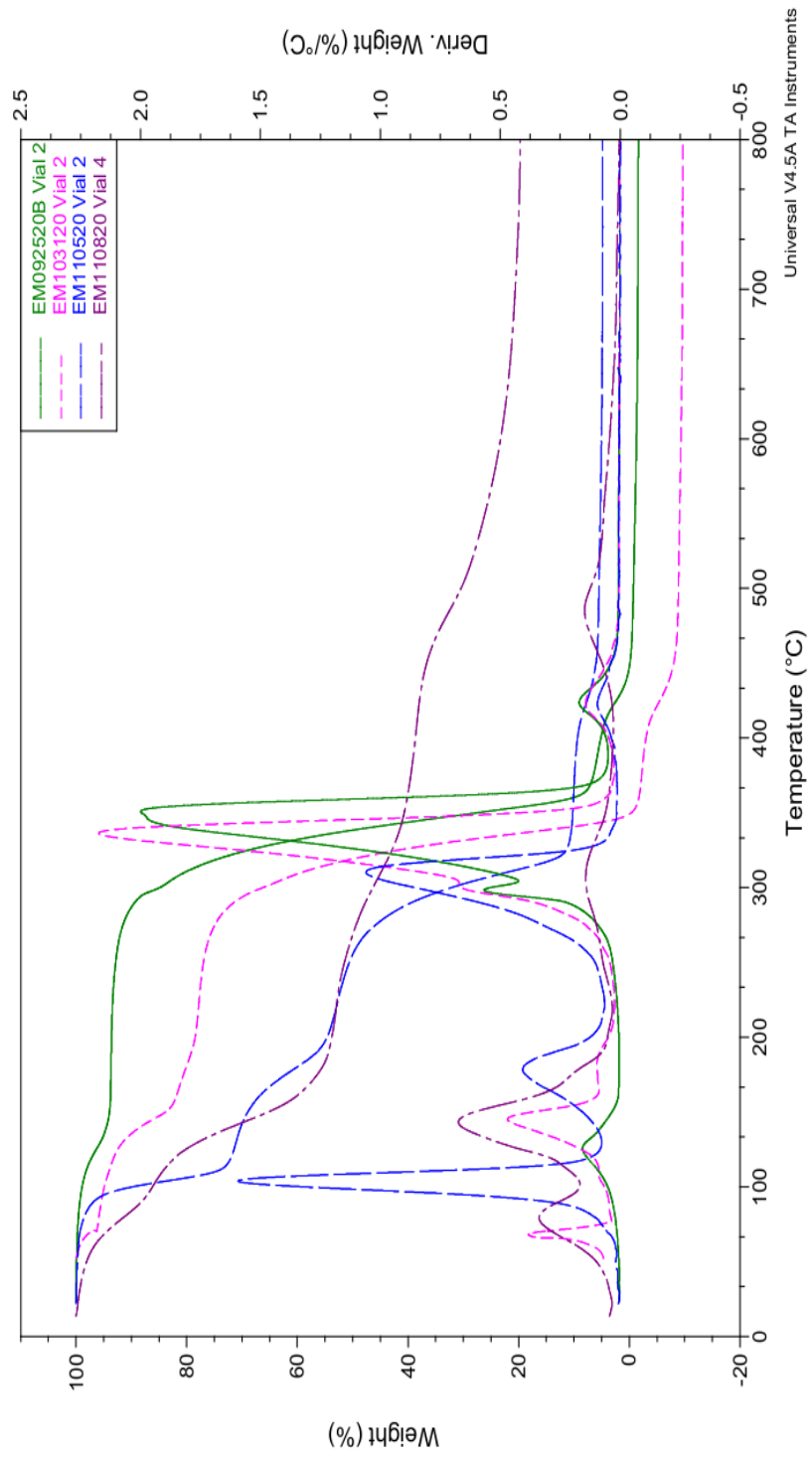
Figure 43: 1,3,5-PPTBDA insoluble product outliers.

Sample EM100419 (1,3,5-DPP) had the highest onset of degradation temperature of all three synthesized products. Samples EM110820 and EM111220 (1,3,5-PPTBDA) had the highest mass remaining at 600°C.

E. DSC

The following DSC samples were heated, cooled, and heated to observe the second heating cycle. The second heating cycle for sample EM100419 is shown in Figure 44. Figure 44 is the DSC thermogram and Table 20 contains the onset values for thermal events T_g and T_m. EM100419 had a glass transition at 0°C and three melting temperatures at 122°C, 158°C, and 180°C. These three different T_m values indicate that there are multiple species present or that the crystals sizes and perfections vary.

Table 20: DSC T_g and T_m Analysis of 1,3,5-DPP.

1,3,5-DPP	T_g (°C)	T_m (°C)
EM100419	0	122,158,180
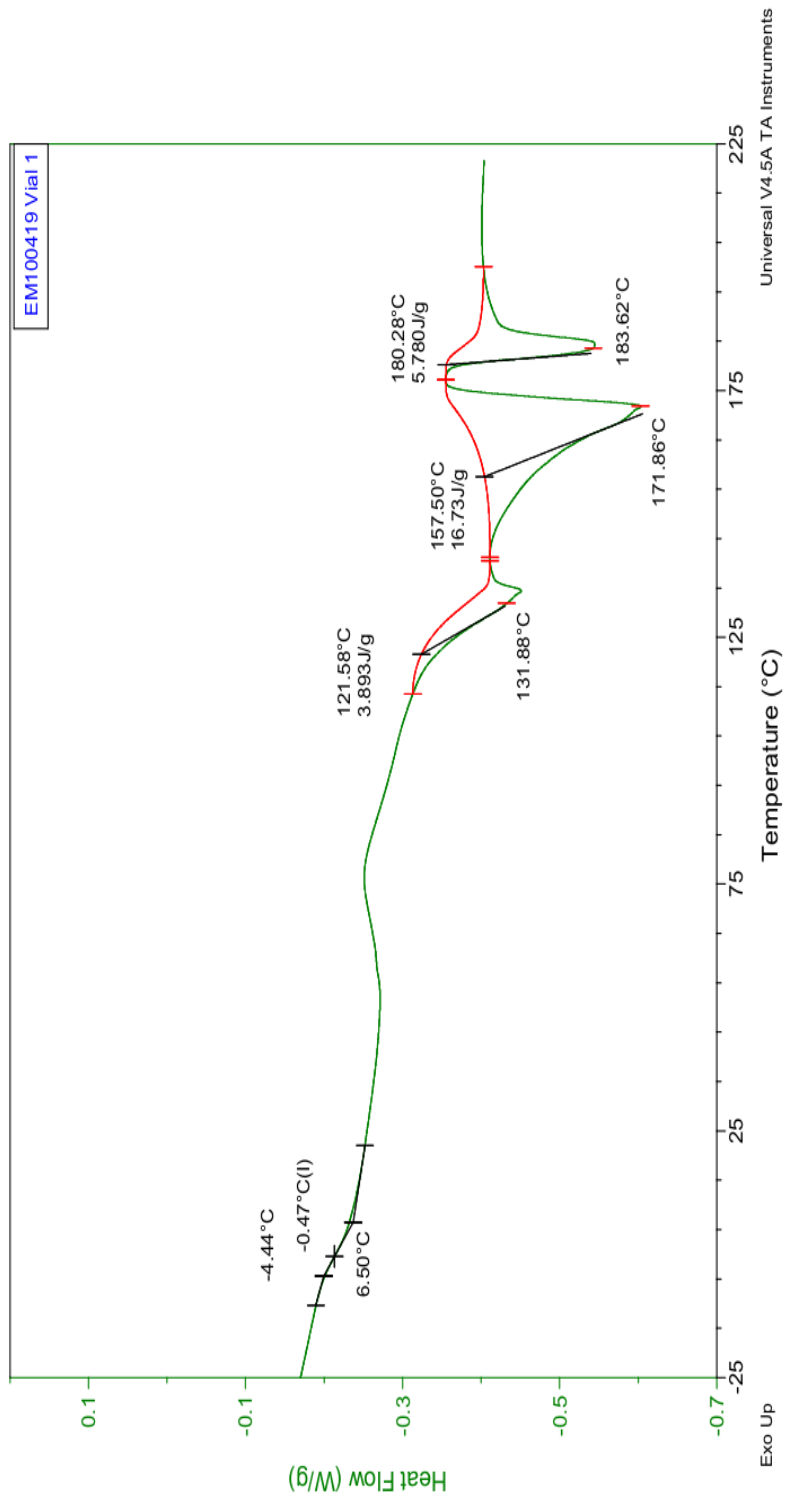
Figure 44: DSC Thermogram of EM100419.

The 1,3,5-PPDP samples were not carried out to higher temperature testing due to an early onset degradation temperature. Table 21 shows the observed temperature transitions that were determined from the samples thermograms (Figure 45) indicating only glass transition temperatures.

Table 21: DSC T_g and T_m Analysis of 1,3,5-PPDB.

1,3,5-PPDB	T_g (°C)	T_m (°C)
EM081720	39	-
EM082820	42	-
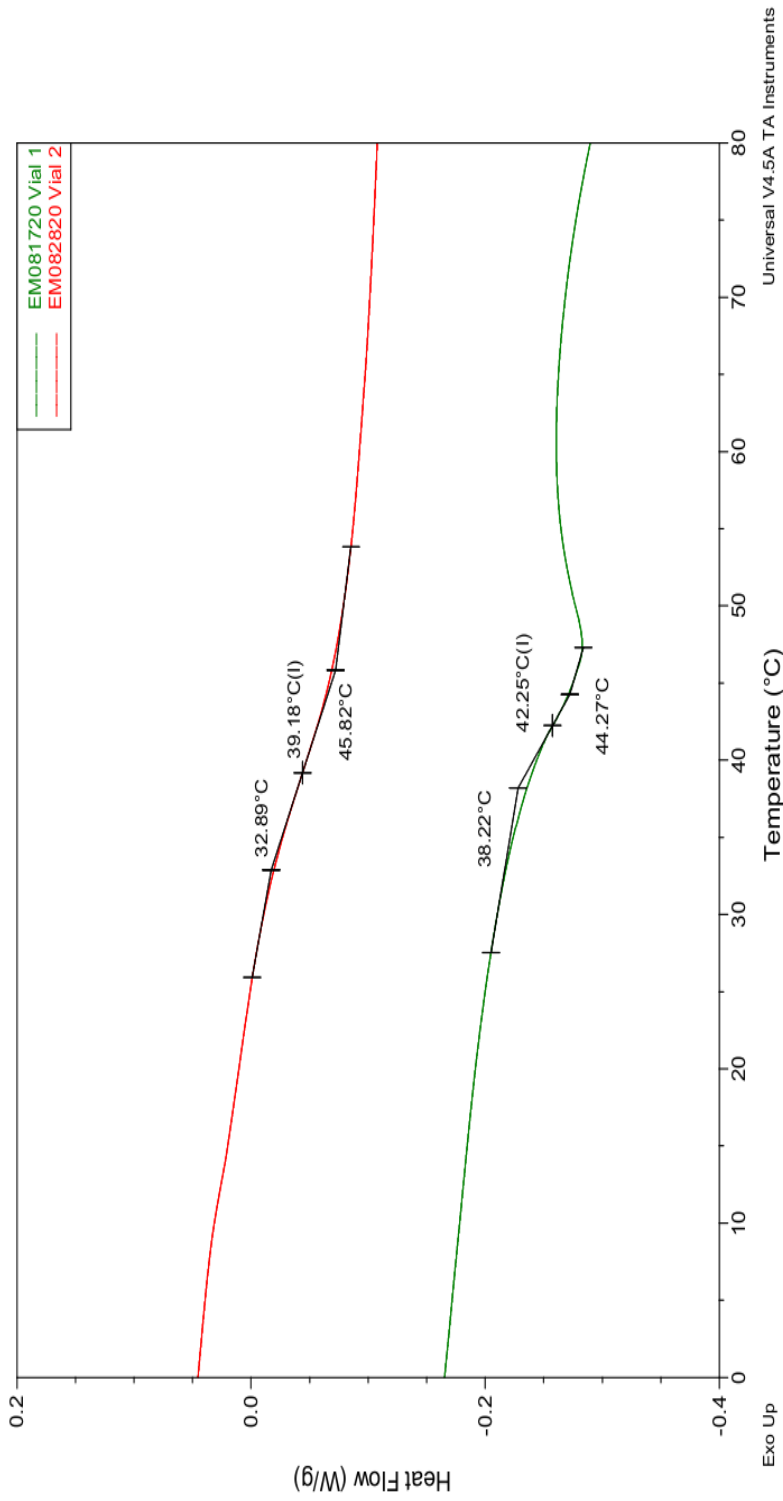
Figure 45: DSC Thermogram for 1,3,5-PPDB samples.

The soluble sample thermograms (Figure 46 and Figure 47) were combined in Table 22 below. None of the soluble samples contained T_m values and samples EM092520B and EM103120 also did not contain any T_g values.

Table 22: DSC T_g and T_m Analysis of 1,3,5-PPTBDA Soluble Samples.

1,3,5-PPTBDA	T_g (°C)	T_m (°C)
EM110520 Vial 1	97	-
EM092520B Vial 1	-	-
EM103120 Vial 1	-	-
EM110820 Vial 1	159,226	-
EM111220 Vial 1	154, 222	-
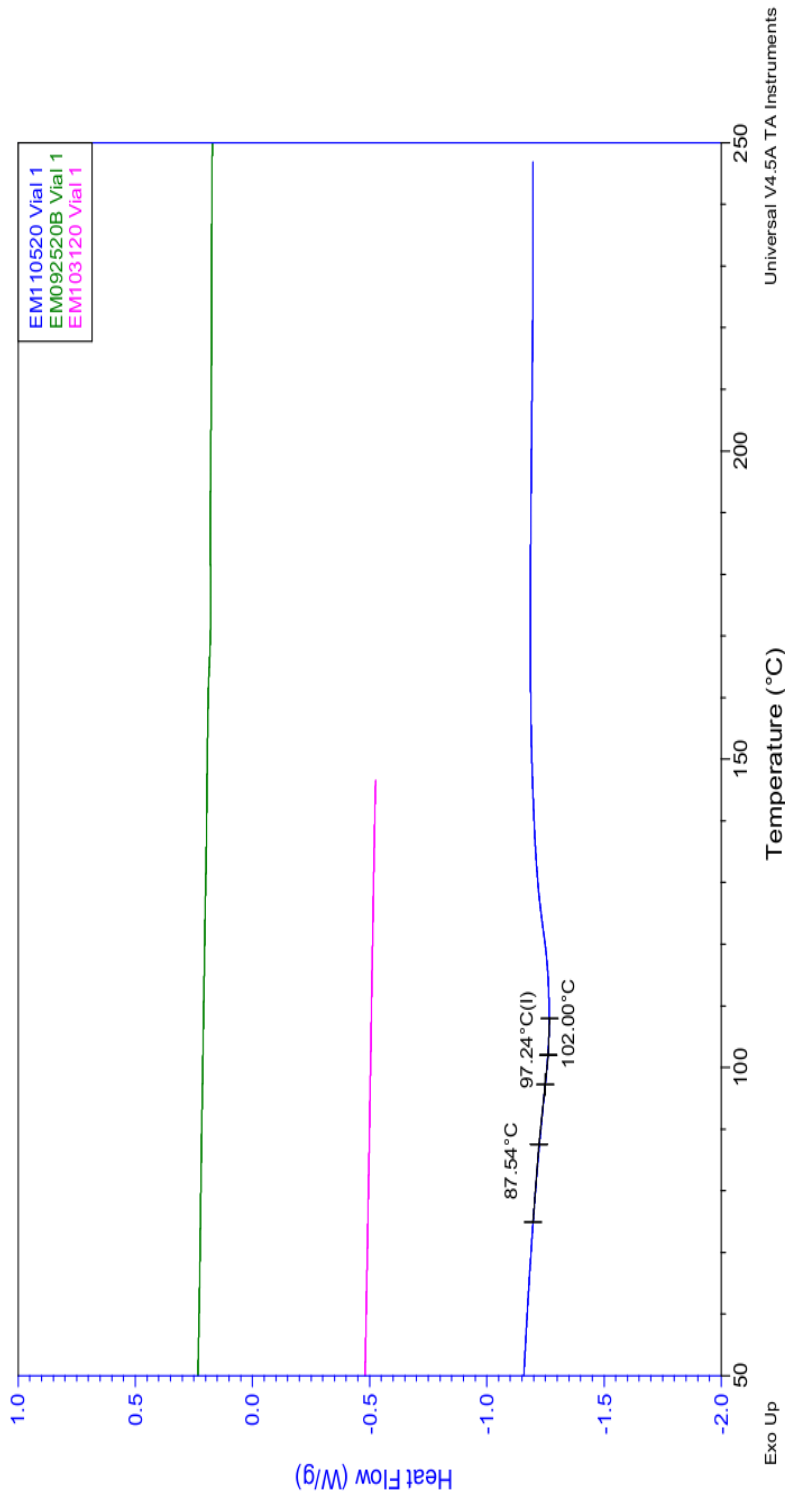
Figure 46: DSC Thermogram of soluble 1,3,5-PPTBDA samples.
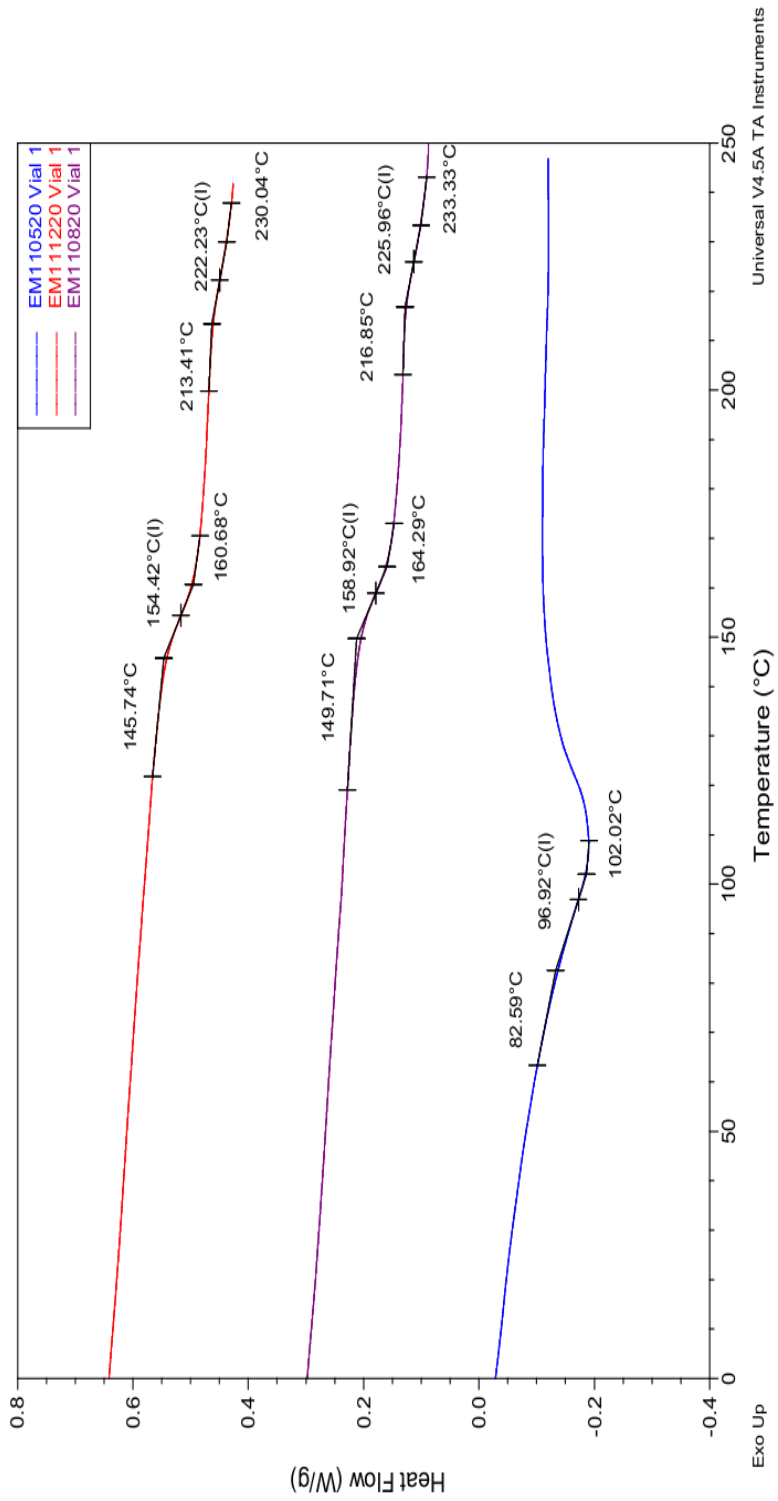
Figure 47: DSC Thermogram of 1,3,5-PPTBDA samples.

Figure 48 observes the 1,3,5-PPTBDA insoluble samples. EM110820 vial 3 and 4 contain possible T_g values or it may be degradation of the samples. The onset of degradation was so low for samples EM110820 and EM111220 that it is difficult to determine.

Table 23: DSC T_g and T_m Analysis of 1,3,5-PPTBDA insoluble samples.

1,3,5-PPTBDA	T_g (°C)	T_m (°C)
EM110820 Vial 2	-	-
EM110820 Vial 3	103	-
EM110820 Vial 4	109	-
EM111220 Vial 2	-	-
EM111220 Vial 3	-	-
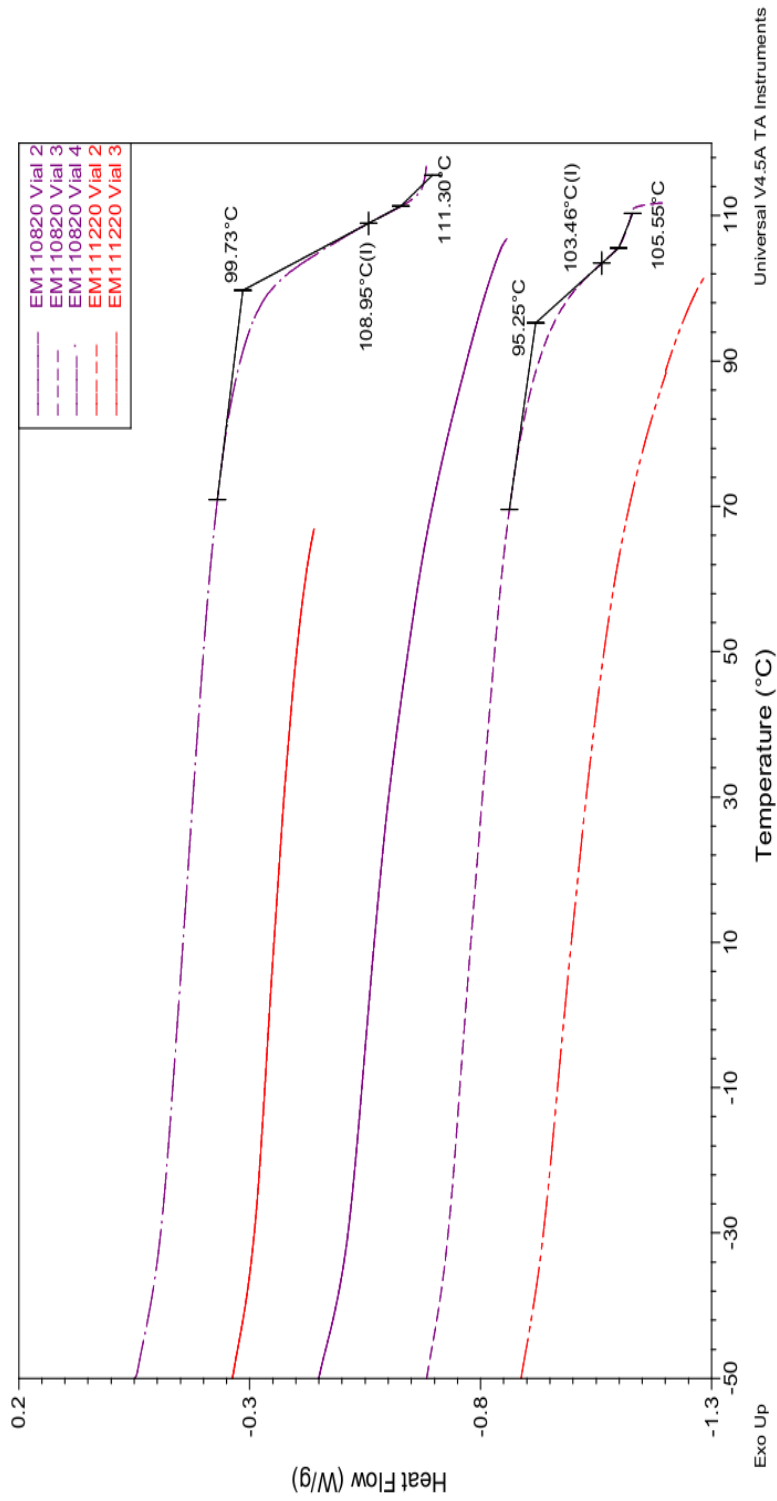
Figure 48: DSC Thermogram of insoluble 1,3,5-PPTBDA samples.

F. NMR

The spectras for ^{13}C, ^{1}H, and ^{31}P have been obtained for sample EM100419 (1,3,5-DPP) and are shown in Figures 49,50, and 51. Table 24 is a summary of the proposed chemical shifts of sample EM100419.

Table 24: ^{13}C NMR peak assignment of sample EM100919 (1,3,5-DPP) final washed product relative to TMS.

Peak Assignment	Chemical Shift (ppm)	Comment on Carbon
5	119.9	phenyl group carbon
7	125.9	phenyl group carbon
6	130.3	phenyl group carbon
3	132.5	central aromatic ring carbon
2	134.7	central aromatic ring carbon
4	150.4	phenoxy carbon
1	165.4	ester carbonyl

Sample EM100419 shows carbonyl peaks at 165, 163, and 162ppm. The presence of two additional carbonyls were observed.[32] This may indicate incomplete esterification of some acid groups on TMA. There should be one carbonyl present around 165ppm.[2] The additional peaks indicate residual impurities or products from side reactions. The 120-

134ppm appears to be what is expected but with noise as previously mentioned. The same goes for the proton and phosphorus NMR.

Table 25: ^{1}H NMR peak assignment of sample EM100919 (1,3,5-DPP) final washed product relative to TMS.

Peak Assignment	Range of Chemical Shift (ppm)	Comment on Carbon
4	7.3-7.4	phenyl group proton
3	7.5	phenyl group proton
2	7.5	phenyl group proton
1	8.7-8.8	central aromatic ring proton

Table 25 is a summary of the proposed chemical shifts of the proton NMR. Multiple peaks present indicate multiple species or products. The ^{31}P contains a peak around -16.1ppm indicating a trisubstituted phosphate.[2,32] Phosphate species may be present around 5 and -10ppm, which would indicate monosubstituted and disubstituted phosphates.

There are no NMR spectra for 1,3,5-PPDB due to the insolubility of the samples. Even if samples seemed to go into solution, small crystals would form at the bottom of the NMR tube or the sample would appear as a gel-like substance indicating crosslinking within the 1,3,5-PPDB samples. The samples were heated to 95°C within the NMR with

failed results due to shimming issues for the NMR at that temperature. The 1,3,5-PPDB

products appear to have a solid and liquid phase present that will require future analysis.

98
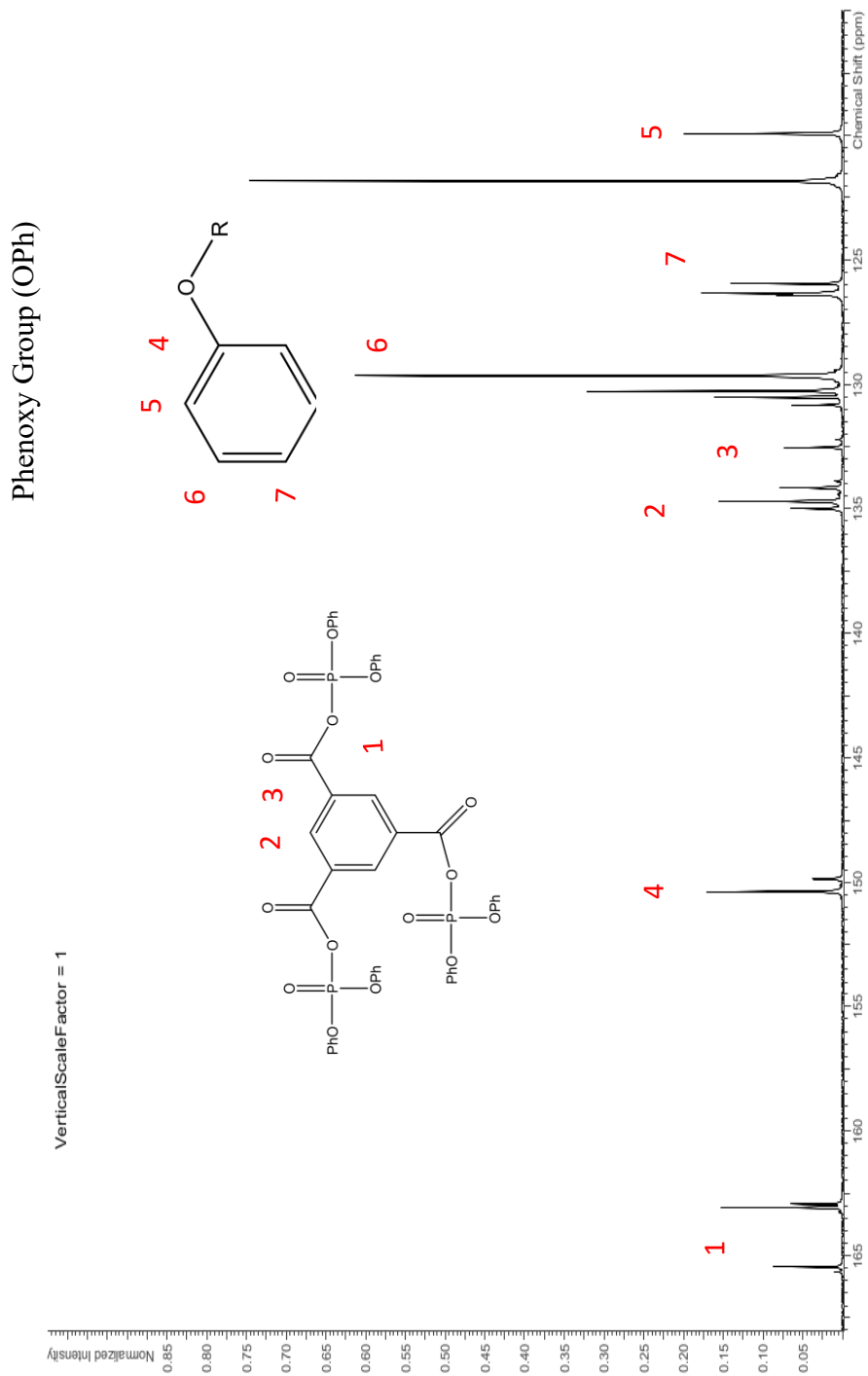
Figure 49: Sample EM100419 (1,3,5-DPP) ^{13}C NMR.
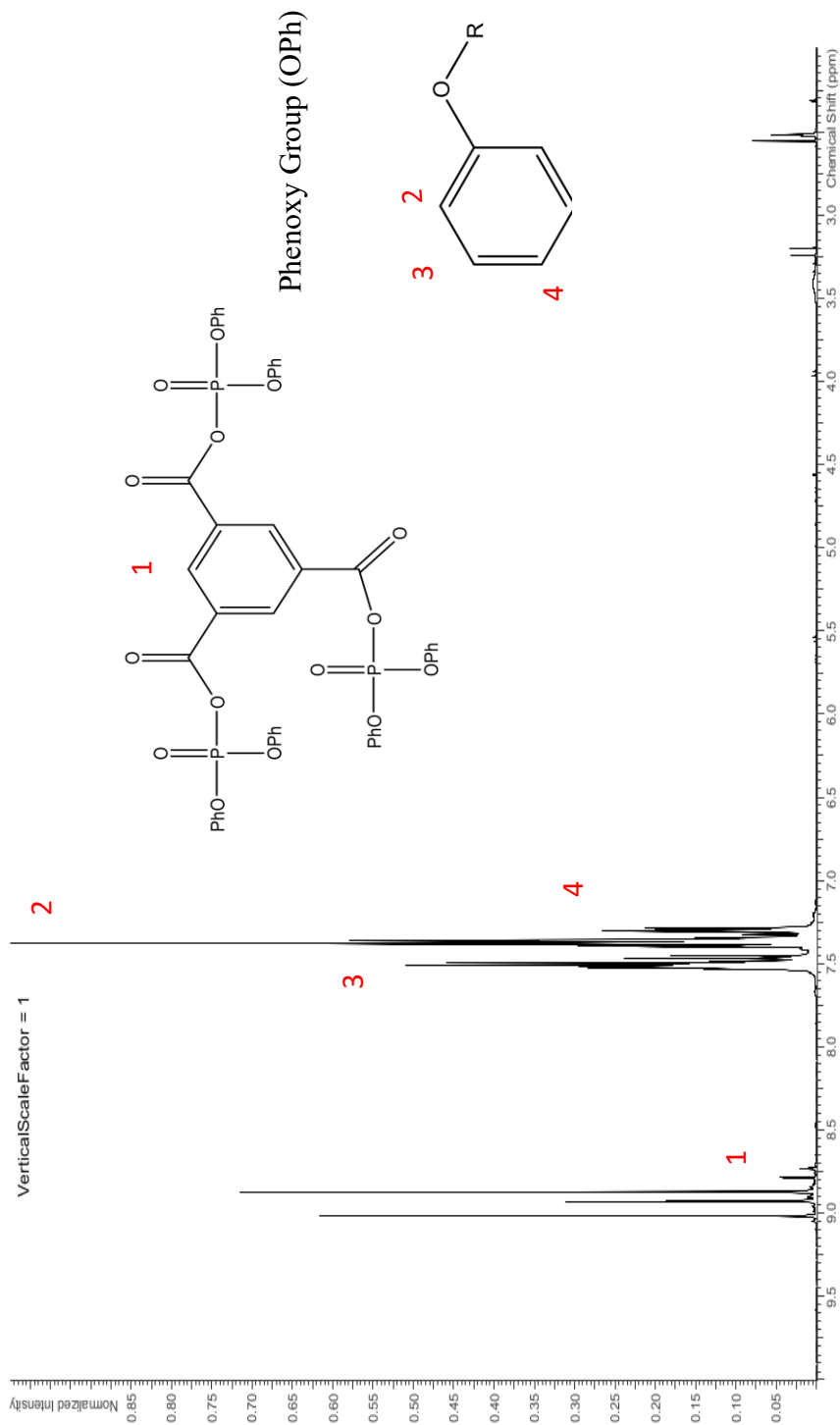
Figure 50: Sample EM100419 (1,3,5-DPP) ¹H NMR.

VerticalScaleFactor = 1

Normalized Intensity

Chemical Shift (ppm)
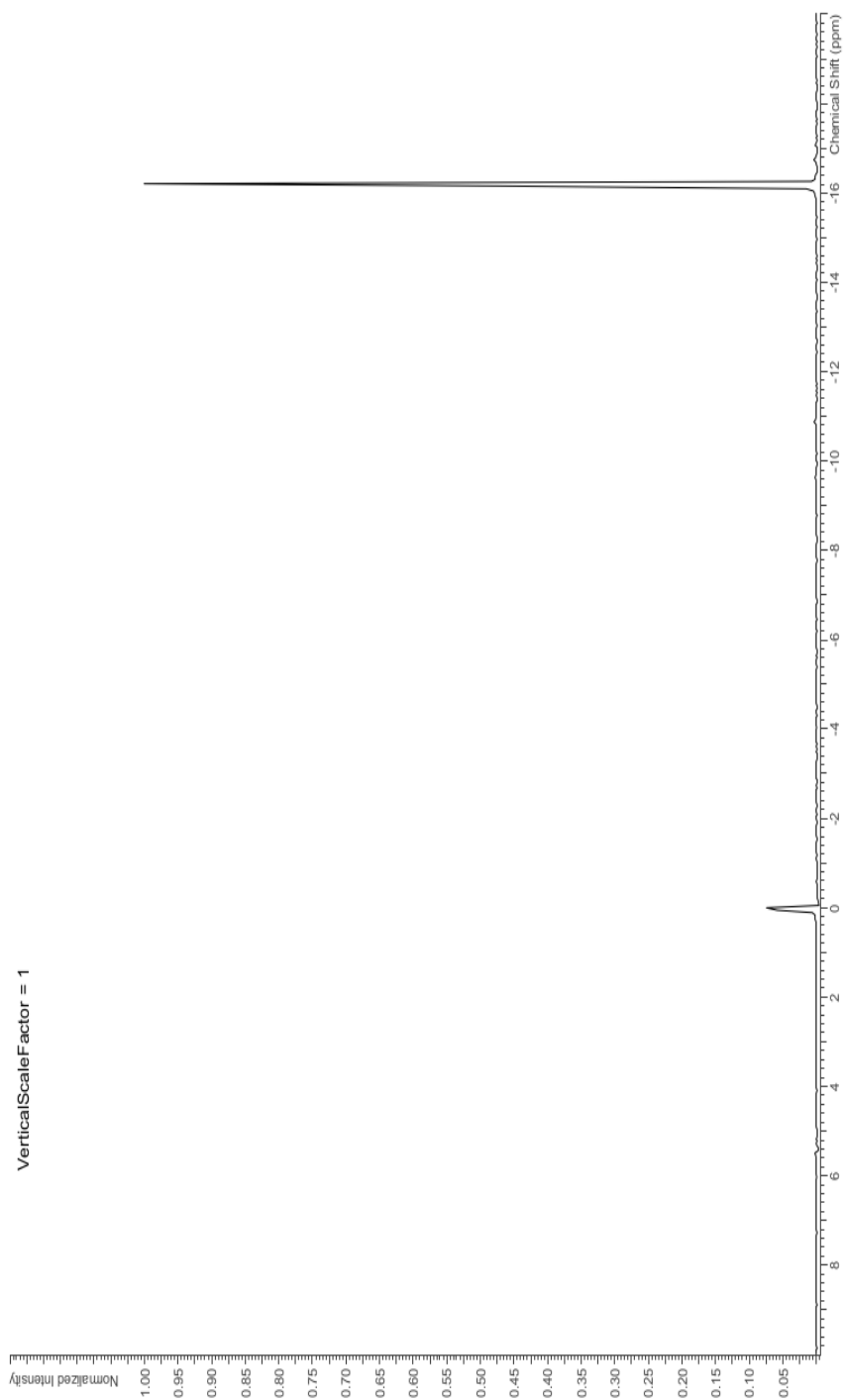
Figure 51: Sample EM100419 (1,3,5-DPP) ^{31}P NMR.

The spectras for ^{13}C, ^{1}H, and ^{31}P obtained for the EM110520 sample are shown in Figures 52-54. These spectra have many similarities to the trimesic acid NMR. In fact, they have almost the exact same signals except for a few small peaks present in the EM110520 in the aliphatic region. Since this sample is supposed to be 1,3,5-PPTBDA, which is capped with carboxylic acid end groups from the addition of trimesic acid, it may be that the resonance peaks are not impurities but part of the NMR profile for this sample. However, the ^{31}P spectra (Figure 54) has a signal at -5.5ppm, which indicates the presence of a monosubstituted species.[2] Table 26 and 27 summarize the peaks for the trimesic acid sample and may serve as a comparison to sample EM110520. The proton for the trimesic acid carboxylic acid group did not show a signal in the ^{1}H.

Table 26: ^{13}C NMR peak assignment of trimesic acid relative to TMS.

Peak Assignment	Chemical Shift (ppm)	Comment on Carbon
3	132.0	central aromatic ring carbon
2	133.8	central aromatic ring carbon
1	166.1	carboxylic acid carbon

Table 25: ^{1}H NMR peak assignment of trimesic acid relative to TMS.

Peak Assignment	Chemical Shift (ppm)	Comment on Carbon
1	8.7	central aromatic ring proton
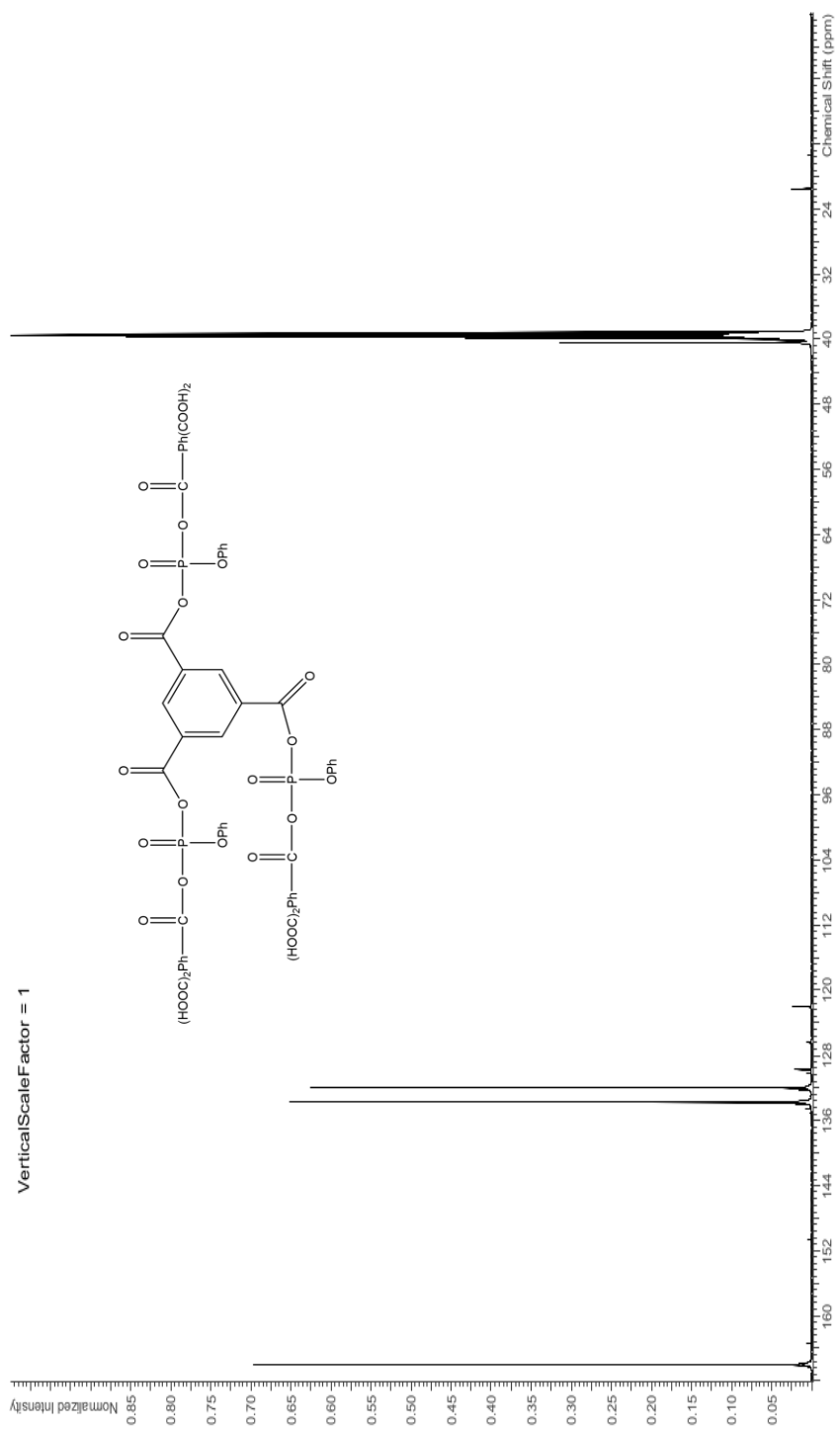
Figure 52: Sample EM110520 (1,3,5-PPTBDA) 13C NMR.

VerticalScaleFactor = 1

Normalized Intensity

Chemical Shift (ppm)
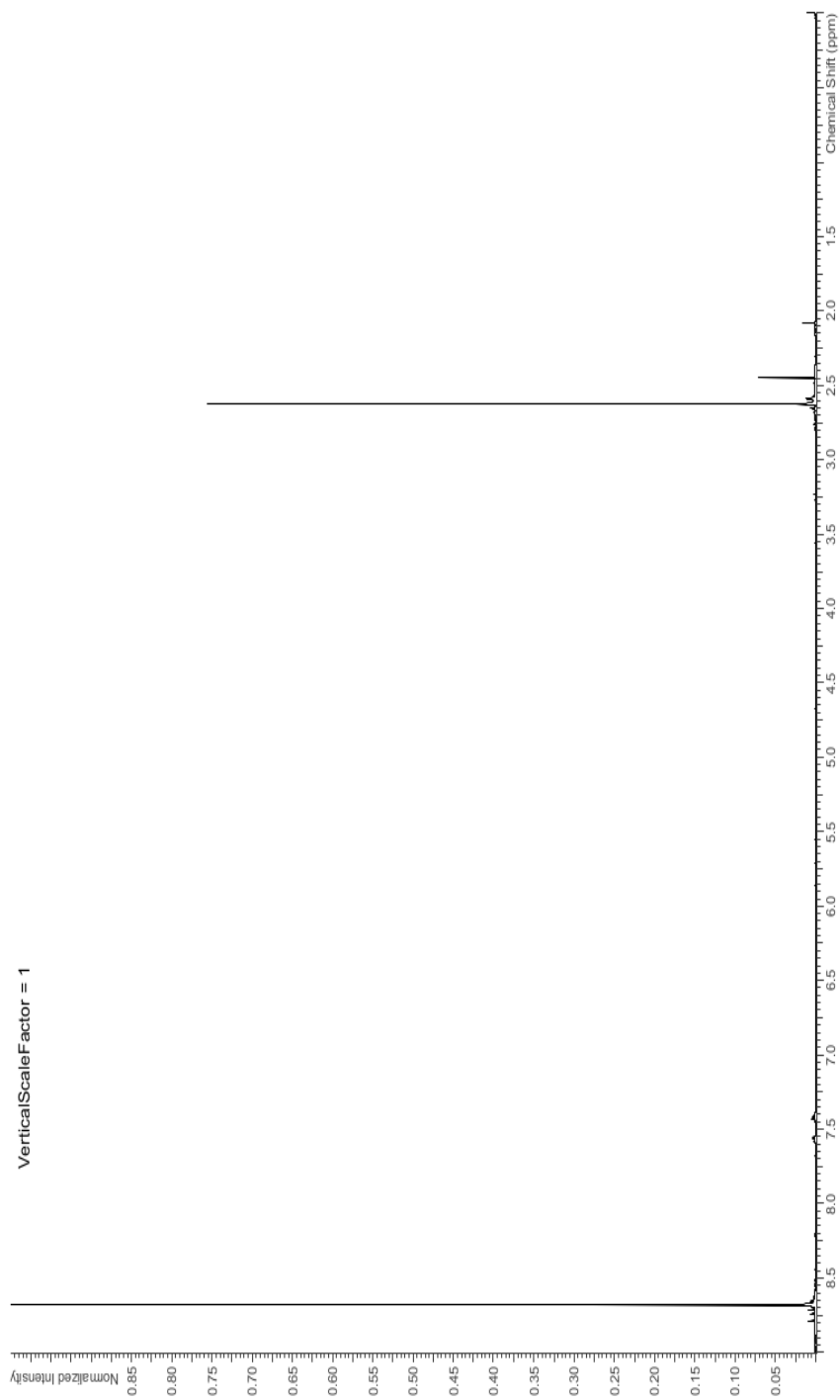
Figure 53: Sample EM110520 (1,3,5-PPTBDA) ^{1}H NMR.
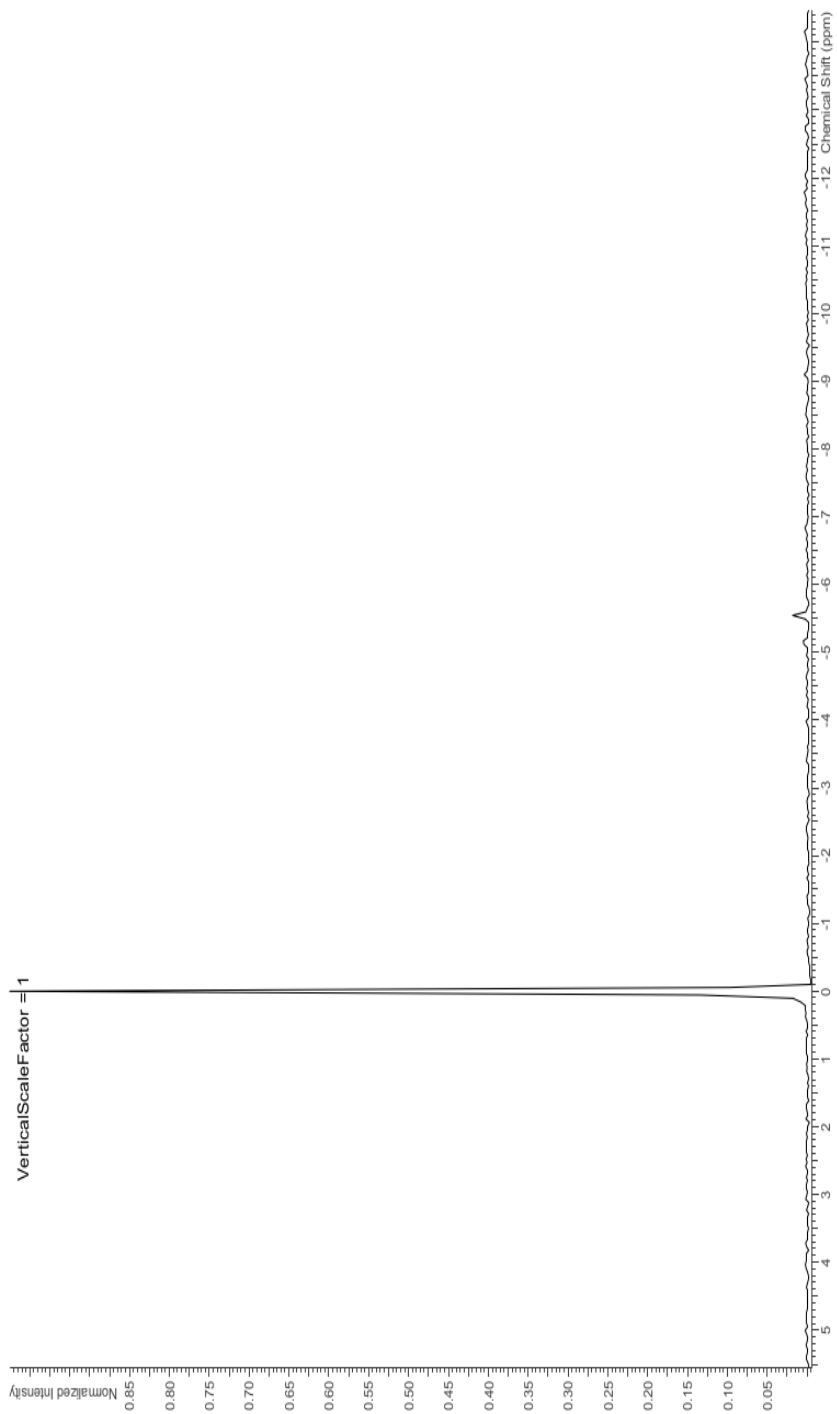
Figure 54: Sample EM110520 (1,3,5-PPTBDA) ^{31}P NMR.
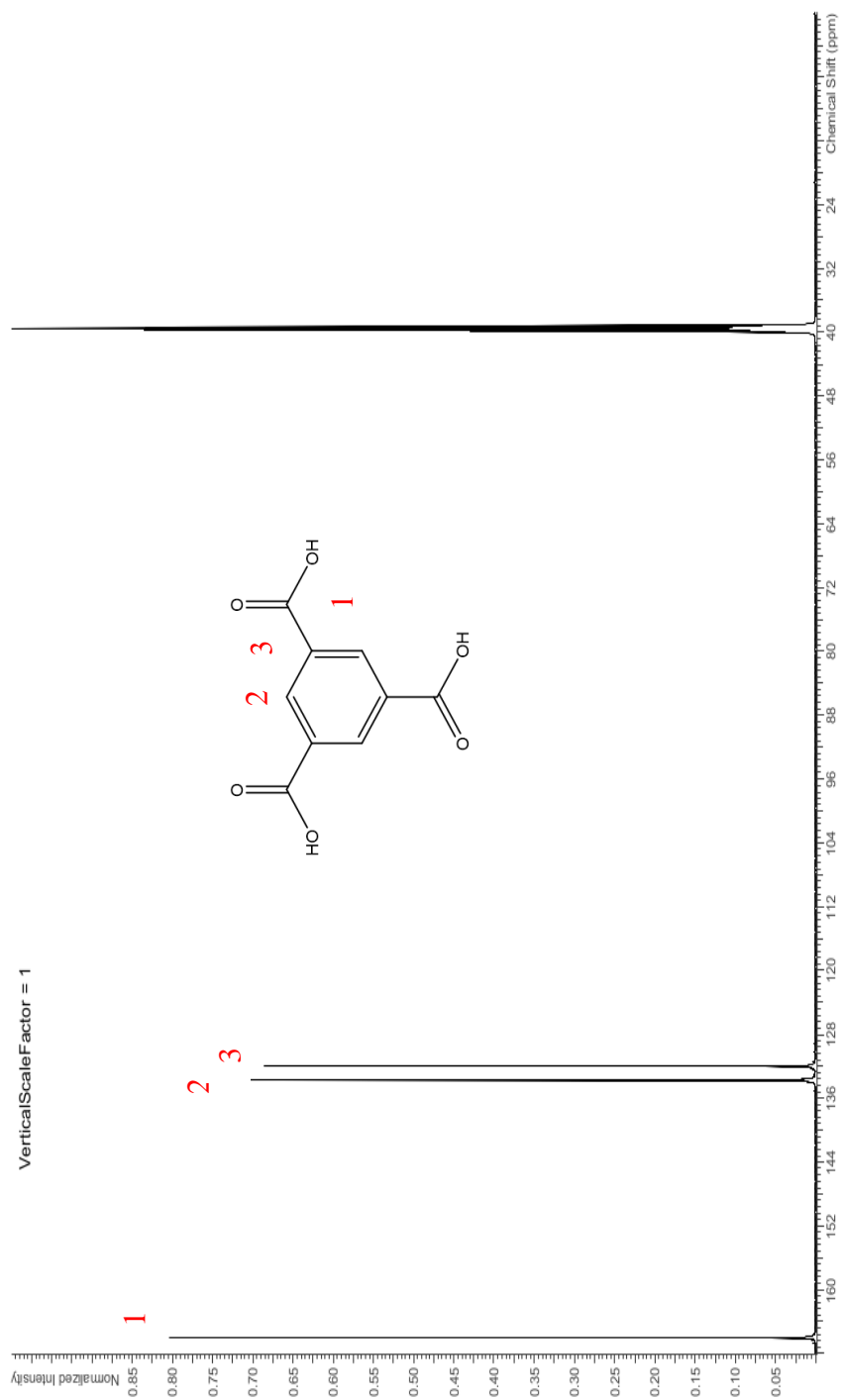
Figure 55: Trimesic Acid ^{13}C NMR.

105

VerticalScaleFactor = 1

Normalized Intensity

0.85 0.80 0.75 0.70 0.65 0.60 0.55 0.50 0.45 0.40 0.35 0.30 0.25 0.20 0.15 0.10 0.05

1

Chemical Shift (ppm)

8.5 8.0 7.5 7.0 6.5 6.0 5.5 5.0 4.5 4.0 3.5 3.0 2.5 2.0 1.5
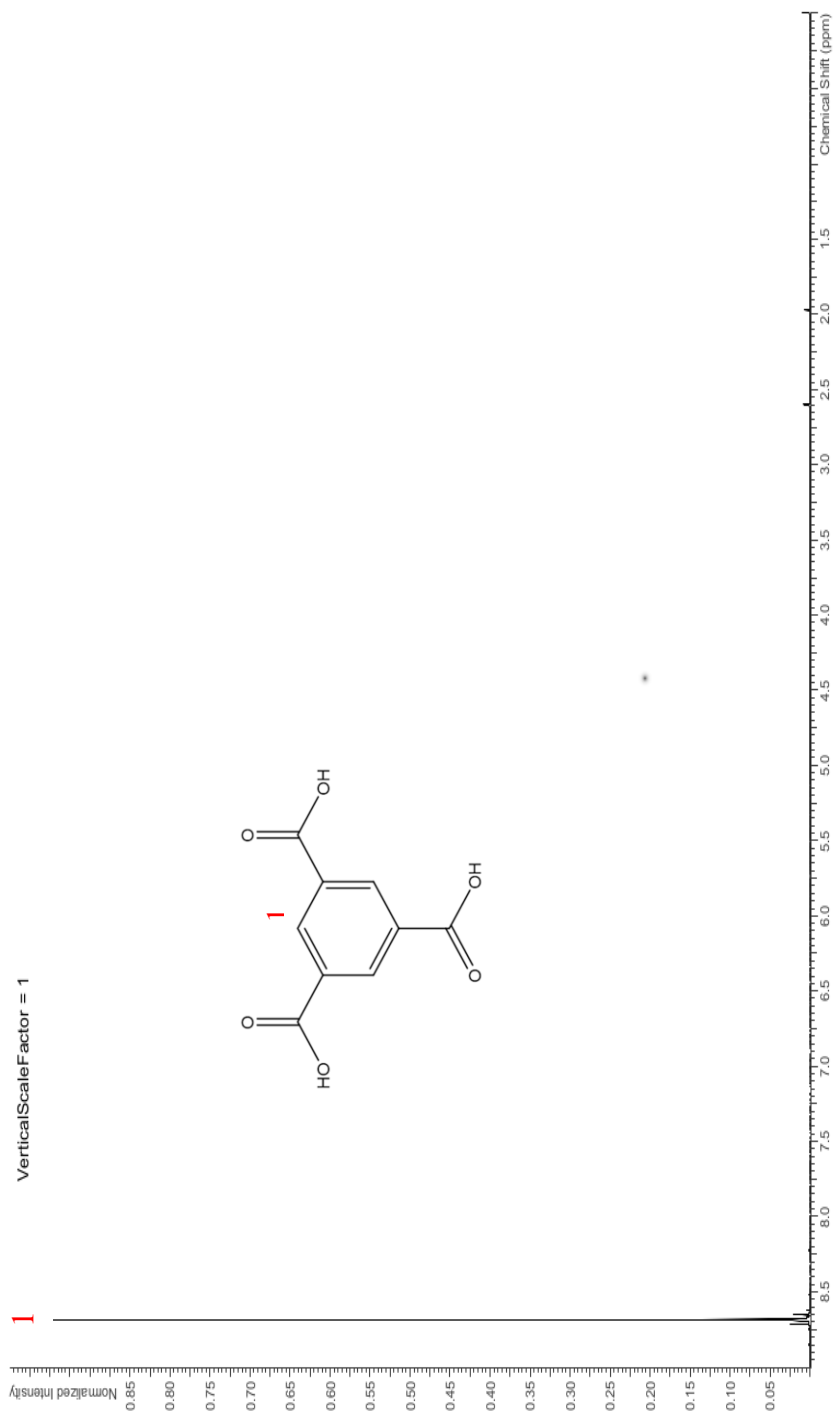
Figure 56: Trimesic Acid ^{1}H NMR.

CHAPTER III

CONCLUSIONS

The microwave-assisted syntheses of the phosphorus based compounds was proven successful, but FTIR, TGA, DSC, and NMR show that this method needs improvement and is not sufficient as is based on evidence of impurities or partially reacted materials.

Samples that were synthesized indicate a mix of products still existed after the purification steps. Sample EM100419 (1,3,5-DPP) appears to have multiple products present due to the multiple carbonyl peaks present in the FTIR, NMR, and the DSC analysis. Sample 1,3,5-DPP was a dark amber before the wash and a white solid with a dense yet soft texture.

The 1,3,5-PPDB samples were insoluble in DMSO solvent. The 1,3,5-PPDB samples synthesized appeared to be a crosslinked material. Crosslinking may also explain why the 1,3,5-PPDB samples would gel-up in DMSO solvent. The products from the 1,3,5-PPDB synthesis were brittle solids and varied in color from yellow to brownish red/black.

The 1,3,5-PPTBDA samples had the highest yields and was the easiest to handle for analysis as the product was a crystalline solid after the purification. ^{31}P NMR suggests that it contains a monosubstituted phosphate species. NMR predictions suggested that more aromatic species should have been present in the ^{13}C and the ^{1}H NMR. 1,3,5-PPTBDA also appeared to the onset of mass loss at much lower temperatures. These low

temperature mass loss maybe due to low-molecular volatile material being vaporized during the heating.

The 1,3,5-DPP samples may need different purification methods. The solvent used for the purification step for the 1,3,5-DPP decreased the yield dramatically for sample EM100419. This result requires further investigation as to why so much product was lost.

Microwave-assisted synthesis is an efficient method of synthesizing materials with faster reaction time. In this research project, the synthesis times were dramatically decreased where they took 24-48 hours of heating alone with traditional methods. The samples synthesized can be studied further as potential flame retardant additives in the future by adding them to a polymer resin and comparing the thermal degradation profiles.

1,3,5-DPP was optimal in this study with a power of 50W, temperature of 130°C, and a time of 15 minutes (EM100419). 1,3,5-PPDB and 1,3,5-PPTBDA had the same first microwave step with optimal settings of 50W, 130°C, and 15 minutes. Based off the amount of TGA char an estimation would be for 1,3,5-PPDB that the optimal time is 5-7minutes, 80-100°C, and with a power of 50W (EM081720 and EM082720). Based off the amount of TGA char for the 1,3,5-PPTBDA samples, it is probable that optimal settings are between 15-20minutes, between 115°C and with a power of 90W (EM110820 and EM111220).

Future improvement on this project could be to try the reaction in DMSO solvent or another compatible solvent. The products were viscous when heated and solidified in

some cases at room temperature. Using a solvent could decrease the reaction time even more and make the products easier to handle after the synthesis.

The goal was to decrease the reaction time using microwave-assisted synthesis. Now the products may be applied to engineering resin to test their FR performance via industrial testing protocols such as UL-94 and LOI.

REFERENCES

1. Hoogenboom, R.; Schubert, U.S.; Wiesbrock, F. Advances in Polymer Science 274. *Microwave-assissted Polymer Synthesis*. Springer. 2016.

2. Mnirajd, P. *Synthesis of Non-Halogenated Phosphorus Flame Retardants For Engineering Resins*. Middle Tennessee State University. 2012. pp. 1-21.

3. Huo, S.; Song, P.; Yu, B.; et.al. Progress in Polymer Science: Phosphorus-containing flame retardant epoxy thermosets: Recent advances and future perspectives, Volume 114. Elvsvier, 2021. April 2021.

4. Wypych, George. Mechanisms of Flame Retardants In *Handbook of Flame Retardants*. Chem Tec Publishing, 2021. pp 53-88.

5. Hindersinn, R. Historical Aspects of Polymer Fire Retardance. (A. S. 465, Ed.) *Fire and Polymers: Hazards Identification and Prevention*, 1990. pp. 87-97.

6. All About Bromine. Retrieved from http://www.bromine-info.org/when-did-flame-retardants-start-to-be-used/. 2008.

7. Leadbeater, N., McGowan, Cynthia. *Clean, Fast Organic Chemistry: Microwave-assisted laboratory experiments*. Mathews, North Carolina: CEM Publishing. 2006.

8. Microwave Ovens. Retrieved from https://ethw.org/Microwave_Ovens/. 2017.

9. Gallawa, C.J., A Brief History About The Microwave Oven. Retrieved from https://www.smecc.org/microwave_oven.htm. 2001.

10. Microwave Synthesis 101. CEM Corporation. Retrieved from https://cem.com/microwave-101/. April 2021.

11. Kempe, K.; Becer, R.; Schubert, U. Microwave-Assisted Polymerizations: Recent Status and Future Perspectives. Macromolecules, 2011. pp 5825-5842.

12. Mello, Paola A., Barin, Juliano S., Guarnieri, Ricardo A. Microwave-Assisted Sample Preparation for Trace Element Analysis. Erico Marlon de Moraes Flores (Eds.) Elsevier, 2014. Chapter 2- Microwave Heating. pp 59-75.

13. Kappe, C.O., Comprehensive Medicinal Chemistry II. Volume III. Microwave-Assisted Chemistry. John B. Taylor, David J. Triggle (Eds.), Elsevier, 2007. Chapter 3.36. pp 837-860.

14. Mishra, A.; Vats,T.; Clark, J. Microwave Radiations: Theory and Instrumentation, *Micorwave-Assisted Polymerizations*. Royal Society of Chemistry, 2016. Chapter I. pp 1-

15. Haynes, H.J. *FIRE LOSS IN THE UNITED STATES*. National Fire Protection Association. 2021.

16. Constanintine D. Papaspyrides, Pantelis Kiliaris. *Polymer Green Flame Retardants*. Amsterdam: Elsevier, 2014.

17. Bart, J.C. *Additives in Polymers: Industrial Analysis and Applications*. John Wiiley & Sons. 2005.

18. SpecialChem. Retreived from https://polymer-additives.specialchem.com/selection-guide/flame-retardants-for-fire-proof-plastics/flame-retardants-mechanism-of-action-and-chemistries. April 2021.

19. Hull, T., Law, R., & Bergman, A. Environmental Drivers for Replacement of Halogenated Flame Retardants. In D.C. Papaspyrides, & P. Kiliaris (Eds.), Polymer Green Flame Retardants. Amerstdam: Elsevier, 2014. pp. 126-134.

20. Kundu, Chanchal K., Lei Song, Zhiwei L., Hu, Yuan. An Overview of Fire Retardant Treatments for Synthetic Textiles: From Traditional Approaches to Recent Applications. Volume 137. European Polymer Journal. Retrieved from https://www.sciencedirect.com/science/article/abs/pii/S0014305720316256. 2020.

21. Laoutid, F., Bonnaud, L., Alexandre, M., Lopez-Cuesta., & Dubois, P. New Prospects in Flame Retardant Polymer Materials: From Fundamentals to Nanocomposites. *Materials Science and Engineering* (63), 2009. pp 100-125.

22. Marosi, G., Szolnoki, B., Bocz, K., & Toldy, A. Reactive and Additive Phosphorus-Based Flame Retardants of Reduced Environmental Impact. In C.D. Papaspyrides, & P. Kiliaris (Eds.), Polymer Green Flame Retardants. Amsterdam: Elsevier, 2014. Pp 181-220.

23. Flame Retardants Online, Mode of Action. Retrieved from https://www.flameretardants-online.com/flame-retardants/mode-of-action.

24. Roth, Thomas; Wolf, Marion; Pohlein, Manfred; van Eldik, Rudi. Analysis of Flame Retardants and Elements of Concern in Printed Writing Boards with Respect to Originand Year of Construction. Bioanalytical Chem. 2013. 405, 7215-7229.

25. Flame Retardants. Retrieved from https://www.niehs.nih.gov/health/topics/agents/flame_retardants/. May 2021.

26. Birnbaum, L.S., Health Effects of Brominated Flame Flame Retardants (BFRS). Presented at 27th International Symposium on Halogenated Persistent Organic Pollutants .Dioxin 2007, Tokyo, JAPAN, 2007.

27. Salmeia, Khalifah; Gooneie, P.; Simonetti, P.; et. al. Comprehensive study on flame retardant polyesters from phosphorus additives, Volume 155; Polymer Degredation and Stability. Switzerland. Elsevier, 2018. pp 22-34. April 2021.

28. Wang, H.; Wang, S.; Du, X.; Wang, H.; Chenga, X.; Zongliang, D. RSC Advances: Synthesis of a Novel Flame Retardant Based on DOPO Derivatives and its Application in Waterborne Polyurethane. Royal Society of Chemistry, 2019. RSC Adv., 2019,9, 7411-7419. April 2021.

29. Chung, HW.; Ding, WH. Determination of organophosphate flame retardants in sediments by microwave-assisted extraction and gas chromatography–mass spectrometry with electron impact and chemical ionization. *Anal Bioanal Chem* 395**,** 2325–2334, 2009.

26. RTI Laboratories. FTIR Analysis Techniques. https://rtilab.com/techniques/ftir-analysis/.

27. Vollhardt, K.P.; Schore, N.E. *Organic Chemistry: Structures and Functions*; W.H. Freeman and Company: New York, 2007.

28. Thermofisher Scientific. FTIR Sample Techniques: Attenuated Total Reflection (ATR). https://www.thermofisher.com/us/en/home/industrial/spectroscopy-elemental-isotope-analysis/spectroscopy-elemental-isotope-analysis-learning-center/molecular-spectroscopy-information/ftir-information/ftir-sample-handling-techniques/ftir-sample-handling-techniques-attenuated-total-reflection-atr.html

29. Campbell, D.; White, J.R. Thermal Analysis. In Polymer Characterization: Physical Techniques; Chapman & Hall: New York, 1989. pp 362-382.

30. Janovick, Jennifer, Spyros, Apostolos, Dais, Photis, Hatzakis, Emmanuel. 4-Nuclear Magnetic Resonance. Chemical Analysis of Food. 2nd Edition Yolando Pico (Ed.) Academic Press, 2020. pp 135-175.

31. Coates, J. In *Encyclopedia of Analytical Chemistry*; R.A. Meyers. John Wiley & Sons Ltd, Chichester, 2000. pp 10815-10837.

32. Nguyen, C.; Kim, J. Polymer Degradation and Stability: Thermal stabilities and flame retardancies of nitrogen–phosphorus flame retardants based on bisphosphoramidates. Elsevier, 2008. Vol.93. pp 1037-1043.